119
21

Rain Scatter Interference In Satellite Links

by

Fatim M. Haidara

Thesis submitted to the Faculty of the

Virginia Polytechnic Institute and State University

in partial fulfillment of the requirements for the degree of

Master of Science

in

Electrical Engineering

APPROVED:

C. W. Bostian, Chairman

W. L. Stutzman

T. Pratt

December, 1988

Blacksburg, Virginia

Rain Scatter Interference In Satellite Links

by

Fatim M. Haidara

C. W. Bostian, Chairman

Electrical Engineering

(ABSTRACT)

Scattering by rain in addition to inducing attenuation and depolarization in satellite links can create intersystem interference. This type of interference was investigated extensively in the 1970 's for terrestrial links, but little has been done to study its effects on modern and future satellite links. This thesis reports on studies of the potential interference created by the scattering of an uplink signal into an adjacent satellite and the inverse case where a downlink signal is scattered into the earth station of an adjacent satellite system. The thesis describes the rain medium in a way which emphasizes the computation of the needed single-drop scattering coefficients using the extended boundary condition method (EBCM). The development of the experimental and theoretical study of rain scattering interference is then reviewed. Three computation methods for the interfering power are presented and compared. The first one, based on the radiative transfer equation, includes multiple scattering considerations, while the two other techniques take only the first order multiple scattering into account. The impact of such interference is then studied and an experiment involving the OLYMPUS and ACTS spacecraft is proposed.

Acknowledgements

I first would like to express my deep gratitude and sincere appreciation to Professor C.W. Bostian for giving me extremely helpful and valuable guidance, encouragement and advice. I am also indebted to Professor T. Pratt and W.L. Stutzman for their willingness to serve on my committee and for their valuable suggestions. Appreciation is extended to C. P. Marshall for her expert and patient help in typing this thesis, and to all the members of the Satellite Communication Group for their kind assistance.

In addition I would like to express my appreciation to the African American Institute for it financial support and to Mrs. Elizabeth Ward for effective assistance. Appreciation is extended also to the Malian government. I would like to thank Tijan M. Sallah, Cheryl L. Kyle, Fatima El Abdaoui, Peter Materu, Patricia Webber, Paul Werntz and Koichiro Takamizawa for their friendship.

Finally I would like to thank my parents Baba Akhib Haidara and Selly Haidara, my sisters Aminata, Habibatou, and Khadidjatou, and my brothers Alhassane and Mansour for their continuing love and support.

Table of Contents

List of Illustrations

1.0 Introduction

1.1 Statement of the Problem

The worldwide technological explosion of the past decades and the consequent expanding need in telecommunications has led to the saturation of the C band (4-8 GHz) and lower bands and to the use of higher frequencies for satellite communications. More and more systems are operating at frequencies ranging from the Ku (12-18 GHz), K (18-27 GHz) and Ka (27-30 GHz) bands to the millimeter waves (> 30 GHz). In addition to alleviating the existing congestion, such systems have the advantages of offering more bandwidth and higher antenna gain, thus allowing for more flexibility in improving the channel capacity. The primary problem is that an electromagnetic wave propagating in the earth's atmosphere may be strongly impaired and, at frequencies above 10 GHz, the degradations are more serious than for lower frequencies (except for the case of Faraday rotation). Oxygen and water vapor absorption, the increase of the thermal noise, and the scintillations due to tropospheric turbulence all exemplify this. The major impairments are the result of the interactions between

the electromagnetic wave and tropospheric hydrometeors (rain, snow, hail, etc.). These phenomena have been widely studied both theoretically and experimentally by engineers and scientists.

Rain drops absorb and scatter electromagnetic energy so that a wave traveling in precipitation is attenuated and depolarized. The attenuation may critically affect any satellite link (operating above 10 GHz) and the depolarization may impair frequency reuse systems using dual polarization by creating cochannel interference and crosstalk. This is often called self-interference. Another important problem arises because rain scatters electromagnetic waves not only in the forward direction (i.e. in the direction of the incident wave), but also in all other directions. This phenomenon, also called side-scattering or bistatic-scattering (from radar terminology) is a potential source of interference between two communications systems because the power scattered out of the intended propagation path can be intercepted by the side lobe of an antenna looking at another transmitter; a widely studied example of this is the interference between terrestrial radio relay and satellite links at 4-6 GHz that is involved in the determination of coordination distance. Radar systems, remote sensing systems, and radiometric measurements can also be seriously degraded by bistatic scattering of energy from another system.

The problem of rain scatter interference was investigated widely in the early 1970's, and it has had relatively little attention since then. This thesis was written to bring together all of the existing literature on the topic and to establish the severity of the interference problem that might be expected for the satellite systems of the 1990's. The particular case treated in this thesis involves the interference created by the electromagnetic energy scattered out of the downlink propagation path of a geostationary satellite system into the side lobe of the receiving earth station antenna of an adjacent geostationary satellite link (see Figure 1); it corresponds to a planned experiment using the spacecraft OLYMPUS and ACTS. The orbital spacing between the two satellites is assumed to be 2 degrees, the minimum allowed by the

F.C.C. regulations. Thus this is a worst-case condition. In this study the pattern of the receiving antenna is chosen to be as broad as possible in order to increase the probability of intercepting the interfering signal scattered by the rain. This choice allows us to model widely used domestic and commercial systems with VSATs (Very Small Aperture Terminals). A VSAT has a large beamwidth because of the small size of its antenna. The side-lobe to side-lobe interference is the other sources of interference and can be estimated using the side lobe envelope specified by the F.C.C. The purpose of this thesis is twofold. The first is to predict the interfering signal both qualitatively (coherent vs incoherent) and quantitatively (i.e. finding the interfering power received by the impaired antenna) for frequencies above 10 GHz. This involves a close study of the single and multiple scattering processes in the random rain media taking into account the rain parameters (rain rate, drop size distribution, location of the rain , etc.) as well as the system parameters (frequency, elevation angles, incident power, beamwidth of the sidelobe receiving the interference etc.). This also includes the analysis of the impact of such interference on the overall performance of the impaired system. For this, the two classical systems, analog FM and digital modulation, are studied. Our second purpose is to propose an experiment using OLYMPUS and ACTS that would characterize the phenomena.

1.2 Description of the Thesis.

Following this introductory section, Chapter 2 gives the mathematical statement of the problem by first describing the microscopic characteristics of the rain medium, then by presenting the EBCM (extended boundary condition method) to compute the scattering coefficient of the raindrops, and finally by introducing a mathematical description of the side

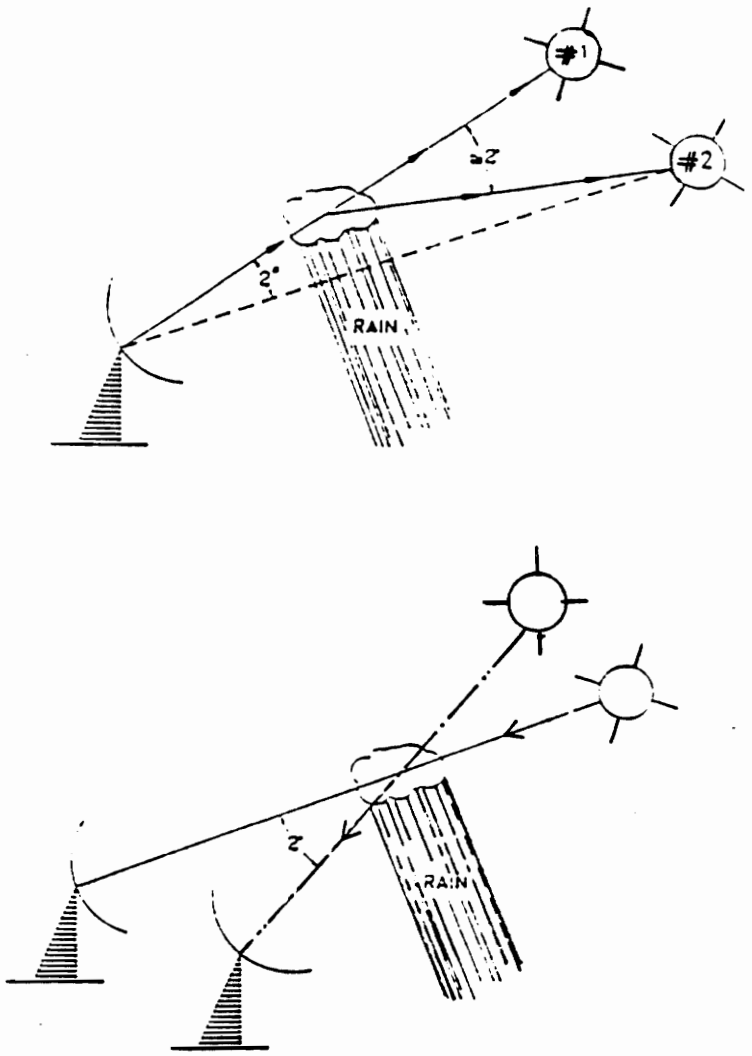

Figure 1. Interference from an adjacent satellite system in presence of rain: (1) Uplink case (2) downlink case.

scattering problem. The third chapter contains a review of the literature. In Chapter 4 we propose three prediction methods for the power scattered by the rain ; the first one is based on the vector radiative transfer equation and includes multiple scattering considerations, while the two other techniques are founded on the bistatic radar equation and on Chu's derivations and assume single scattering. This chapter also present an analysis of the effect of rain scatter interference on typical commercial systems. The fifth chapter presents recommendations for an experiment that would characterize the rain side scattering for satellite links using the OLYMPUS and ACTS satellites. Finally, the results of this thesis are summarized in the conclusion chapter.

2.0 Mathematical Statement of the Problem

In this chapter our purpose is to present the mathematical and physical definitions necessary for the understanding of the rain scatter interference problem. The microscopic characteristics of the rain medium are described, emphasizing the calculation of the scattering properties of a single raindrop, and a mathematical description of the side scattering problem ends the chapter.

2.1 The Rain Medium

2.1.1 Physical Properties

The rain medium has been extensively studied by meteorologists and telecommunications engineers. Oguchi [1] and Stutzman [2] give excellent reviews of this work. Therefore we will only stress here the relevant characteristics.

A raindrop may be modeled by a dielectric material whose complex dielectric constant may be written as [1]:

$$\varepsilon = \varepsilon_r - i\varepsilon_i \tag{2.1}$$

and its complex refractive index is

$$N = N_r - iN_i \tag{2.2}$$

The relation between the above quantities is

$$N = \sqrt{\varepsilon} \tag{2.3}$$

The complex refractive index of a raindrop depends on both the temperature and the wavelength. An empirical model of the refractive index was derived by Ray [3] for temperatures between $-20°C$ and $50°C$ and wavelengths ranging from $2\mu m$ to several hundred meters. This model was coded by Barksdale [4] and will be used in the computation of raindrop single scattering coefficients.

Another important factor in computing scattering coefficient is the shape of the drop, which depends on its size. Pruppacher and Pitter [5] have investigated this dependence, and

found the following widely used theoretical model (Figure 2) based on $\bar{a}$, the equivalent radius or equivolumetric radius of the drop ($\bar{a}$ is defined as the radius of a sphere containing the same volume of water as the spheroidal drop).

- For $\bar{a} < 0.17$ mm the drop is spherical

- For $0.17 \text{ mm} \leq \bar{a} < 0.5$ mm the drop is an oblate spheroid: i.e. an ellipse rotated around its minor axis .

  The axial ratio $\frac{a}{b}$, where a is the minor axis and b the major axis, is well approximated by:

$$\frac{a}{b} = 1 - \bar{a} \quad (\bar{a} \text{ in mm}) \tag{2.4}$$

- For $0.5 \text{ mm} \leq \bar{a} < 2$ mm the drop is an asymmetric oblate spheroid with an increasingly flat base.

- For $2 \text{ mm} \leq \bar{a} < 4$ mm , the drop is oblate with a concave depression at the base.

- Larger drops ($\bar{a} \geq 4$ mm) break up into smaller ones.

The choice of the raindrop shape depends on the propagation phenomenon, which is studied. For example, rain attenuation has been widely modeled using a population of spherical raindrops. Depolarization, on the contrary, because it is produced by differential attenuation involving non-spherical raindrops, is usually studied using either an entirely oblate spheroidal drop population or a mixture of spherical and oblate drops [2], [6]. When modeling propagation through rain using non-spherical raindrop shapes, one must also consider the canting angle of the drop; i.e., the angle between the minor axis of the drop and the vertical.

Canting occurs because aerodynamic forces tilt the drop, and (Figure 3) the canting angle distribution is critical in modeling depolarization. Studies [1], [2] show that a gaussian distribution of canting angles gives good results.

The final, but none the less important factor, in the rain medium characterization is the drop size distribution which can be defined as the number $n(\bar{a})$ of drops per unit volume whose equivalent radius is between $\bar{a}$ and $\bar{a} + d\bar{a}$. This quantity depends on the rain rate. Three drop size distributions are used in modeling millimeter wave propagation through rain. The first is the Laws and Parson (LP)[6] drop size distribution which was obtained experimentally and is representative of widespread rain the in a temperate climate zone. The Marshall and Palmer (MP)[7] distribution is similar but has an analytical form which make it more suitable for calculation; it can be expressed as:

$$n(\bar{a}) = N_0 e^{-\Lambda \bar{a}} \quad m^{-3} mm^{-1} \tag{2.5}$$

with

$$N_0 = 16000$$

$$\Lambda = 8.2R^{0.21}$$

where $\bar{a}$ is the equivalent volume radius in millimeters and R is the rain rate in mm/hr.

The above distribution is suitable for widespread rains; Joss [8] gives different parameters Λ and N_0 for thunderstorm and drizzle. In this thesis we will use the MP drop size distribution because it has a simple functional expression. Besides, since we are not concerned with depolarization effects, we will assume that all the drops are oblate spheroids with no canting angle. The axial ratio will be given by Equation 2.4.

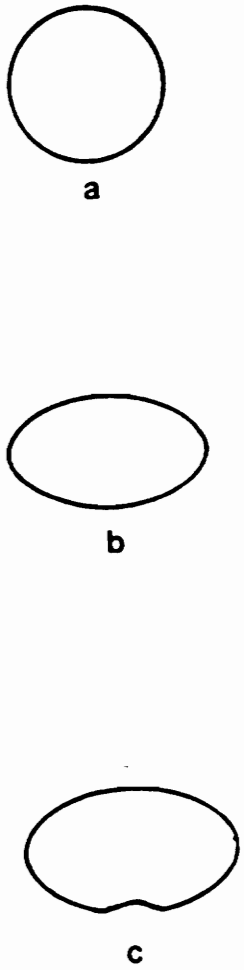

Figure 2. Pruppacher and Pitter rain drop: (a)spherical drop; (b) oblate spheroidal drop ; (c) distorted oblate spheroidal drop

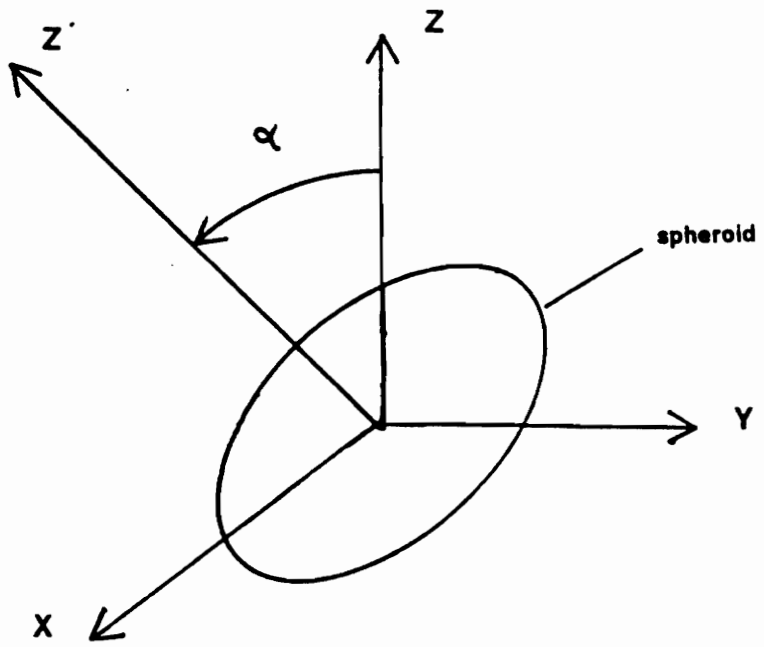

Figure 3. Tilted oblate spheroidal drop; alpha is the canting angle.

2.1.2 Single Scattering Properties of a Raindrop.

2.1.2.1 General Properties.

In order to solve the macroscopic problem of scattering in rain , it is necessary first to know the scattering properties of a single water drop. Since this topic is exhaustively treated in the literature [1],[4],[9],[10],[11],[12],[13] we restrict this study to the essential core by first defining the single scattering terminology and geometry, then briefly reviewing the method used to compute the scattering amplitude, and finally presenting the extended boundary condition method (EBCM).

Consider the scattering geometry on Figure 4 where a monochromatic linearly polarized unit plane wave $(\vec{E}_i,\vec{H}_i)$ is incident on a particle of arbitrary shape and complex dielectric constant $\varepsilon(\vec{r})$.The electromagnetic wave propagates in the direction $\hat{i}$ with a wave number k .The dielectric particle absorbs part of the incident energy and scatters the remaining part. $(\vec{E}_s, \vec{H}_s)$ represents the scattered field at a distance r in a direction $\hat{o}$; it is very complex in the near field of the particle [14]. But in the far field of the drop, the electromagnetic wave is spherical and can be expressed as :

$$\vec{E}_s(\vec{r}) = \vec{f}(\hat{o},\hat{i})\frac{e^{-jkr}}{r} \tag{2.6}$$

with $\vec{r} = r\hat{o}$ and $r >> \frac{D^2}{\lambda}$ (λ is the wavelength and D is a typical dimension for the particle). The vector function $\vec{f}(\hat{o},\hat{i})$ is the scattering amplitude and represents the magnitude, the phase, and the polarization (generally elliptical) of the scattered electromagnetic wave.

We can then define various cross sections of a particle [1],[14],[15]. A cross section has the dimension of an area and depends on the size and shape of the particle and on the angle of incidence and polarization of the incoming wave :

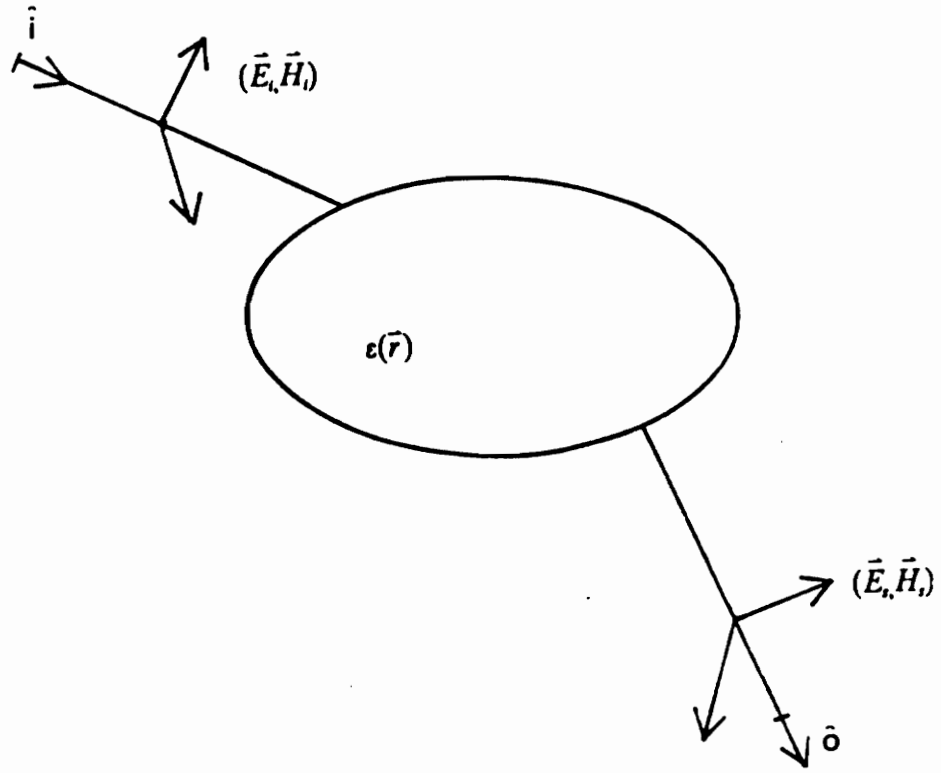

Figure 4. Single scattering geometry .

- First the absorption cross section, which represents the amount of power absorbed by the particle when it is illuminated by a unit plane wave, is denoted σ_a.

- The scattering cross section σ_s is the power scattered in all directions by the raindrop when it is illuminated by a unit plane wave. σ_s is related to the scattering amplitude defined earlier (2.6) by the following equation:

$$\sigma_s = \int_{4\pi} |\vec{f}(\hat{o}, \hat{i})|^2 d\omega \tag{2.7}$$

$d\omega$ is an element of solid angle and the integration is for all scattering directions $\hat{o}$.

- Then we define the extinction or total cross section which is the sum of the scattering cross section σ_s and the absorption cross section σ_a :

$$\sigma_t = \sigma_a + \sigma_s \tag{2.8}$$

This represents the amount of power subtracted from the incident unit plane wave by absorption and scattering. The total cross section is linked to the forward scattering amplitude by a relation denoted as the forward scattering theorem [1],[14],[15] :

$$\sigma_t = -\frac{4\pi}{k} Im[\vec{f}(\hat{i}, \hat{i})] \cdot \hat{e}_i \tag{2.9}$$

where $\hat{e}_i$ is the direction of the incident field. From (2.9) we may compute the attenuation of the coherent field and the extinction cross section.

To model bistatic scattering one may use :

- The differential cross section σ_d

$$\sigma_d(\hat{o},\hat{i}) = |f(\hat{o},\hat{i})|^2 \tag{2.10}$$

- The radar cross section or bistatic radar cross section :

$$\sigma_{bi}(\hat{o},\hat{i}) = 4\pi\sigma_d(\hat{o},\hat{i}) \tag{2.11}$$

- The phase function (this term is not linked to the phase of the wave , but it has its origins in the astronomical term "lunar phase") represents the amount of scattered power :

$$p(\hat{o},\hat{i}) = \frac{4\pi}{\sigma_t}|f(\hat{o},\hat{i})|^2 \tag{2.12}$$

The scattering amplitude depends on the shape, the size, the frequency, the temperature and the dielectric parameters of the particles. Several techniques to evaluate it have been developed. They can be classified depending on the shape and the size of the scatterers.

The computation of the scattering amplitude can be carried out exactly when the shape of the particles is simple. The Mie theory [14],[15] which gives the exact field scattered by an isotropic homogeneous sphere of arbitrary size exemplifies this . An exact general integral equation for the scattering amplitude is given by Ishimaru [15] :

$$f(\hat{o},\hat{i}) = \frac{k^2}{4\pi}\int_V \left\{-\hat{o}\times[\hat{o}\times\vec{E}(\vec{r'})]\right\}\left\{\frac{\varepsilon(\vec{r'})}{\varepsilon_0}-1\right\}e^{-jk\vec{r'}\cdot\hat{o}}\,dV' \tag{2.13}$$

Where $\vec{E}(r')$ is the field inside the particle, ε_0 is the dielectric constant of the medium surrounding the particle and V the volume occupied by the dielectric. The main difficulty in using (2.13) is to know $\vec{E}(r')$, the internal field; it is generally necessary to use approximations:

- For an electrically small dielectric body ($D << \lambda$) the internal field can be approximated by a uniform electrostatic field . This method is referred to as Rayleigh scattering. The pattern of the field scattered by a small spherical particle computed using the aforementioned approximation is similar to that of an electric dipole.

- When $(\varepsilon(r) - 1)kD << 1$, the internal field can be replaced by the incident field thus giving Rayleigh-Debye scattering.

- When $(\varepsilon(r) - 1)kD >> 1$ and $\varepsilon(r) - 1 < 1$ the internal field is approximated by a plane wave propagating inside the particle with the propagation constant of the particle. This technique is called the WKB interior wave number approximation.

Electrically large scatterer cases are treated using geometrical optics methods [14]. The above techniques , however do not hold for scatterers in the resonance region where the size of the scatterers is of the same order as the wavelength; the following methods have been developed for such particles :

- the geometrical theory of diffraction for high frequencies and perfectly conducting bodies.

- the moment method for bodies of size smaller than 0.1λ. This limitation arises from computing reasons .

- the perturbation method for scatterers whose shape is a small distortion of a sphere.

- the point matching method .

- the extended boundary condition method (EBCM) for homogeneous dielectric.

- the global-local finite element method.

The most suitable methods for our purpose, to compute the scattering amplitude of an oblate spheroid raindrops, are the EBCM and the global-local finite method [12] [13]; the EBCM is chosen for it is adaptable to any shape and size of homogeneous dielectric particles and simpler to code.

2.1.2.2 The EBCM: The EBCM (also called T-matrix method) was first developed by P.C.Waterman [16] for conducting bodies in the region of resonance; it was then extended to dielectrics by using the Huygens' principle. A detailed treatise on this method can be found in H. Barksdale's dissertation [4] or in Barber et al. [13] In the following we describe the main steps of this technique and present some numerical results.

Consider a homogeneous and isotropic dielectric (ε, μ_o) particle illuminated by a monochromatic, linearly polarized plane wave $(\vec{E}_i, \vec{H}_i)$ as depicted in Figure 4. The problem is to find the scattered field $(\vec{E}_s, \vec{H}_s)$ at a point P, referred to as the observation point. P belongs to a sphere including the dielectric. The total field at a given point is:

$$\begin{aligned} \vec{E} &= \vec{E}_i + \vec{E}_s \\ \vec{H} &= \vec{H}_i + \vec{H}_s \end{aligned} \tag{2.14}$$

So the scattered field can be expressed as:

$$\begin{aligned} \vec{E}_s &= \vec{E} - \vec{E}_i \\ \vec{H}_s &= \vec{H} - \vec{H}_i \end{aligned} \tag{2.15}$$

Let $\vec{M}_i, \vec{J}_i$ be the magnetic and electric source currents creating ($\vec{E}_i, \vec{H}_i$). Schelkunoff's equivalence principle states that [8]: "The field in a source free region bounded by a surface

S could be produced by a distribution of electric and magnetic currents on this surface, and in this sense, the actual distribution can be replaced by an equivalent distribution:

$$\vec{M} = \vec{E} \times \hat{n}$$
$$\vec{J} = \hat{n} \times \vec{H} \tag{2.16}$$

where $\vec{E}, \vec{H}$ are the impressed fields and $\hat{n}$ is the unit vector normal to the surface, pointing into the source-free region." This principle is applied to our problem in four steps to transform it into a simpler equivalent problem:

- Step 1: The field $\vec{E}_s$ and $\vec{H}_s$ can be considered as being produced by a current distribution $\vec{J}_s, \vec{M}_s$. The Schelkunoff principle allows us to define surface currents $\vec{J}_s$ and $\vec{M}_s$ generating $(\vec{E}_s, \vec{H}_s)$ (Figure 5) with:

$$\vec{J}_S = \hat{n} \times \vec{H}_S$$
$$\vec{M}_S = \vec{E}_S \times \hat{n} \tag{2.17}$$

- Step 2: Consider now the situation described by Figure 6-a where the internal field is equal to the opposite of the incident field $(\vec{E}_i, \vec{H}_i)$. The equivalence principle applied to this problem, gives Figure 6-b where the external field is null, and the internal field is $(-\vec{E}_i, -\vec{H}_i)$ with the current distribution:

$$\vec{J}_i = \hat{n}' \times \vec{H}_i$$
$$\vec{M}_i = \vec{E}_i \times \hat{n}' \tag{2.18}$$

- Step 3: Using the superposition principle we combine the results of Step 1 and 2 (Figure 6-b and Figure 5-b), obtaining thus the configuration depicted by Figure 7 where the surface currents:

$$\vec{J}_+ = \hat{n} \times (\vec{H}_s + \vec{H}_i)$$
$$\vec{M}_+ = (\vec{E}_i + \vec{E}_i) \times \hat{n} \tag{2.18}$$

generate the scattered field ($\vec{E}_s$ and $\vec{H}_s$) outside S and $-\vec{E}_i, -\vec{H}_i$ inside S.

- Step 4: Finally we add the sources $\vec{J}_i$ and $\vec{M}_i$ (Figure 8).

We obtain after these manipulations the new but equivalent problem consisting of the same sources and fields as in the initial problem, but the scatterer is replaced by a surface current distribution over S, producing the scattered field in the free space. The field inside the surface is null. To solve the equivalent problem, we first express the external field and the internal field. The boundary conditions at the surface S are then stated and the scattered field evaluated. The terms "external" and "internal" are relative to the surface S.

The scattered fields in the equivalent problem are due to the sources $\vec{J}_+$, $\vec{M}_+$; one can compute them using the magnetic and electric potential $\vec{A}$, and $\vec{F}$ as in Harrington [17]:

$$\vec{E}_s = -\nabla \times \vec{F} - \frac{1}{j\omega\varepsilon_0}(\nabla \times \nabla \times \vec{A})$$
$$\vec{H}_s = \nabla \times \vec{A} - \frac{1}{j\omega\varepsilon_0}(\nabla \times \nabla \times \vec{F}) \tag{2.19}$$

and

$$\vec{A} = \int_S \vec{J}_+ \, G(kR) \, ds$$
$$\vec{F} = \int_S \vec{M}_+ \, G(kR) \, ds \tag{2.20}$$

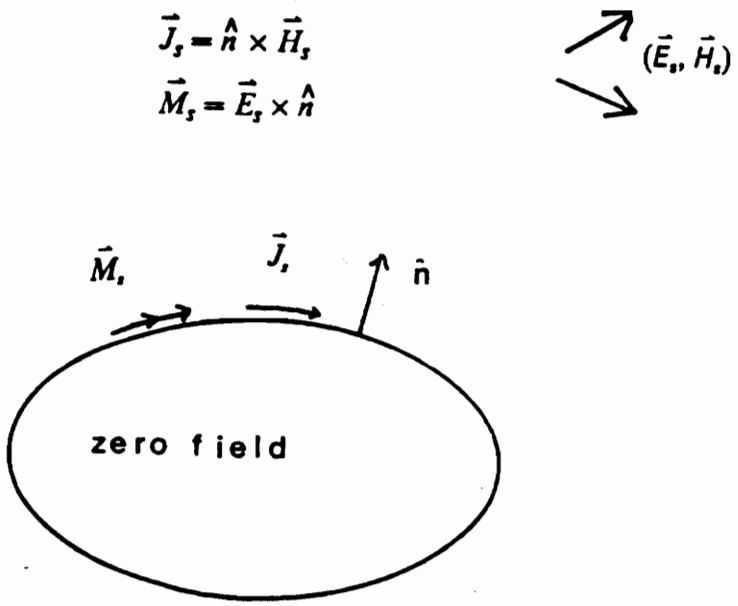

Figure 5. Step 1 of EBCM: Schelkunoff's principle for the scattered field.

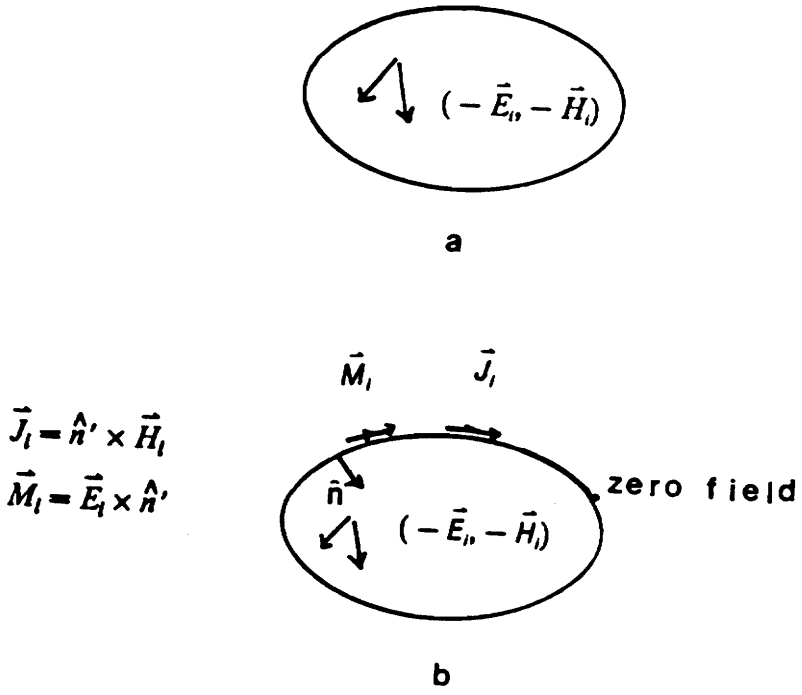

Figure 6. Step 2 of EBCM: Internal problem

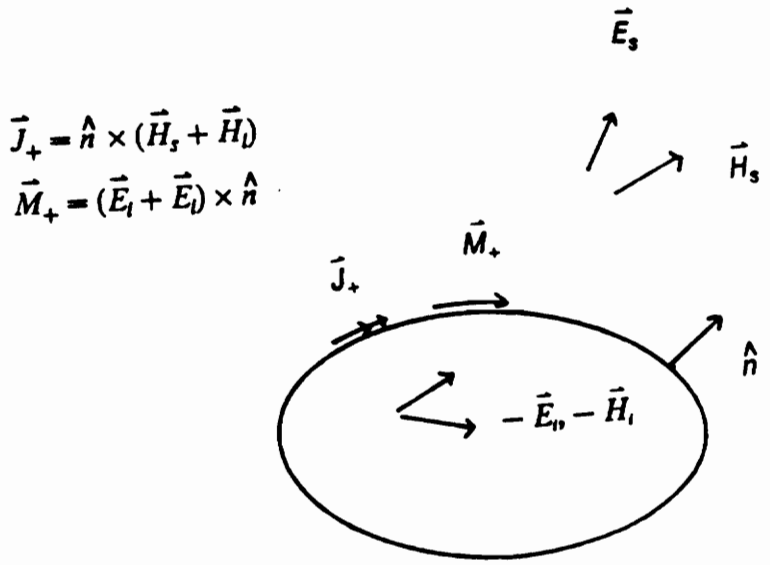

Figure 7. Step 3 of EBCM: Superposition of Figures 6-b and 5

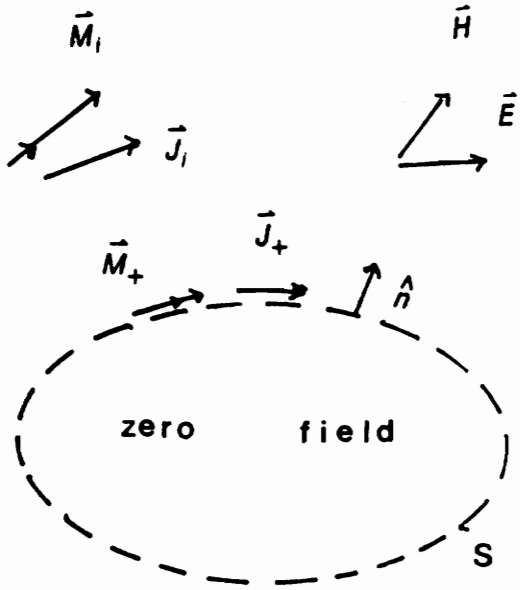

Figure 8. Step 4 of EBCM: Equivalent problem

$$\vec{J}_+ = \hat{n} \times \vec{H}_+$$
$$\vec{M}_+ = \vec{E}_+ \times \hat{n}$$

Where $G(kR) = \frac{e^{jkR}}{4\pi R}$ is the free space Green's function and $R = |\vec{r} - \vec{r}'|$. Substituting (2.20) into (2.19) yields:

$$\vec{E}_s(\vec{r}) = \nabla \times \int_S (\hat{n} \times \vec{E}_+) G(kR) ds - \nabla \times \nabla \times \int_S \frac{1}{j\omega\varepsilon_0} (\hat{n} \times \vec{H}_+) G(kR) ds \tag{2.21}$$

The total field is then:

$$\vec{E}(\vec{r}) = \vec{E}_i(\vec{r}) + \nabla \times \int_S (\hat{n} \times \vec{E}_+) G(kR) ds - \nabla \times \nabla \times \int_S \frac{1}{j\omega\varepsilon_0} (\hat{n} \times \vec{H}_+) G(kR) ds \tag{2.22}$$

Since inside the scatterer the total field is null, the incident field can be expressed as:

$$\vec{E}_i(\vec{r}) = -\nabla \times \int_S (\hat{n} \times \vec{E}_+) G(kR) ds + \nabla \times \nabla \times \int_S (\hat{n} \times \vec{H}_+) G(kR) ds \tag{2.23}$$

The field E_i is then expanded (inside the volume) using the spherical vector harmonics M_{mn} and N_{mn} defined by Stratton [18]:

$$\vec{M}_{\sigma mn}(\vec{r}) = \nabla \times \vec{r} \begin{Bmatrix} \cos m\phi \\ \sin m\phi \end{Bmatrix} P_n^m(\cos\theta) Z_n(kr) \tag{2.24}$$

$$\vec{N}_{\sigma mn}(\vec{r}) = \frac{1}{k} \nabla \times \vec{M}_{\sigma mn}(\vec{r})$$

with

σ = even or odd

$P_n^m(\cos\theta)$ = appropriate Legendre function

$Z_n(kr)$ = appropriate Bessel function

(r, θ, ϕ)represent the spherical coordinates of $\vec{r}$

For solutions where the value of the field must be finite at $r = 0$, the Bessel function $Z_n(kr)$ must be $J_n(kr)$, and the corresponding functions will be written as $\vec{M}^1_{\sigma mn}$ and $\vec{N}^1_{\sigma mn}$. The Hankel function $H_n(kr)$ is used for spherical outgoing waves; the equivalent functions will then be denoted as $\vec{M}^3_{\sigma mn}$ and $\vec{N}^3_{\sigma mn}$.

So the incident field is :

$$\vec{E}_i = \sum_{\nu=1}^{\infty} D_\nu [a_\nu \vec{M}^1_\nu(k\vec{r}) + b_\nu \vec{N}^1_\nu(k\vec{r})] \tag{2.25}$$

where

ν is a combination of n,m,σ

a_ν, b_ν are the expansion coefficients

D_ν is a normalization factor equal to :

$$D_{mn} = \varepsilon_m \frac{(2n+1)(n-m)!}{4n(n+1)(n+m)!}$$

$$\varepsilon_m = \begin{cases} 1 \text{ if } m = 0 \\ 2 \text{ if } m > 0 \end{cases}$$

The dyadic free space Green's function is expanded as follows:

$$\bar{\bar{G}}(kr) = \frac{j}{k}\pi \sum_{\nu=1}^{\infty} D_\nu \left[\vec{M}_\nu^3(k\vec{r}_>)\vec{M}_\nu^1(kr_<) + \vec{N}_\nu^3(k\vec{r}_>)\vec{N}_\mu^1(k\vec{r}_<) \right] \tag{2.26}$$

with $\vec{r}_<$ = Minimum ($|\vec{r}|$, $|\vec{r}'|$) and $\vec{r}_>$ = Maximum($|\vec{r}|$, $|\vec{r}'|$)

The convergence problem of the above expansions has to be studied. For $\vec{E}_i$ there are no singularities within the volume of the scatterer, but for the dyadic Green's function the point R=0 or $\vec{r} = \vec{r}'$ is a singularity and the expansion is valid for points inside an inscribed sphere and outside a circumscribed sphere as shown by the dashed region in Figure 9.

Let us work with an inscribed sphere, and let P be a point inside that sphere. Then $\vec{r}_< = \vec{r}$ and $\vec{r}_> = \vec{r}'$. Substituting (2.25) and (2.26) into (2.24) and using the properties of multiplication of a dyadic by a vector yields the infinite set of equations

$$-a_\nu = j\frac{k^2}{\pi} \int_S \left[\vec{N}_\nu^3(k\vec{r}').(\hat{n}\vec{E}_+) + j(\frac{\mu_0}{\varepsilon_0})^{1/2}\vec{M}_\nu^3(k\vec{r}')(\hat{n} \times \vec{H}_+) \right] ds \tag{2.27}$$

$$-b_\nu = j\frac{k^2}{\pi} \int_S \left[\vec{M}_\nu^3(k\vec{r}').(\hat{n} \times \vec{E}_+) + j(\frac{\mu_0}{\varepsilon_0})^{1/2}\vec{N}_\nu^3 \right] ds$$

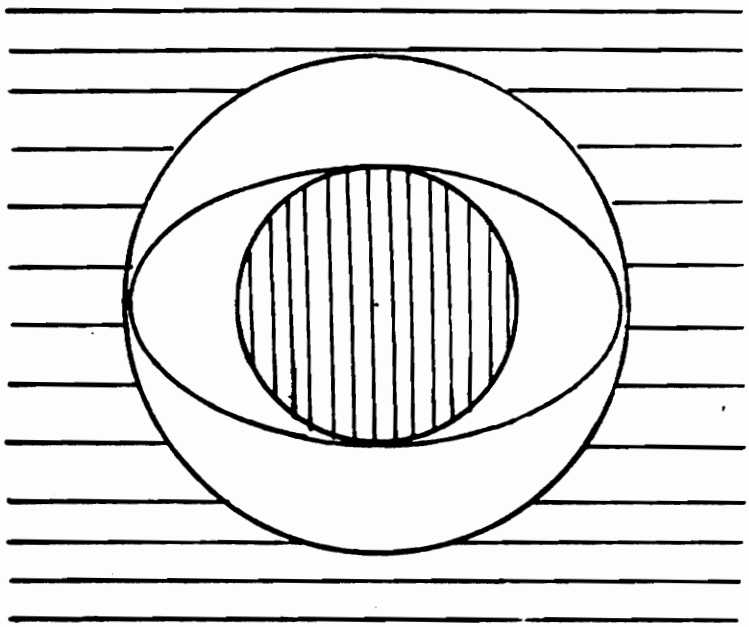

Figure 9. Convergence region for the dyadic Green function: Shaded area

This solution guarantees a zero field inside the circumscribed sphere. To obtain (as we need) a null field in the complete internal volume of the scatterer we use the concept of analytic continuation. Waterman [16] describes this principle as follows:

A function can be expanded about a point Q inside the internal sphere in a region going up to the closest singularity; this process may be repeated and the volume where the function is known is enlarged little by little. It is therefore possible to expand the total field in the interior volume of the inscribed sphere.

The internal problem is then solved by expanding the total field as

$$\vec{E}(k'\vec{r}) = \sum_{\mu=1}^{N} c_\mu \vec{M}_\mu^1 + d_\mu \vec{N}_\mu^1(k'\vec{r}) \tag{2.28}$$

where

μ stands for σ, m, n

$k' = \omega(\mu\varepsilon)^{\frac{1}{2}}$ is the wave number inside the scatterer

Then $\vec{H}(k'\vec{r})$ is computed using :

$$\vec{H}(k'\vec{r}) = \frac{1}{j\omega\mu} \nabla \times \vec{E}(k'\vec{r})$$

So

$$\vec{H}(k'\vec{r}) = -j\left(\frac{\varepsilon}{\mu}\right)^{1/2} \sum_{\mu=1}^{N} c_\mu \vec{N}_\mu^1(k'\vec{r}) + d_\mu \vec{M}_\mu^1(k'\vec{r}) \tag{2.29}$$

The boundary conditions at the spherical surface S are the continuity of the tangential components of the fields:

$$\hat{n} \times \vec{H}_+ = \hat{n} \times \vec{H}_-$$
$$\hat{n} \times \vec{E}_+ = \hat{n} \times \vec{E}_- \qquad (2.30)$$

$\vec{E}_-$ and $\vec{H}_-$ are the internal fields on the surface S; they have been expanded in (2.28) and (2.29). We substitute (2.28) and (2.29) into (2.30), replace $(\hat{n} \times \vec{E}_+)$ and $(\hat{n} \times \vec{H}_+)$ by the expression thus obtained in (2.27) and use the vectorial identity $\vec{a}.(\vec{b} \times \vec{c}) = \vec{b}.(\vec{c} \times \vec{a})$ together with the fact that M_μ and N_μ form an orthogonal family (Stratton [18]) to get:

$$-ja_\nu = [K + (\varepsilon_r)^{1/2} J]c_\mu + [L + (\varepsilon_r)^{1/2} I]d_\mu \qquad (2.31)$$

$$-jb_\nu = [I + (\varepsilon_r)^{1/2} L]c_\mu + [J + (\varepsilon_r)^{1/2} K]d_\mu$$

with

$$I = \frac{k^2}{\pi} \int_S \hat{n}.\vec{M}_\nu^3(k\vec{r}\,') \times \vec{M}_\mu^1(k'\vec{r}\,')ds$$
$$J = \frac{k^2}{\pi} \int_S \hat{n}.\vec{M}_\nu^3(k\vec{r}\,') \times \vec{N}_\mu^1(k'\vec{r}\,')ds$$
$$K = \frac{k^2}{\pi} \int_S \hat{n}.\vec{N}_\nu^3(k\vec{r}\,') \times \vec{M}_\mu^1(k'\vec{r}\,')ds$$
$$L = \frac{k^2}{\pi} \int_S \hat{n}.\vec{N}_\nu^3(k\vec{r}\,') \times \vec{N}_\mu^1(k'\vec{r}\,')ds$$

The infinite set of equations which would have given an exact solution has been truncated and is now a finite set of 2N equations.

Evaluation of the scattered field

It is now possible to find d_μ and c_μ the expansion coefficients of the internal field by using (2.31). The surface magnetic and electric currents $\hat{n} \times \vec{E}_-$ and $\hat{n} \times \vec{H}_-$ can then be computed using (2.30) and then the scattered field can be computed using (2.15) and the boundary conditions. Finally we obtain

$$E_s(kr) = \sum_{\nu=1}^{N} p_\nu \vec{M}_\nu^3(kr) + q_\nu \vec{N}_\nu^3(kr) \tag{2.32}$$

with:

$$p_\nu = -jD_\nu \sum_{\mu=1}^{N} \left[K' + \varepsilon_r^{1/2} J'\right] c_\mu + \left[L' + \varepsilon_r^{1/2} I'\right] d_\mu$$

$$q_\nu = -jD_\nu \sum_{\mu=1}^{N} \left[I' + \varepsilon_r^{1/2} L'\right] c_\mu + \left[J' + \varepsilon_r^{1/2} K'\right] d_\mu$$

$$I' = \frac{k^2}{\pi} \int_S \hat{n}.\vec{M}_\nu^3(k\vec{r}\,') \times \vec{M}_\mu^1(k'\vec{r}\,')ds$$

$$J' = \frac{k^2}{\pi} \int_S \hat{n}.\vec{M}_\nu^3(k\vec{r}\,') \times \vec{N}_\mu^1(k'\vec{r}\,')ds$$

$$K' = \frac{k^2}{\pi} \int_S \hat{n}.\vec{N}_\nu^3(k\vec{r}\,') \times \vec{M}_\mu^1(k'\vec{r}\,')ds$$

$$L' = \frac{k^2}{\pi} \int_S \hat{n}.\vec{N}_\nu^3(k\vec{r}\,') \times \vec{N}_\mu^1(k'\vec{r}\,')ds$$

The far field value of the scattered field is: $E_s = \vec{F}(\theta_S, \phi_S/\phi_i, \theta_i) \exp(jkr)/r$ when kr goes to infinity :

$$\vec{F}(\theta_S, \phi_S/\theta_i, \phi_i) = \vec{F}(o, i) = \sum_{\mu=1}^{N} p_\mu c_\mu + j\, q_\mu b_\mu(\theta, \phi) \tag{2.33}$$

(θ_i, ϕ_i) define the direction of the incident field (θ_s, ϕ_s) define the direction of the scattered field in which one is interested. $f(\hat{o}, \hat{i})$ is the far field vector amplitude.

Barksdale [4] and Barber [13] give an exhaustive study of the problem. They present the specialization of the EBCM to oblate spheroidal particles. Besides, Barksdale wrote a program to compute the forward scattering coefficient of an oblate spheroidal raindrop using EBCM that we modify to obtain scattering amplitude for all direction. (See program SCAMP in Appendix A). The geometry is described in Figure 10. Two incident polarizations are considered:

Case I: $\vec{E}_i(\vec{r}) = \vec{E}_1(\vec{r}) = (\hat{x}\cos\alpha - \hat{z}\sin\alpha)e^{-jk(x\sin\alpha + z\cos\alpha)}$ (2.34)

Case II: $\vec{E}_i(\vec{r}) = \vec{E}_2(\vec{r}) = \hat{y}\, e^{-jk(x\sin\alpha z\cos\alpha)}$

We use the program SCAMP to calculate the phase and amplitude of the scattering coefficients of an oblate raindrop of radius 3.5 mm and an incidence angle of 90 degrees. The results are in good agreement with those of Morgan [12], see Figures 11-18. Our program will be extensively used to implement the vector radiative transfer equation (VRTE).

2.2 The Problem

A global geometry of the problem is presented in -- Figure id 'AB20' unknown --page no.. The geosynchronous satellites S_A and S_B are 2° apart and the main lobes of the antennas A_A and A_B are directed to S_A and S_B, respectively. In the absence of rain the interference (downlink only) from the system A into B consists of the side lobe to side lobe direct interference. We do not consider the specular reflection and multipath signals. In the presence of rain at the intersection of two side lobe beams of the transmitting antenna of S_A and the receiving antenna A_B, the downlink field of the system A is scattered into the antenna A_B. This intersection is called the common volume Vc. The main problem in this thesis is to compute the interference created. For this we make the following assumptions:

- Considering the range involved (about 36000 km) it is reasonable to assume that the rain is illuminated uniformally by a plane wave $\vec{E}_i$. In addition the satellite is supposed to

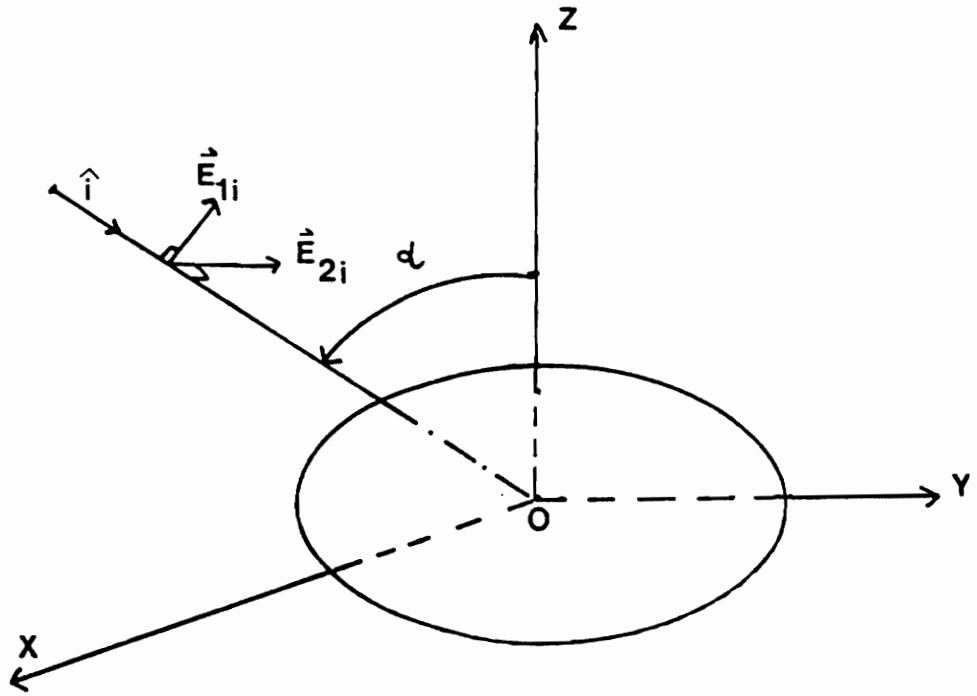

Figure 10. Polarizations of the incident field.

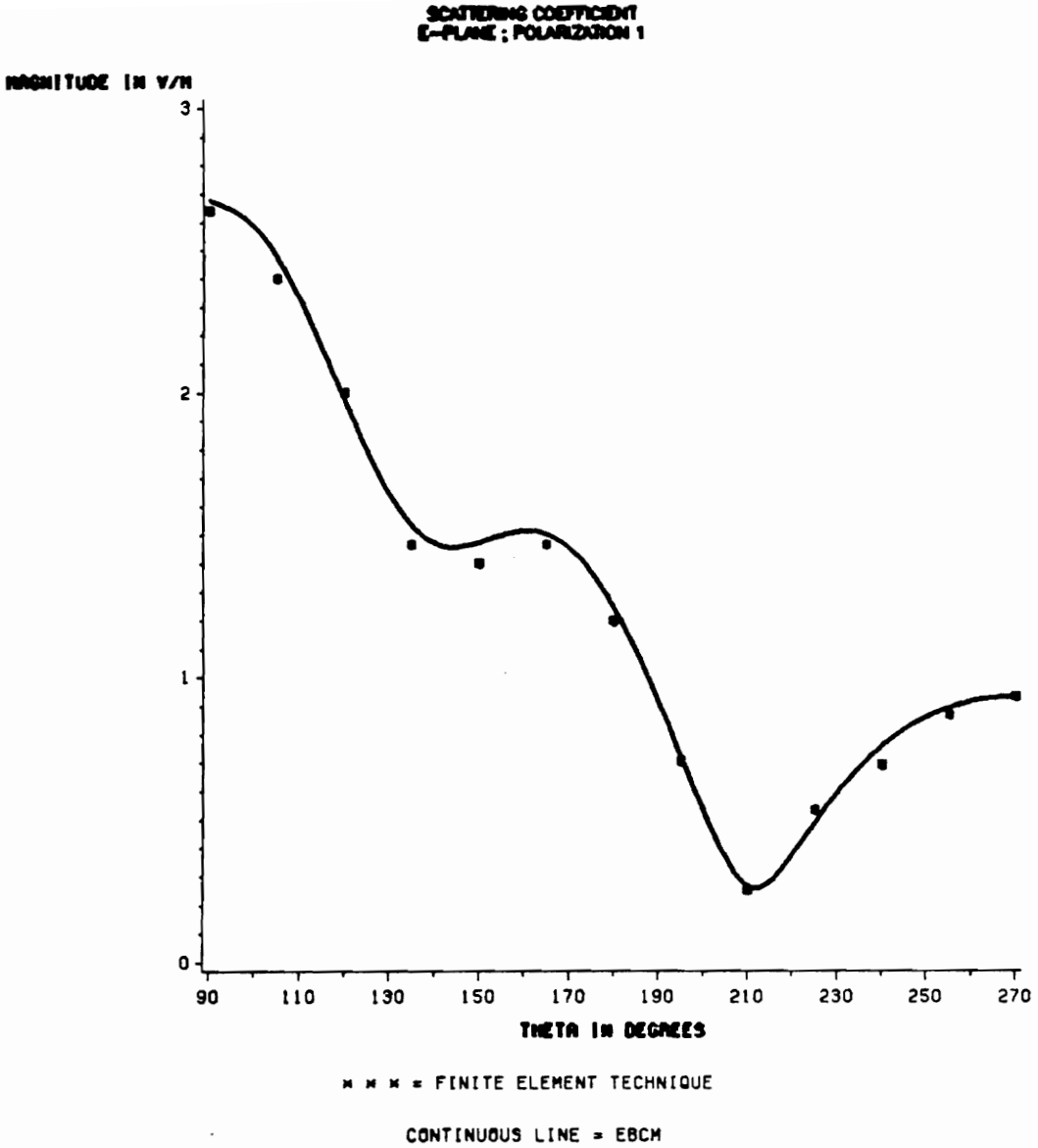

Figure 11. Scattering coefficient of an oblate spheroid of radius 3.5mm; the incident angle is 90 degree.

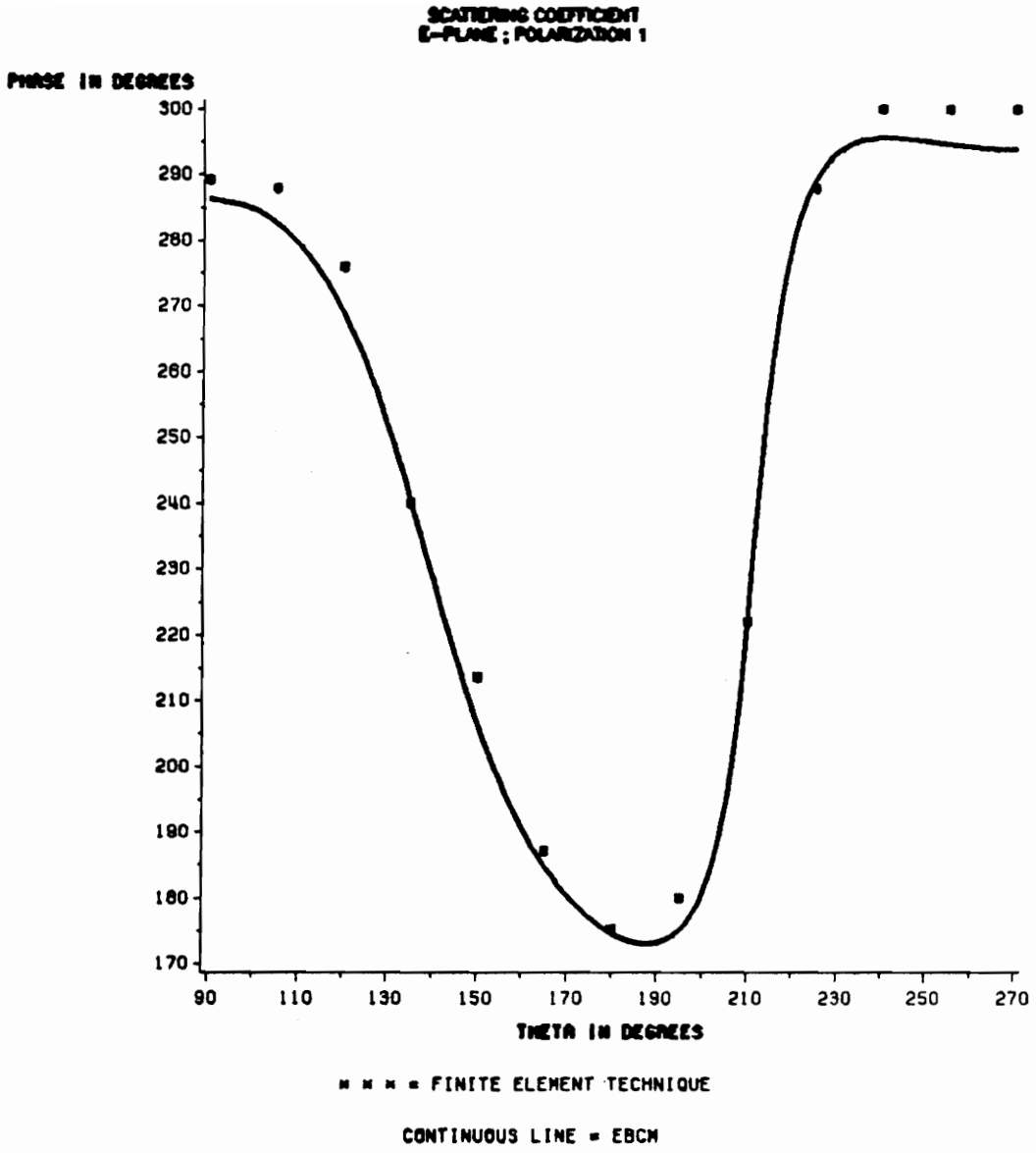

Figure 12. Scattering coefficient of an oblate spheroid of radius 3.5mm; the incident angle is 90 degree.

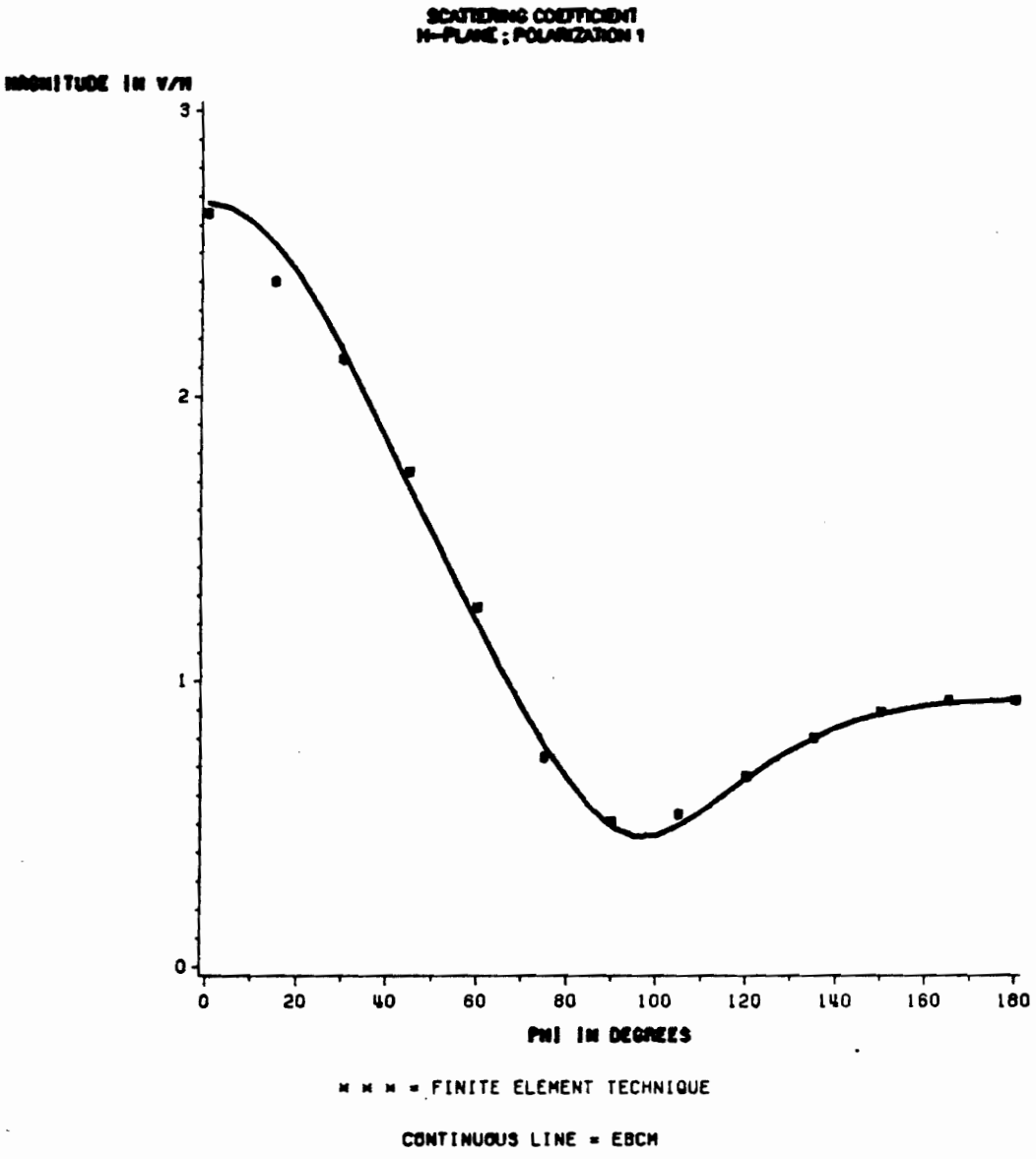

Figure 13. Scattering coefficient of an oblate spheroid of radius 3.5mm; the incident angle is 90 degree.

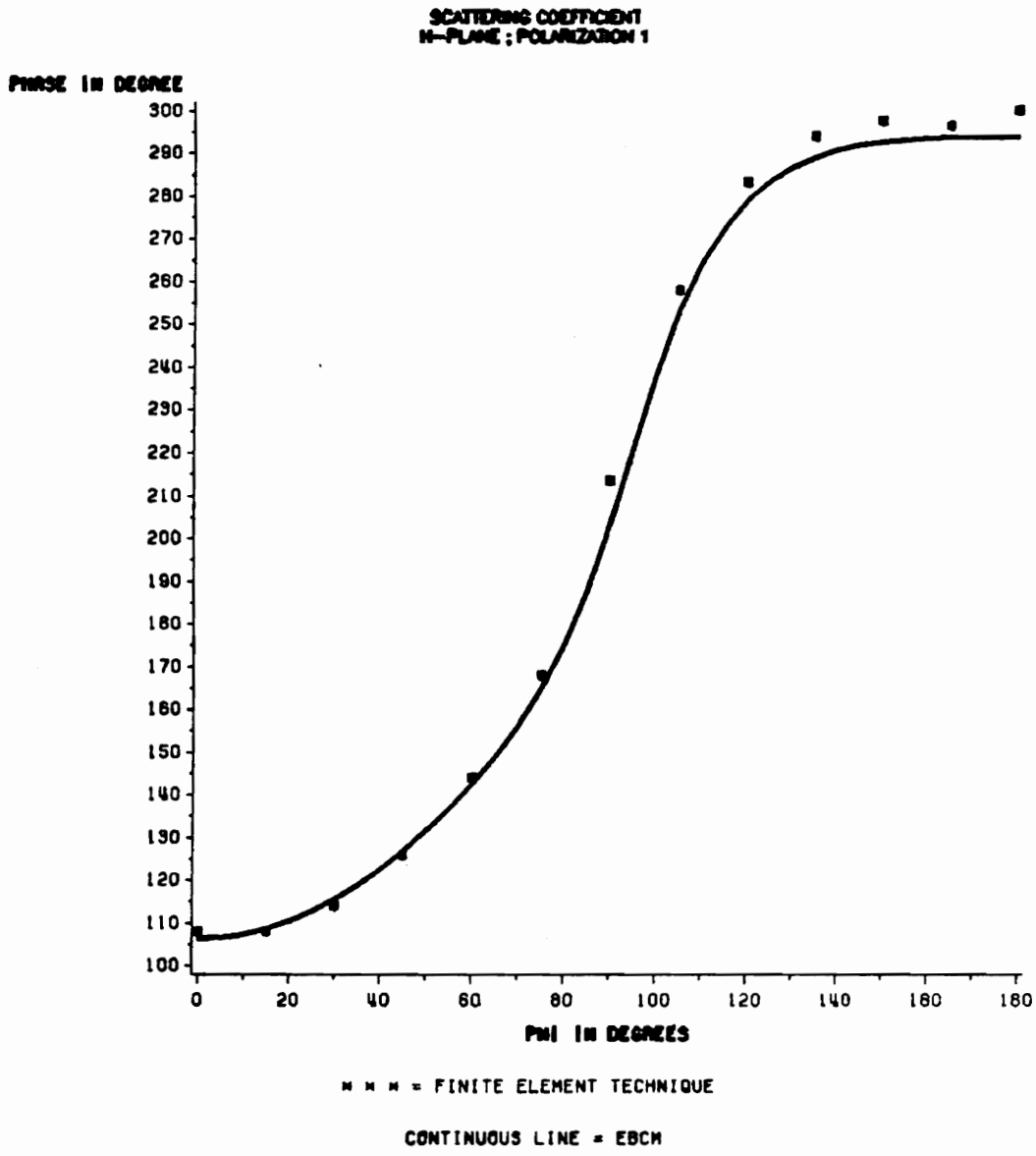

Figure 14. Scattering coefficient of an oblate spheroid of radius 3.5mm; the incident angle is 90 degree.

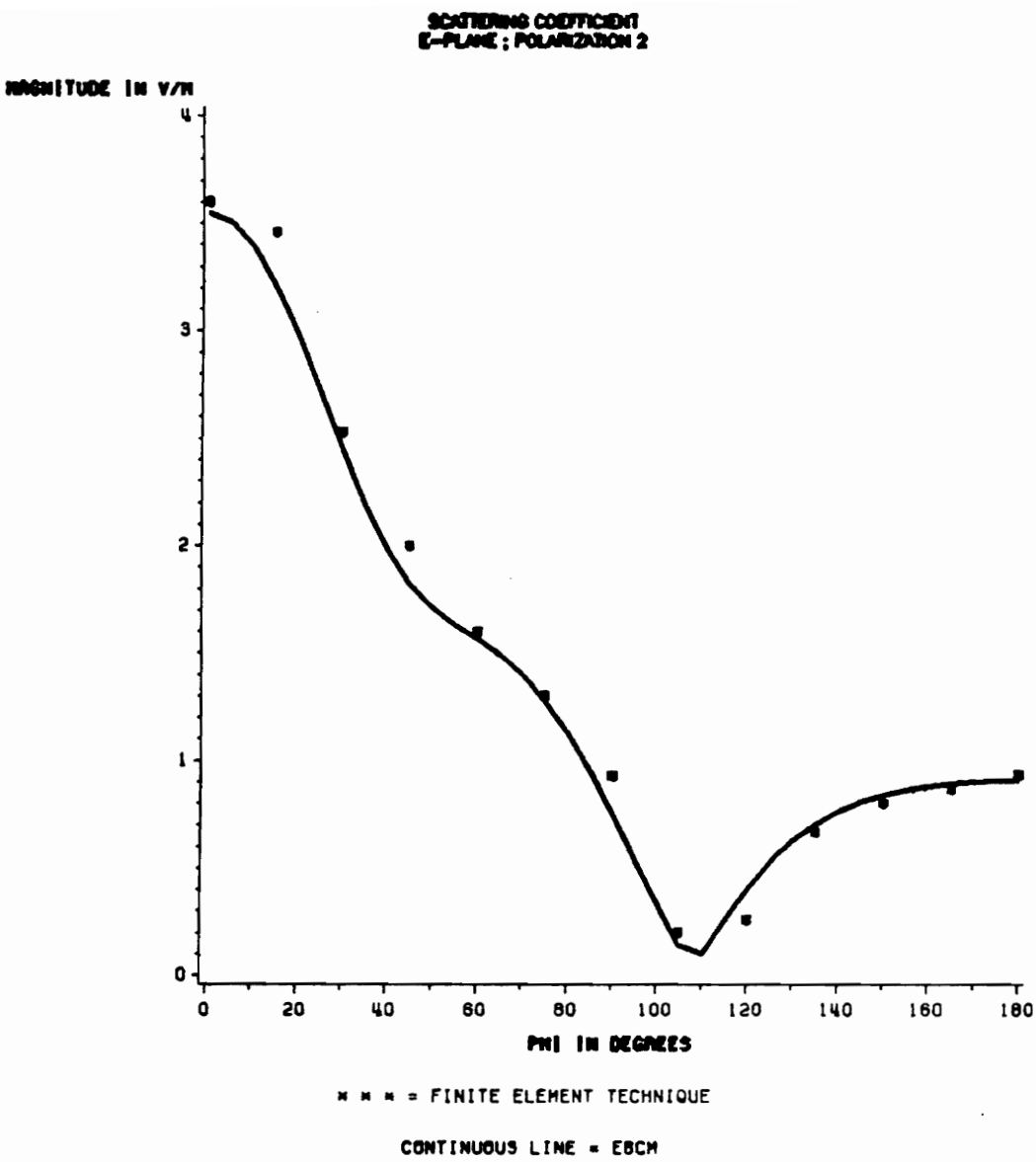

Figure 15. Scattering coefficient of an oblate spheroid of radius 3.5mm; the incident angle is 90 degree.

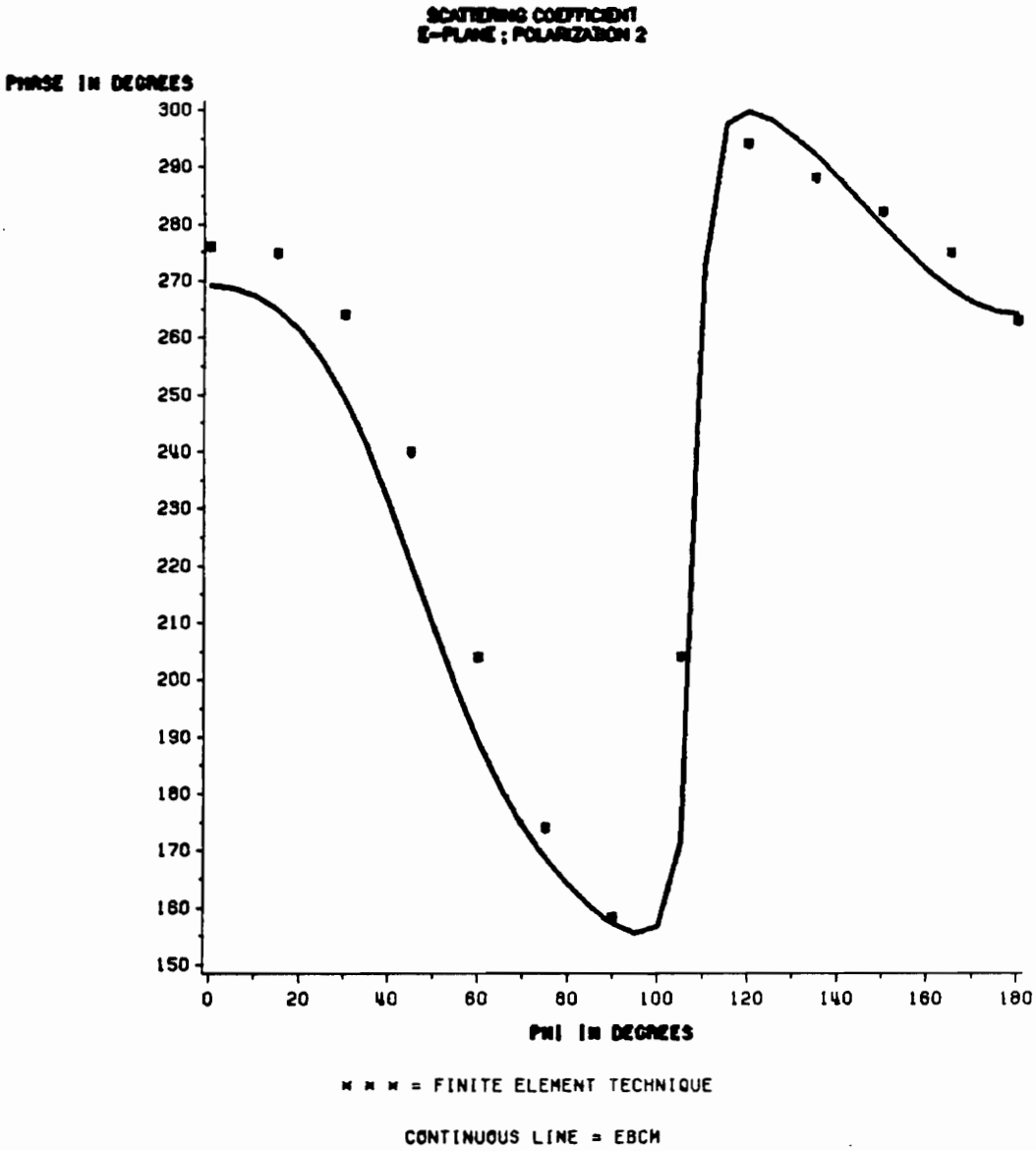

Figure 16. Scattering coefficient of an oblate spheroid of radius 3.5mm; the incident angle is 90 degree.

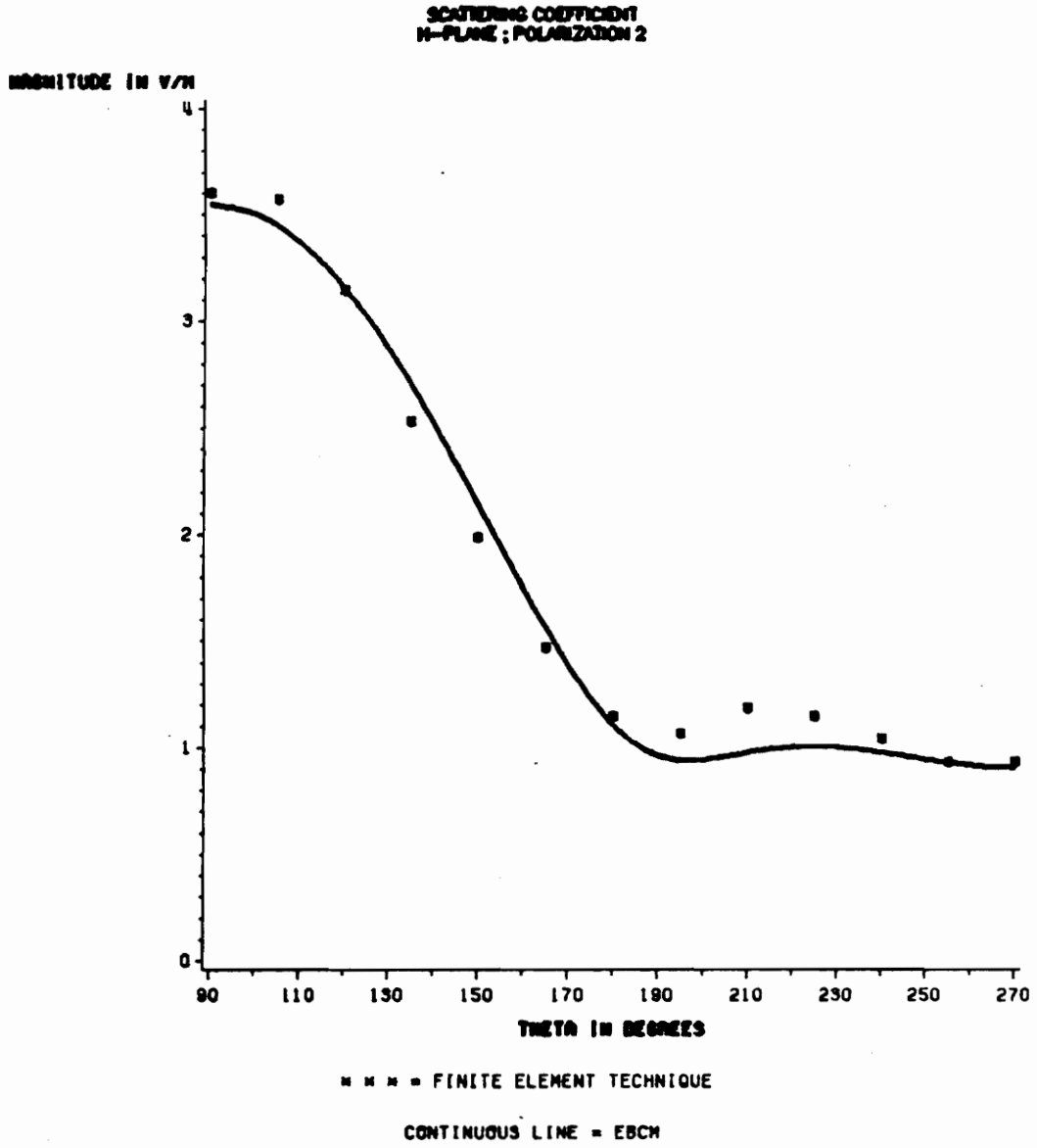

Figure 17. **Scattering coefficient of an oblate spheroid of radius 3.5mm; the incident angle is 90 degree.**

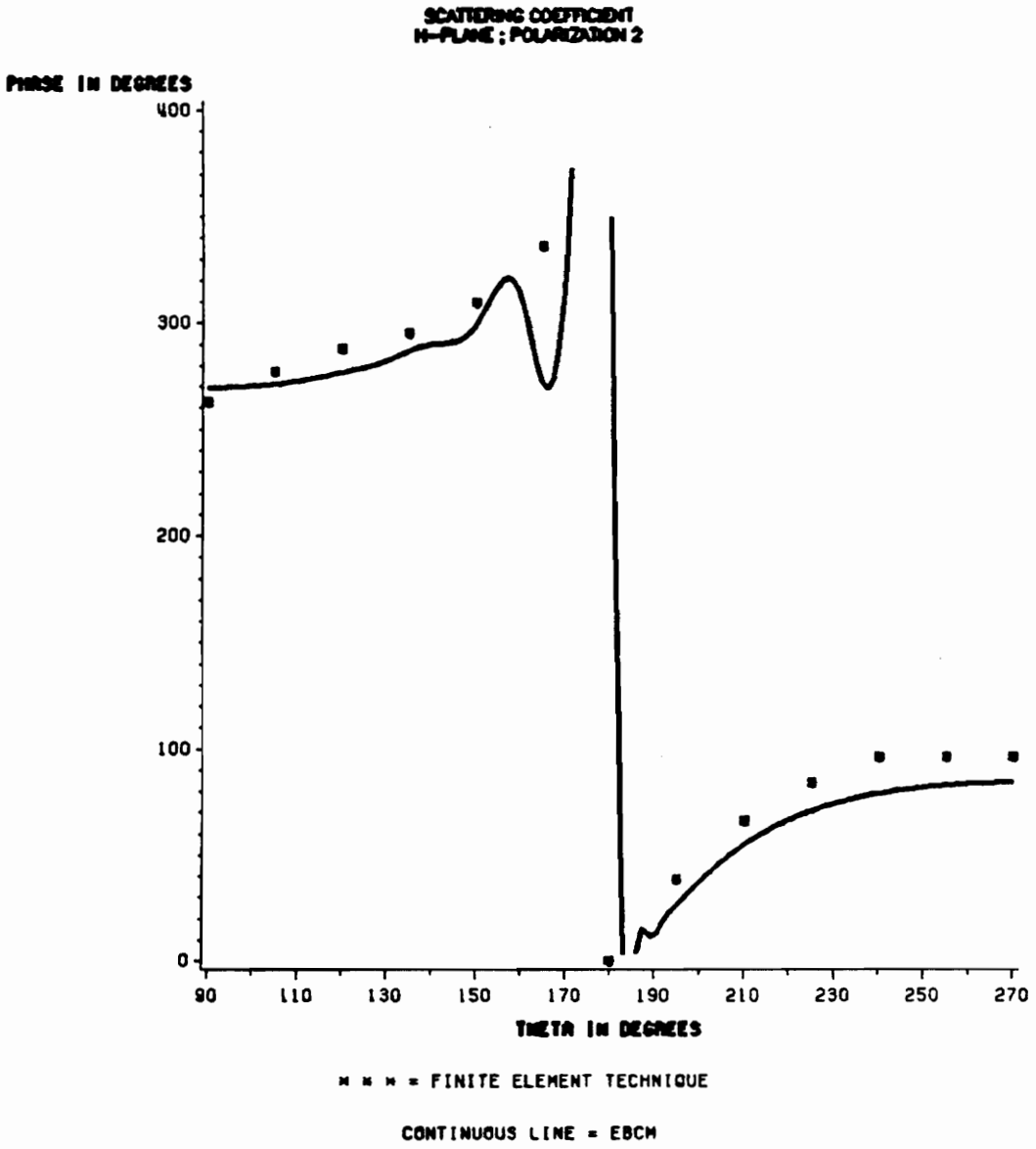

Figure 18. Scattering coefficient of an oblate spheroid of radius 3.5mm; the incident angle is 90 degree.

transmit a linearly polarized wave. The common volume is therefore reduced to the intersection of the illuminated rain and the beam of the receiving antenna.

- The receiving system is assumed to be a VSAT. The diameter of the aperture of such an antenna is usually smaller than 1 m. The far field for a frequency ranging from 10 to 30 GHz therefore starts at around 100 m. So we can assume that the rain is in the far field of the receiving antenna.

- The rain is assumed to have a uniform rate and a MP drop size distribution; the rain drops are uncanted oblate spheroidal. In addition each rain drop is supposed to be in the the far field of the others .

- Three approaches will be used to solve the side scattering problem; the first two use the bistatic radar equation (BRE) and Chu 's technique with a first order multiple scattering assumption to compute the average power scattered by the rain, while the third uses the vector radiative transfer equation (VRTE) taking the multiple scattering process into account to evaluate the scattered incoherent intensity.

Before applying these methods the main experimental and theoretical contributions of importance to this thesis are reviewed in the following chapter.

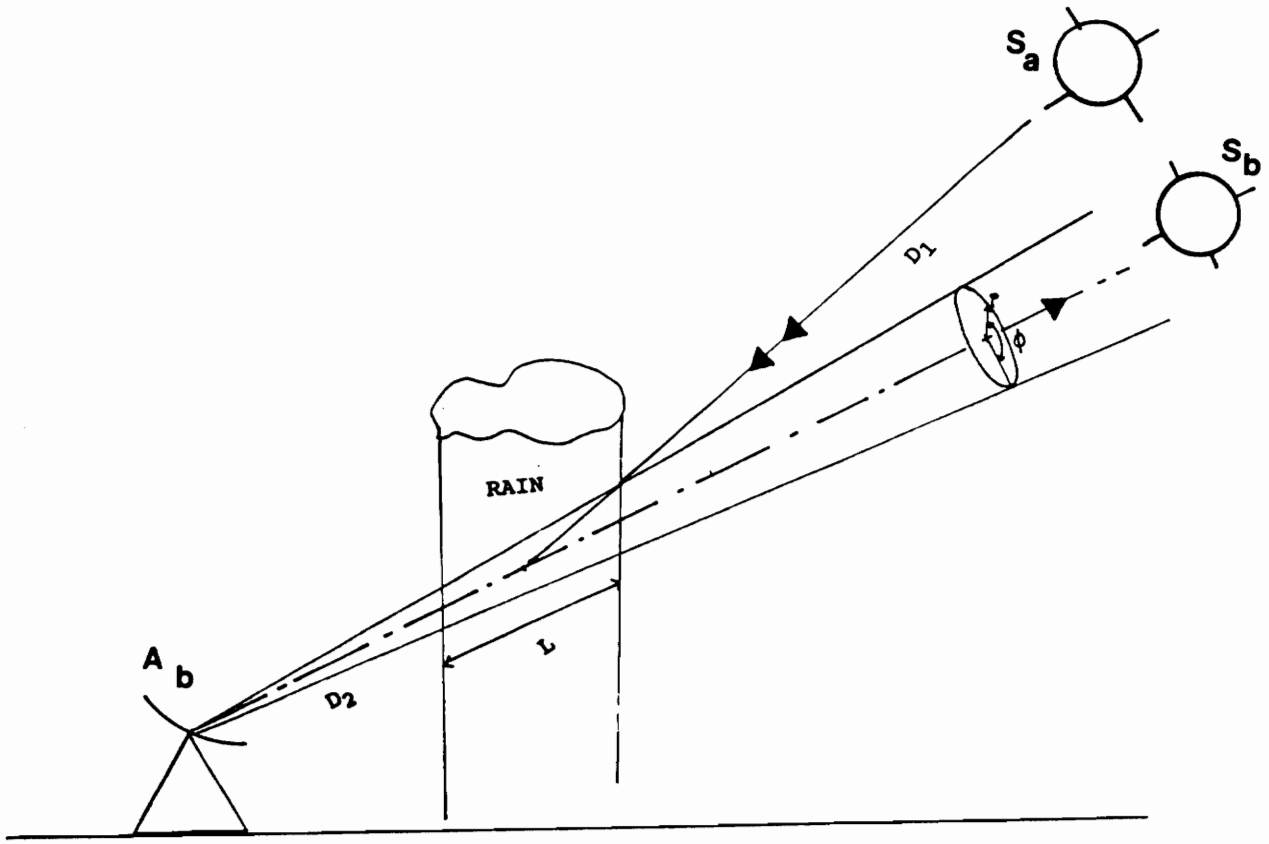

Figure 19. Geometry of the rain side scatter problem on an earth-space link

3.0 Literature Survey

The object of this chapter is to review the main experimental and theoretical contributions related to the rain scattering interference problem. After summarizing the early experimental work we present the bistatic radar equation and its application to non-attenuating and attenuating frequencies for terrestrial path rain scatter interference, and finally we investigate the influence of the multiple scattering.

The first observations of rain scattering interference were made in the late nineteen fifties and early nineteen sixties. In 1960 Doherty and Stone [22] reported a measurement of the power scattered by rain at 2.72 GHz. As in most of the experiments conducted so far, the coupling between the main beam of a ground based transmitter and a terrestrial receiver was measured. The scattering angles were 3° and 18° and the rain was detected using a weather radar. The results showed a scattered power which could exceed the normal tropospheric scattered power by 15 dB and were in good agreement with the theoretical predictions based on the simple formula :

$$P_r = P_t f \theta_R V_c \tag{3.1}$$

where :

P_i is the incident power

P_r is the scattered power

V_c is the common volume

θ_R is the solid angle subtended by the receiving beam

$f = 4.610^{-15} R^{1.6} \lambda^{-4}$ is the scattering coefficient per unit volume

(Isotropic scattering is assumed together with a LP distribution)

λ is the wavelength and R the rain rate

Similarly, the experiment performed by Hogg, Semplak and Gray in 1963 [23] measured the rain scatter interference between a terrestrial transmitter and a horn reflector antenna pointed to the zenith. The coupling was, therefore, between the main lobe of the transmitter and a far side lobe of the receiver. The measured scattered power which was expressed in degrees Kelvin could be 5 to 6 times higher than the thermal noise for high rain rate. In 1970 Hogg and Gusler [24] published theoretical calculations of the coupling due to rain between an earth station looking at a geostationary satellite and a terrestrial radio relay system. They assumed that the receiving antenna has a gaussian illumination and is electrically large so it has low side lobes, that the transmitting antenna in the first approach is radiating isotropically and that in the second approach its pattern is directive (the two cases have consistent results), and finally that the rain drops are spherical and scatter isotropically with a scattering coefficient which follows an empirical formula similar to that of (3.1). The computations were made for various geometrical configurations. The rain rate ranged from 0 to 400 mm/h, the frequencies from 4 to 30 GHz and the spacing between the antennas from 5 to 200 km. The ratio of the received power to the transmitted power representing the the coupling between the two antennas was plotted versus the rain rate for various frequencies and spacings. These plots showed that for frequencies below 10 GHz the power ratio increases with rain rate, confirming

the absence of attenuation ; but for higher frequencies the curves reach a maximum and then decrease. This maximum is reached for lower rain rates when the frequency is increased. This occurs because higher frequencies produce stronger attenuation. Besides, the coupling is higher for smaller spacing between the antennas. The maximum value of the coupling was found to be -140 dB. Practically, this level is significant because the power scattered by the rain can be higher than the thermal noise at the earth station receiver. The same year Setzer [25] examined the case of anisotropic scattering by spherical drops using both Rayleigh and Mie theories together with a LP distribution and compared the results to the isotropic scattering case developed by Gusler and Hogg. He found that the three studies agreed within 3 dB and claimed that his uncertainty was negligible for coupling on the order of -140 dB.

The above work showed the necessity to take the rain scattering interference into account when doing link budget calculation for both satellite and terrestrial systems, and subsequently to model theoretically this type of interference .

3.1 The Bistatic Radar Equation (BRE)

The BRE has been widely used to compute the power scattered by the rain for terrestrial paths [25]-[30]. It use has been recommended by Study Group 5 of the CCIR [31] to predict bistatic link measurements, compute the intersystem interference and and finally determine the coordination distance. A general form of the BRE is [32]:

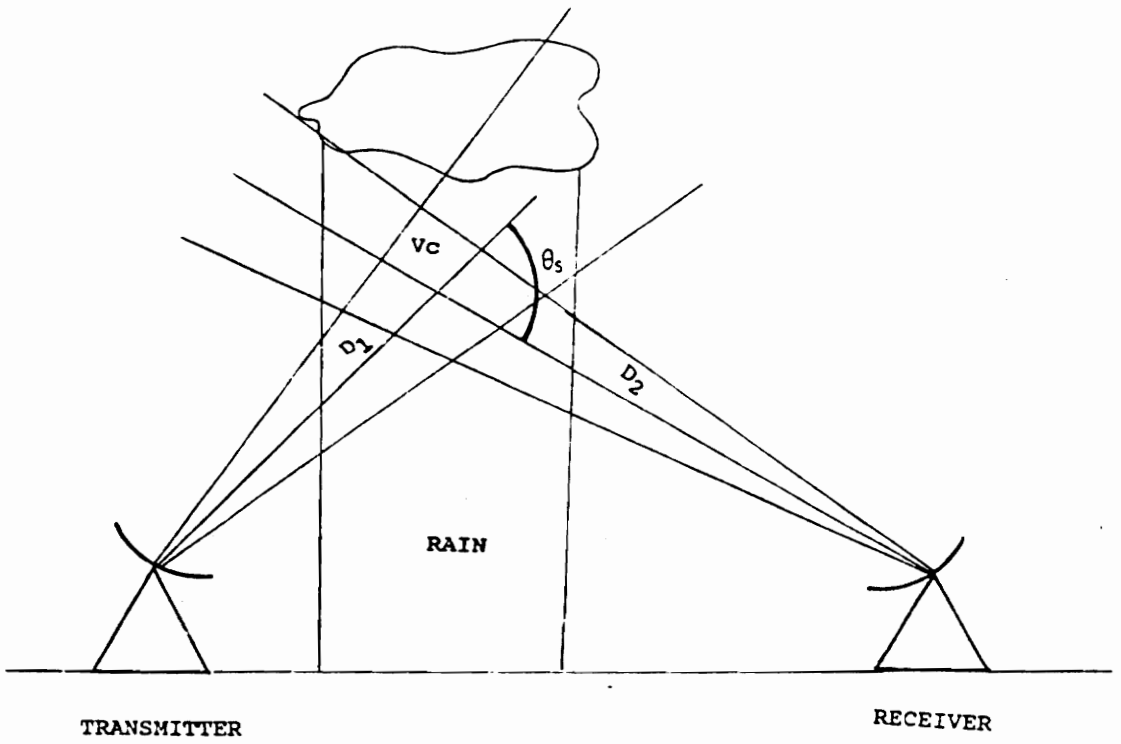

Figure 20. Rain scatter interference geometry for terrestrial paths

$$P_r = P_t \int_0^{\bar{a}_{max}} d\bar{a} \int_{V_c} dv \frac{\gamma(D_1)\gamma(D_2)A(\hat{o})G_t(\hat{i})\sigma_{bi}(\hat{i}, \hat{o}, \bar{a})n(\bar{a})}{(4\pi)^2 D_1^2 D_2^2} \tag{3.2}$$

with :

P_r = received interference power

P_t = transmitted power

$\bar{a}$ = equivolume radius of the particle

$\bar{a}_{max}$ = maximum value of $\bar{a}$

V_c = common volume

dv = volume element in the common volume

D_1 = distance from the transmitter to dv

D_2 = distance from the receiver to dv

$\gamma_t(D_1)$ = attenuation along the path D_1

$\gamma_t(D_2)$ = attenuation along the path D_2

$\hat{o}$ = unit vector along D_2

$\hat{i}$ = unit vector along D_1

$G_t(\hat{i})$ = gain of the transmitter antenna in the direction $\hat{i}$

$A(\hat{o})$ = effective aperture of the receiving antenna

(a perfect polarization match is assumed) in the direction $\hat{o}$

$\sigma_{bi}(\hat{i}, \hat{o}, \bar{a})$ = bistatic scattering cross section of drop of equivolume radius $\bar{a}$;

the incident direction is $\hat{i}$ and the scattering direction is $\hat{o}$

$n(\bar{a})$ = drop size distribution

This expression assumes a first order multiple scattering process (FOMS) (Figure 21 on page 52); i.e. the incident wave is attenuated by the rain before reaching the volume element dv, then it is scattered by dv, and finally attenuated again on the path to the receiver .This assumption does not take into account all the multiple scattering but it gives very good results for frequencies where the multiple scattering is neglectable .

Because the integration in the BRE can be complex, it is common to use simplifications. The first one [25],[30],[32] arises from the assumptions that the extent of the common volume is small compared to D_1 and D_2 and that the antenna beams are narrow and their patterns are modeled by gaussian functions.The BRE becomes:

$$P_r = P_t \frac{\gamma_t \gamma_r G_t(\hat{i}) G_r(\hat{o}) V_c}{(4\pi)^3 D_1^2 D_2^2} \bar{\sigma}_{bi}(\hat{i}, \hat{o}) \tag{3.3}$$

where :

$$\bar{\sigma}(\hat{i}, \hat{o}) = \int_0^{\bar{a}_{max}} n(\bar{a}) \sigma_{bi}(\hat{i}, \hat{o}, \bar{a}) d\bar{a} \tag{3.4}$$

is the bistatic cross section per unit volume; it is usually expressed in terms of the radar reflectivity factor Z [25]-[32]. For Rayleigh scattering [30]:

$$\bar{\sigma}_{bi} = \frac{\pi^5}{\lambda^4} \left| \frac{\varepsilon - 1}{\varepsilon + 2} \right| Z \quad m^2/m^3 \tag{3.5}$$

where

$$Z = \sum d^6 = \sum \frac{\bar{a}^{\,6}}{64} \qquad (3.6)$$

The summation is over all the drop diameters d (or radii $\bar{a}$) of the drops within a unit volume. Empirical formulas for the radar reflectivity depend on the type of drop size distribution and on the type of scattering considered. For Rayleigh scattering and a LP distribution $Z = 400R^{1.4}$ while for a MP distribution $Z = 200R^{1.6}$. At frequencies where Rayleigh scattering does not hold, the bistatic reflectivity $Z_b = \bar{\sigma}_{bi}$ is used instead of the radar reflectivity factor.

Equation (3.3) may be rewritten as in Awaka 's paper [28] :

$$\frac{P_r}{P_t} = C + 10 \log Z - A \quad dB \qquad (3.7)$$

where C is a constant factor which is system dependent (geometry, gains , etc...) and independent of the rain rate, A is the attenuation due to the rain along the path and Z is the reflectivity factor . Both A and Z are linked to the rain parameters. According to (3.7) the prediction of the coupling due to rain is equivalent to the prediction of Z and A. Legitimately most of the researchers tried to relate the statistics of the rain to those of A and Z [25]-[29],[32]. For frequencies below 10 GHz the attenuating effect of rain may be neglected so the problem is reduced to the prediction of Z (see Crane [25], Hubbard [26], Sagakami [27]). More recent work deals with attenuating frequencies. Awaka [28] in 1984 described a prediction method for the power scattered by rain based on the assumption that both the rain rate and the rain attenuation follow a lognormal distribution . The comparison with experimental results showed very good agreement at 14.3 GHz . But at 34.86 GHz and for weak rain rate predicted and measured values diverged. Crane [25] with the two component model offered a new possibility of predicting statistics of bistatic scattering by rain. This was

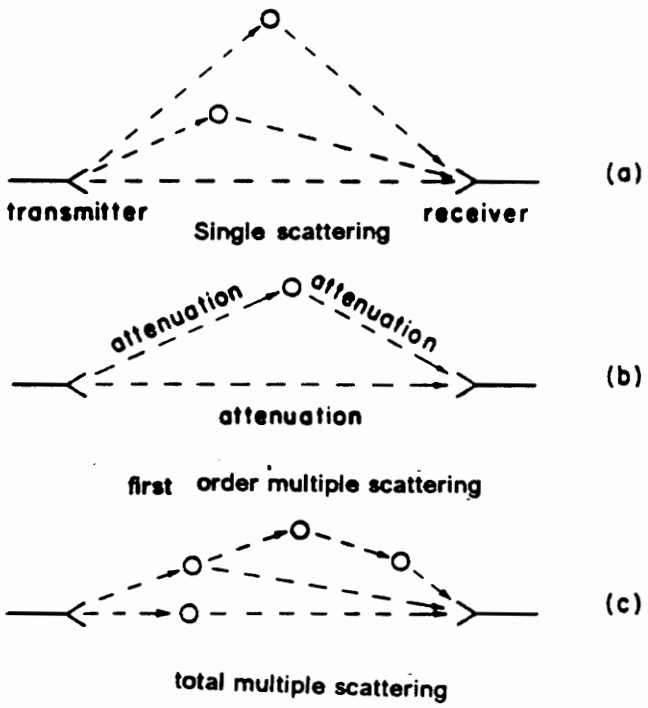

Figure 21. Multiple scattering processes (from reference [15])

developed by H.C.Shieh [32] in 1986 and compared to both Awaka's lognormal model and measurements made in Japan. The results were consistent. Even though the simplified BRE gives an accurate model for rain scatter interference between ground based receivers and transmitters it has some limitations as far as space-earth paths are concerned. The main restrictions arise because the dimension of the common volume are assumed to be small compared to D_2 . In fact, the common volume as assumed in Chapter 2 is the intersection between the rain and the beam of the receiving antenna because the rain is uniformly illuminated by the wave transmitted by the satellite .

3.2 Rain Scatter Interference on Earth-Space Paths

The aforementioned works treat the interference induced by a terrestrial transmitter into a ground based receiver, thus involving a large scattering angle. Studies by Chu [33] and Arnold et al.[34] are noteworthy because they address the issue of calculating and measuring the power scattered by rain from the down link of a satellite system into the ES receiving antenna of an adjacent satellite system. The scattering angle in this case is small (a few degrees) . Chu [33] (1977) presents a theoretical computation of the rain scatter coupling in the geometry described above under the assumption that the receiving antenna has a gaussian beam, that there is single scattering, and that the rain drops scatter isotropically. Also, he assumes that the rain is uniform and is located in the vicinity of the ES. The wanted power received by the ground station is :

$$P_r = P_s A_g e^{-\alpha L} \tag{3.8}$$

where

P_s is the power density at the ground station in clear weather

A_g effective receiving aperture of the ground station

αL is the rain attenuation

The interfering power is (see the geometry in Figure 19 on page 43 page= no.):

$$P_i = P_s e^{-\alpha L} \frac{\lambda^2}{4\pi} \left[\int \sigma(\bar{a}) n(\bar{a}) d\bar{a} \right] \int_0^L \int_0^{2\pi} \int_0^{\infty} \frac{2}{\pi \omega^2} e^{-\frac{2\rho^2}{\omega^2}} \rho d\rho d\phi dz \tag{3.9}$$

where :

L is the path length in the rain

$n(\bar{a})d\bar{a}$ is the drop size distribution

$\sigma(\bar{a})$ is the scattering cross section of a drop

$\omega^2 = \omega_0^2[1 + (\frac{\lambda z}{\omega_0})^2]$

ω_0 is the waist of the gaussian beam;

it correspond to the value of ω when $z = 0$.

After integration, Chu obtains a simple expression for the ratio between the interfering power and the wanted power :

$$\frac{P_i}{P_r} = \frac{\beta \alpha L}{G} = \frac{\beta A}{4.34G} \tag{3.10}$$

where

$\beta = \frac{\text{scattering cross section}}{\text{extinction cross section}}$ is the albedo

$G =$ gain of the ES antenna

$A =$ attenuation in dB

This formula shows that the ratio $\frac{P_i}{P_r}$ increases with the attenuation and the albedo β . The important factor given the range of A (10 to 20 dB) and β(about 0.1) is the gain G, which can reach 60 dB. The gaussian beam assumption somewhat restricts the range of application of the formula . Further limitations arise because the formula leaves out any dependance on the angular dimensions of the beam and thus of the common volume. Equation (3.10) was verified by Li [35] in an experiment involving the measurement of side scattering by rain with a scattering angle of 3.25 degrees at 11 GHz on a horizontal terrestrial link.

A COMSTAR propagation experiment reported by Cox, Arnold and Hoffman in 1982 [34] attempted to measure the rain scatter interference for two satellites with an orbital spacing of 0.85 degree at 19 and 28 GHz. Our search of the literature indicates that this experiment is unique. The COMSTAR satellite was located at a longitude of 95° W on the geostationary orbit and it had two experimental beacons (19 and 28 GHz) pointed toward the earth . The earth station antenna was a 7 meter Cassegrain reflector and had low side lobes (less than -40 dB at 1° off axis) and high gain for both frequencies. A displaced feed created an offset beam at 0.85° from the main beam axis. The main beam corresponded to sidelobe peaks of -46 dB at 28 GHz and -41dB at 19 GHz of the offset beam; it was directed at the satellite so that the offset beam would receive the scattered power during a rain event and at the same time would receive the direct signal on the -46 dB and -41 dB sidelobes. The power ratio $X = \frac{\text{normalized signal off path}}{\text{normalized signal on path}}$ was measured. The signal levels were normalized to the corresponding value in clear weather. The values of X to which 99%, 90% and 50% of the data are inferior were plotted versus the attenuation. At 19 GHz the spread of the data were due to noise in the receiver and to the random gain variation of $\mp 1dB$ in the off-path-beam

receiver. For $0 < A < 15$ dB (A is the attenuation) X, is was found to be -41 dB which corresponded to the side lobe level. For $A > 15$ dB the values of X represented the receiver noise. Similar results were found at 28 GHz except that the plot started at a lower level (side lobe level of -46 dB) and reached the receiver noise limit for lower rain rates. The antenna beam pointing errors were more important in the spreading of the data. In both cases the rain scatter coupling could not be measured because of the limitations imposed by the side lobe level of the antenna at low rain rate (low attenuation) and the receiver noise at higher rain rate. The rain scattered power was below the threshold of the experiment; Cox et al. verified this by using Chu's formula (3.8). We have to note though that the 7 meter antenna is very directive compared to a VSAT antenna which would intercept much more scattered power (especially incoherent power).

3.3 *Multiple Scattering*

The models described in the first part of this chapter do not take multiple scattering fully into account . It has been shown [40], however that for frequencies above 10 GHz, the effect of multiple scattering could be noticeable because the scattering cross section of a raindrop is no longer much smaller than its absorption cross section. It is therefore important to study how important multiple scattering would be for the side scattering problem. Two methods have been developed to solve the multiple scattering problem: the multiple scattering or classical theory and the radiative transfer equation (RTE) .The first is rigorously derived from Maxwell's equations and was initiated by Twersky, Foldy, Lax and Dyson (see [15] for references). It leads to an integral equation for the average total intensity and the coherent field. These integral equations can be solved using the method of stationary phase, giving

good results in a small angle approximation. The RTE, on the contrary, is a heuristic theory which can be linked under some assumptions (weak scattering) [15] [36] to the classical theory. The RTE deals with the transfer of energy through a random medium and is expressed either in terms of the specific intensity or in terms of the Stokes vector. More details about the RTE will be given in the next section. The study of the multiple scattering in rain effects has been conducted mainly for line-of-sight propagation and backscattering. Specifically the effect on attenuation and depolarization was characterized (see [37]-[43], [45]-[49] for references). As far as the attenuation is concerned, the reviewed studies evaluate the importance of different orders of scattering (single, FOMS, etc.) on the coherent field. The results are that the use of the single scattering assumption gives good results for frequencies below 10 GHz while the FOMS suffices for frequencies between 10 and 20 GHz, and finally that for higher frequencies a total multiple scattering assumption is necessary. The incoherent intensity is found to be weak compared to the coherent one; its influence increases with the beamwidth of the receiving antenna (small aperture antenna such as VSATs are more sensitive to incoherent interference while large size antennas receive less incoherent power). The incoherent intensity effects on depolarization were also studied [39]-[41], [43], [44]. As a matter of fact, the depolarization in the rain is the result of both the depolarization of the coherent field due to differential attenuation and the generation of an incoherent field by multiple scattering.

Very little has been done concerning the significance of multiple scattering in the side scattering problem. Most of the studies related to that issue assume that the the coherent intensity propagates in a small cone centered on the forward direction and that the side scattering is mostly incoherent,especially for the large scattering angle which is the case for terrestrial path scattering. This assumption arises from the use of the stationary phase method in analyzing the multiple scattering processes [15], [44]. Ishimaru [46]-[48] presents results of incoherent scattered intensity by a plane parallel medium filled with spherical raindrops. He

also give a method for media with spheroidal particles which will be used later in this thesis. Shieh [32] on the other side presents as a part of his study of earth to earth rain scatter interference an evaluation of the multiple scattering effects by solving the RTE for a plane parallel and for a cylindrical medium using the finite element technique. His original method allows one to asses the importance of each order of scattering and to handle inhomogeneities within the scattering volume. He compares the results obtained for the plane parallel medium with that obtained with a single scattering assumption. The scattering angle is 98.6° the frequency is 14.3 GHz, and the rain rates 0.5 and 9.5 mm/h. Shieh finds that the higher orders of scattering are negligible. This may not be the case for higher frequencies and higher rain rates, and we feel that the study of the total multiple scattering is important to the problem of rain scattering interference.

4.0 Predictions

In the previous section we showed that it was important to take all the orders of multiple scattering into account in calculating the power scattered by the rain, the use of the radiative transfer equation is a good method for that. In this chapter we first formulate the vector radiative transfer equation then we solve this equation for a parallel plane rain medium and we use the results to compute the rain side scatter interference for satellite link. The second part of this chapter presents the BRE and Chu's technique. Finally, the implications for commercial systems are studied.

4.1 Radiative Transfer

4.1.1 Basic Definitions

In the previous chapter we characterized single scattering; here, the microscopic problem of scattering in a random medium is addressed. After undergoing multiple scattering, an electromagnetic wave propagating in a random medium fluctuates both in phase and amplitude. These variations are due to the randomness of the location and size of particles (in our case raindrops) which are constantly in motion. Thus, after (Ishimaru [15]) the scattered field $\vec{u}(\vec{r}, t)$ is a random function of both location and time and is composed of two parts:

$$\vec{u}(\vec{r}, t) = <\vec{u}(r, t)> + \vec{u}_f(\vec{r}, t) \tag{4.1}$$

$<\quad>$ is an ensemble average on all the possible spatial configurations of the scatterer and $<\vec{u}(r, t)>$ is the average or coherent field. On the other hand, $\vec{u}_f(\vec{r}, t)$ is the fluctuating or incoherent field; it satisfies:

$$<\vec{u}_f(\vec{r}, t)> = \vec{0}$$

Similar definitions can be stated for the intensities: The average intensity $<I>$ is:

$$\begin{aligned} <I(\vec{r}, t)> &= <|\vec{u}(\vec{r}, t)|^2> \\ <I(\vec{r}, t)> &= |<\vec{u}(\vec{r}, t)>|^2 + <|\vec{u}_f(\vec{r}, t)|^2> \\ &= I_c + I_{inc} \end{aligned} \tag{4.2}$$

where $I_c = |<\vec{u}(r,t)>|^2$ is the coherent intensity and $I_{inc} = <|\vec{u}_f(\vec{r},t)|^2>$ is the incoherent intensity.

The total intensity is

$$I(\vec{r},t) = <I(\vec{r},t)> + I_f(\vec{r},t) \tag{4.3}$$

I_f is the fluctuating intensity and can be expressed as:

$$I_f = <\vec{u}(r,t)>\ ^*\vec{u}_f(r,t) + <\vec{u}(r,t)>\vec{u}_f\ ^*\ (r,t) \tag{4.4}$$

The coherent intensity propagates, according to Van de Hulst [14], in the forward direction. Most of the theories relative to the propagation of electromagnetic fields in random media deal with the average intensity $<I(\vec{r},t)>$ and its two constituents (I_c, I_{inc}) ; this is the case in the bistatic radar equation and the radiative transfer equation.

To describe the polarization state of the waves the modified Stokes parameters are defined (see [14] [15] [20] [21] for a detailed treatise) as:

$$[I] = \begin{bmatrix} I_1 \\ I_2 \\ U \\ V \end{bmatrix} = \begin{bmatrix} <\vec{E}_1\vec{E}_1> \\ <\vec{E}_2\vec{E}_2> \\ 2Re[<\vec{E}_1\vec{E}_2>] \\ 2Im[<\vec{E}_1\vec{E}_2>] \end{bmatrix} \tag{4.5}$$

where $\vec{E}_1$ and $\vec{E}_2$ represent an orthogonal decomposition of the wave; for example they may be the horizontal and vertical components of the wave. The Stokes parameters of two independent waves are additive; they describe completely or partially polarized waves. For this thesis it is necessary to express the single scattering in terms of the Stokes parameters. We use Van de Hulst's [14] classical linear relation between scattered and incident field:

$$\begin{bmatrix} E_{1s} \\ E_{2s} \end{bmatrix} = \begin{bmatrix} f_{11}(\hat{0},\hat{i}) & f_{12}(\hat{0},\hat{i}) \\ f_{21}(\hat{0},\hat{i}) & f_{22}(\hat{0},\hat{i}) \end{bmatrix} \begin{bmatrix} E_{1i} \\ E_{2i} \end{bmatrix} \frac{e^{-jkr}}{r} \tag{4.6}$$

the subscripts i and s stand for incident and scattered and 1 and 2 stand for two orthogonal polarizations of the field. $f_{ij}(\vec{o},\vec{i})$ are the scattering coefficients. They can be obtained directly from the single scattering amplitudes computed in the previous section. Using (4.6) and (4.5) yields:

$$[I]_s = \frac{1}{r^2}\bar{\sigma}[I]_i \tag{4.7}$$

with

$$\bar{\sigma} = \begin{bmatrix} |f_{11}|^2 & |f_{12}|^2 & Re(f_{11}f_{12}^*) & -Im(f_{11}f_{12}^*) \\ |f_{21}|^2 & |f_{22}|^2 & Re(f_{21}f_{22}^*) & -Im(f_{21}f_{22}^*) \\ 2Re(f_{11}f_{22}^*) & 2Re(f_{12}f_{22}^*) & Re(f_{11}f_{22}^* + f_{12}f_{21}^*) & -Im(f_{11}f_{22}^* - f_{12}f_{21}^*) \\ 2Im[f_{11}f_{21}^*] & 2Im(f_{11}f_{22}^*) & Re(f_{11}f_{22}^* + f_{12}f_{21}^*) & Re(f_{11}f_{22}^* - f_{12}f_{21}^*) \end{bmatrix} \tag{4.8}$$

4.1.2 Formulation of the Radiative Transfer Equation

The radiative transfer equation is a heuristic theory initiated by Shuster in 1903 and developed by Chandrasekhar [20]. It has been extensively used in optics, marine biology, photography and in the study of the propagation of radiant energy in the atmosphere of stars [20]. The RTE represents the transport of energy through a medium and is expressed in term of the specific intensities.

Let us consider a random medium with a particle density ρ and, inside the medium, a cylindrical element of volume dV of unit cross section and length ds at a position r receiving an incident specific intensity $I(r, \hat{s})$ from a direction $\hat{s}$. Let us study the variation dI of the specific intensity as the wave propagates through dV. Each particle in the volume absorbs and scatter a total intensity of $\sigma_t I(r, \hat{s})$ where σ_t is the extinction cross section. The corresponding change in intensity is :

$$dI(r, \hat{s}) = -\rho\sigma_t I(r, \hat{s})ds \tag{4.9}$$

The minus sign in the above equation indicates a decrease in the intensity. Furthermore the element of volume will receive the power coming from other directions $\hat{s}'$ and will also scatter and absorb it. It is in addition assumed that the medium is emitting a radiation characterized by the power radiation per unit volume and unit solid angle in the direction $\hat{s}$: $\varepsilon(r, \hat{s})$. (An example of this is the thermal radiation form a cloud.) The total variation of the specific intensity is then :

$$\frac{dI}{ds}(r, \hat{s}) = -\rho\sigma_t I(r, \hat{s}) + \frac{\rho\sigma_t}{4\pi}\int_{4\pi} p(\hat{s}, \hat{s}')I(r, \hat{s}')d\omega' + \varepsilon(r, \hat{s}) \tag{4.10}$$

where :

$d\omega'$ is an element of solid angle
$p(\hat{s}, \hat{s}')$ is the phase function as defined in equation (2.12)

Equation (4.10) is the radiative transfer equation for a scalar intensity. The intensity in the above equation can be decomposed into two terms. The first term, the reduced intensity, represents the part of the intensity which is reduced because of scattering and the second

term, the diffuse intensity, represents the part which is produced within the volume. The boundary conditions for I are defined by setting the diffuse intensity entering the medium to zero. The RTE can be generalized to a partially polarized wave by using the Stokes parameters $[I]$ as follows:

$$\frac{d[I]}{ds}(r, \hat{s}) = -[\Lambda][I(r, \hat{s})] + \rho \int_{4\pi} [S(\hat{s}, \hat{s}')][I(r, \hat{s}')]d\omega' + [\varepsilon(r, \hat{s})] \tag{4.11}$$

$[\Lambda]$ is the extinction matrix; as in the case of the scalar wave, the matrix product $[\Lambda][I]$ represents the decrease in the intensity propagating in the direction $\hat{s}$ due to absorption and scattering. Λ depends on the forward scattering coefficients f_{ij} of the raindrops, on the density ρ of the medium and on the wavelength λ and it can be written as:

$$[\Lambda(\hat{s})] = \lambda\rho \begin{bmatrix} -2Im(f_{11}) & 0 & -Im(f_{12}) & Re(f_{12}) \\ 0 & -2Im(f_{22}) & -Im(f_{21}) & -Re(f_{21}) \\ -2Im(f_{21}) & -2Im(f_{12}) & -Im(f_{11}+f_{22}) & -Re(f_{11}-f_{22}) \\ -2Re(f_{21}) & 2Re(f_{12}) & Re(f_{11}-f_{22}) & -Im(f_{11}+f_{22}) \end{bmatrix} \tag{4.12}$$

$[S(\hat{s}, \hat{s}')]$ is the Mueller matrix , and the product $[S][I]$ is the part of the power arriving from the direction $\hat{s}'$ which is scattered in the direction $\hat{s}$. The Mueller matrix is related to the matrix $\bar{\sigma}$ defined earlier in the following manner:

$$[S(\hat{s}, \hat{s}')] = \rho\bar{\sigma}(\hat{s}, \hat{s}') \tag{4.13.a}$$

or :

$$[S(\hat{s},\hat{s}')] = \rho \begin{bmatrix} |f_{11}|^2 & |f_{12}|^2 & Re(f_{11}f_{12}^*) & -Im(f_{11}f_{12}^*) \\ |f_{21}|^2 & |f_{22}|^2 & Re(f_{21}f_{22}^*) & -Im(f_{21}f_{22}^*) \\ 2Re(f_{11}f_{22}^*) & 2Re(f_{12}f_{22}^*) & Re(f_{11}f_{22}^* + f_{12}f_{21}^*) & -Im(f_{11}f_{22}^* - f_{12}f_{21}^*) \\ 2Im[f_{11}f_{21}^*] & 2Im(f_{11}f_{22}^*) & Re(f_{11}f_{22}^* + f_{12}f_{21}^*) & Re(f_{11}f_{22}^* - f_{12}f_{21}^*) \end{bmatrix} \quad (4.13.b)$$

In equation (4.12) and (4.13) the notation $\rho[X]$ means $\int_0^\infty n(\bar{a})X(\bar{a})d\bar{a}$ where $n(\bar{a})$ is the drop size distribution. This represents an average over the drop size distribution of the quantity X. $[\varepsilon(r,\hat{s})]$ is the Stokes parameters source function; it represents the radiation per unit solid angle in the direction $\hat{s}$. Equation (4.11) is called the vector radiative transfer equation (VRTE).

4.1.3 Application to a Plane Parallel Rain Medium.

The following is based on Ishimaru's paper [48], and the treatment is adapted to spheroidal droplets with an non uniform size distribution (MP in our case).

We consider a medium (see Figure 22) lying between the planes z = 0 and z = d filled with oblate spheroidal equioriented raindrops. The axis of symmetry of the drops is parallel to the z axis. We use a coordinate system convenient for the plane parallel geometry where a vector $\vec{u}$ is described by (r, μ, ϕ) where $\mu = \cos\theta$, and (r, θ, ϕ) are the spherical coordinates of $\vec{u}$, and where a point P is defined by (θ, ϕ, z) (Figure 22). Because the drops are axially symmetric their scattering coefficients $f_{ij}(\hat{s},\hat{s}')$ are such that : f_{11} and f_{22} are even functions of $\phi - \phi'$ and f_{12} and f_{21} are odd functions of $\phi - \phi'$. Specifically for forward scattering $\phi = \phi'$ so $f_{21} = f_{12} = 0$, and the scattering matrix is a diagonal matrix. Consequently

$$[\Lambda(\hat{s})] = [\Lambda](\mu, \phi) = \lambda\rho \begin{bmatrix} -2Im(f_{11}) & 0 & 0 & 0 \\ 0 & -2Im(f_{22}) & 0 & 0 \\ 0 & 0 & -Im(f_{11}+f_{22}) & -Re(f_{11}-f_{22}) \\ 0 & 0 & Re(f_{11}-f_{22}) & -Im(f_{11}+f_{22}) \end{bmatrix} \tag{4.14}$$

The Mueller matrix may be partitioned into four 2x2 matrices :

$$S(\mu, \mu', \phi - \phi') = \begin{bmatrix} S_1(\mu, \mu', \phi - \phi') & S_2(\mu, \mu', \phi - \phi') \\ S_3(\mu, \mu', \phi - \phi') & S_4(\mu, \mu', \phi - \phi') \end{bmatrix} \tag{4.15}$$

With :

$$\begin{aligned} [S_1(\hat{s}, \hat{s}')] &= \rho \begin{bmatrix} |f_{11}|^2 & |f_{12}|^2 \\ |f_{21}|^2 & |f_{22}|^2 \end{bmatrix} \\ [S_2(\hat{s}, \hat{s}')] &= \rho \begin{bmatrix} Re(f_{11}f_{12}^*) & -Im(f_{11}f_{12}^*) \\ Re(f_{21}f_{22}^*) & -Im(f_{21}f_{22}^*) \end{bmatrix} \end{aligned} \tag{4.16}$$

$$\begin{aligned} [S_3(\hat{s}, \hat{s}')] &= \rho \begin{bmatrix} 2Re(f_{11}f_{22}^*) & 2Re(f_{12}f_{22}^*) \\ 2Im[f_{11}f_{21}^*] & 2Im(f_{11}f_{22}^*) \end{bmatrix} \\ [S_4(\hat{s}, \hat{s}')] &= \rho \begin{bmatrix} Re(f_{11}f_{22}^* + f_{12}f_{21}^*) & -Im(f_{11}f_{22}^* - f_{12}f_{21}^*) \\ Re(f_{11}f_{22}^* + f_{12}f_{21}^*) & Re(f_{11}f_{22}^* - f_{12}f_{21}^*) \end{bmatrix} \end{aligned} \tag{4.17}$$

S_1 and S_4 are even functions of $\phi - \phi'$ and S_2 and S_3 are even functions of $\phi - \phi'$.

A linearly polarized plane wave $\vec{E}_i$ propagating in a direction $\hat{s}_i(\mu_i, \phi_i)$ is incident on the $z=0$ boundary of the medium. The VRTE becomes:

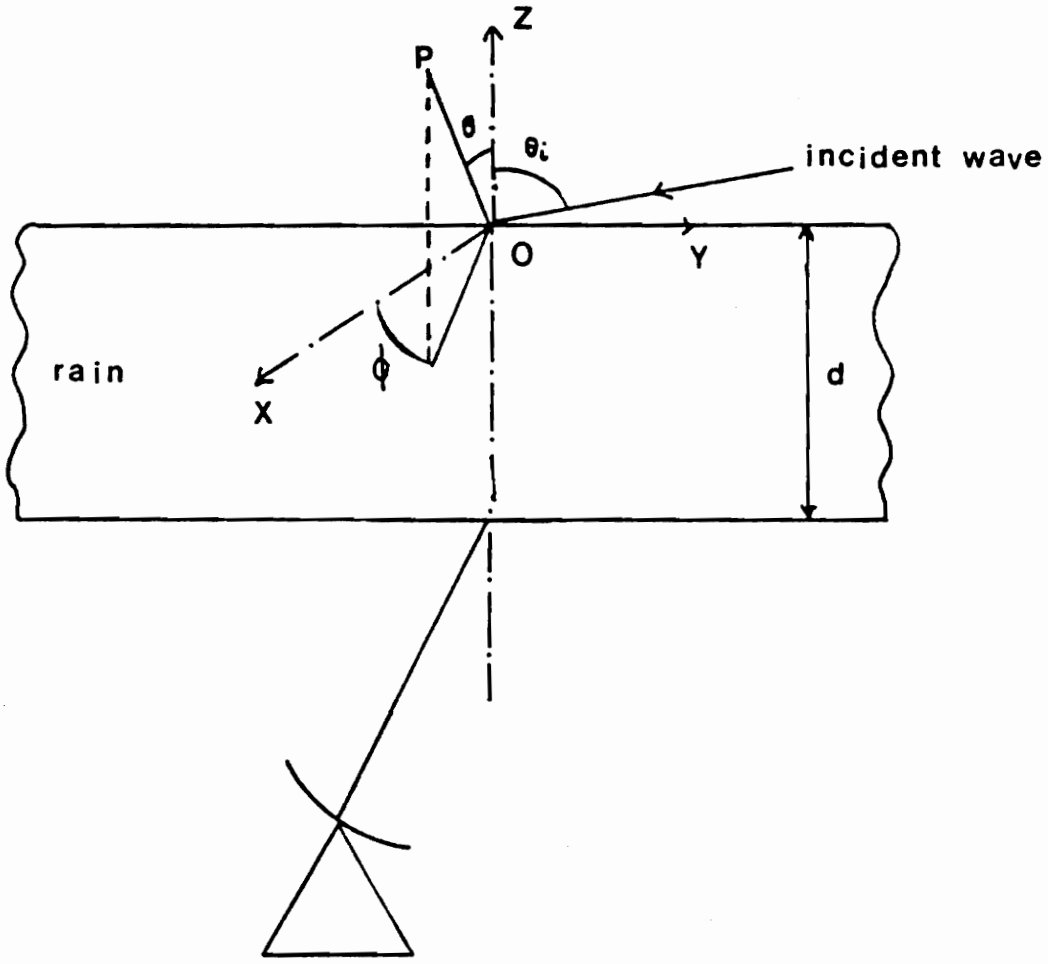

Figure 21. Plane parallel medium geometry.

$$\frac{d[I]}{ds}(z,\mu,\phi) = -[\Lambda(\mu,\phi)][I(z,\mu,\phi)] + \int_{-1}^{1} d\mu' \int_{0}^{2\pi} d\phi' [S(\mu,\mu',\phi-\phi')][I(z,\mu',\phi')] \tag{4.18}$$

4.1.3.1 Propagation of the Coherent Wave

According to Van de Hulst the coherent part of the electromagnetic wave propagates in a random medium only in the forward direction. So it can be written that :

$$\vec{E} = \vec{E}_c \delta(\hat{s}_i - \hat{s}) + \vec{E}_{inc}$$

or

$$[I] = [I_c]\delta(\hat{s}_i - \hat{s}) + [I_{inc}] \tag{4.19}$$

In addition if we omit the coefficient $e^{j(ks-\omega t)}$ it has been shown that the coherent field quantities satisfy:

$$\frac{d}{ds}\begin{bmatrix} E_{c1} \\ E_{c2} \end{bmatrix} = -i\lambda\rho \begin{bmatrix} f_{11} & 0 \\ 0 & f_{22} \end{bmatrix} \begin{bmatrix} E_{c1} \\ E_{c2} \end{bmatrix}$$

or

$$\frac{d}{ds}[I_c] = -[\Lambda][I_c] \tag{4.20}$$

Replacing $\frac{d}{ds}$ by $\mu_i \frac{d}{dz}$ yields:

$$\mu_i \frac{d}{dz}\begin{bmatrix} E_{c1} \\ E_{c2} \end{bmatrix} = -i\lambda\rho \begin{bmatrix} f_{11} & 0 \\ 0 & f_{22} \end{bmatrix} \begin{bmatrix} E_{c1} \\ E_{c2} \end{bmatrix}$$

or

$$\mu_i \frac{d}{dz}[I_c] = -[\Lambda][I_c] \tag{4.21}$$

Solving this equation for I_s and then computing I_s gives :

$$[I_s(z, \mu, \phi)] = [F(\mu, \mu_i, \phi)]\, e^{-\gamma_{ii}\frac{z}{\mu_i}}\, [I_i(0, \mu, \phi)] \tag{4.22}$$

with:

$$[F] = \begin{bmatrix} F_1 \\ F_2 \\ F_3 \\ F_4 \end{bmatrix}$$

and :

- For an x-polarized incident wave ($E_{c2}(z = 0) = 0$)

$$\begin{bmatrix} F_1 \\ F_2 \end{bmatrix} = \rho \begin{bmatrix} |f_{11}|^2 \\ |f_{21}|^2 \end{bmatrix}$$

with :

$$\begin{bmatrix} F_3 \\ F_4 \end{bmatrix} = \rho \begin{bmatrix} 2Re(f_{11}f_{21}^*) \\ 2Im(f_{11}f_{21}^*) \end{bmatrix}$$

and

$$\gamma_{ii} = \gamma_{11} = -2\lambda\rho[Im(f_{11})]$$

- For an y-polarized incident wave ($E_{c1}(z = 0) = 0$)

$$\begin{bmatrix} F_1 \\ F_2 \end{bmatrix} = \rho \begin{bmatrix} |f_{12}|^2 \\ |f_{22}|^2 \end{bmatrix}$$

with :

$$\begin{bmatrix} F_3 \\ F_4 \end{bmatrix} = \rho \begin{bmatrix} 2Re(f_{12}f_{22}^{*}) \\ 2Im(f_{12}f_{22}^{*}) \end{bmatrix}$$

and :

$$\gamma_{ii} = \gamma_{22} = -2\lambda\rho[Im(f_{22})]$$

We note that because of the parity of the coefficients f_{ij} the quantities F_1 and F_2 are even functions of $\phi - \phi'$ while the quantities F_3 and F_4 are odd functions of $\phi - \phi'$.

4.1.3.2 Equation for the Incoherent Intensity

Substituting (4.19) into the VRTE (4.17) yields:

$$\begin{aligned} \frac{d}{ds}\left([I_{inc}] + [I_c]\delta(\hat{s}_i - \hat{s})\right) = &-[\Lambda]\left([I_{inc}] + [I_c\delta(\hat{s}_i, \hat{s})]\right) \\ &+ \int_1^{-1} d\mu' \int_0^{2\pi} d\phi' [S](\mu, \mu', \phi - \phi')\left([I_c]\delta(\hat{s}_i - \hat{s}) + [I_{inc}(z, \mu', \phi')]\right) \end{aligned} \tag{4.23}$$

Then using (4.20) and replacing $\frac{d}{ds}$ by $\mu\frac{d}{dz}$ yields the integrodifferential equation:

$$\begin{aligned} \mu\frac{d}{dz}[I_{inc}] = &-[\Lambda(\mu)][I_{inc}(z, \mu, \phi)] \\ &+ \int_1^{-1} d\mu' \int_0^{2\pi} d\phi' [S(\mu, \mu', \phi - \phi')][I_{inc}(z, \mu', \phi')] \\ &+ [I_s(z, \mu, \phi)] \end{aligned} \tag{4.24}$$

where $[I_s(r, \hat{s})]$ is a 4x1 matrix representing the the Stokes parameters of the part of the coherent incident wave propagating in the direction $\hat{s}_i(\mu_i, \phi)$ that is scattered in the direction $\hat{s}(\mu, \phi)$:

$$[I_s(z, \mu, \phi)] = [S(\mu, \mu_i, \phi)][I_c(z, \mu_i)]$$

The boundary conditions are :

$$\begin{aligned} I_{inc}(z, \mu, \phi) &= 0 \qquad \text{for} \quad 0 \le \mu \le 1 \text{ and } z = 0 \\ I_{inc}(z, \mu, \phi) &= 0 \qquad \text{for} \quad -1 \le \mu \le 0 \text{ and } z = d \end{aligned} \tag{4.25}$$

These boundary conditions state that no incoherent intensity is produced outside the common volume of the rain medium and therefore no incoherent field enters the medium at its plane boundaries z=0 and z=d.

4.1.3.3 Solving the Equation for the Incoherent Wave

The solution that we will use is based on Ishimaru's method [48]. It includes the following steps:

1. Taking the Fourier transform of the equations using the parity of the affected functions.

2. Using Gauss quadrature to approximate the integral part of the resulting equation.

3. Solving the system of first order linear differential equation by using the eigenvalue-eigenvectors method.

Several other methods have been developed to solve this problem. Delogne et al. [37] and Crane [50] used an iterative technique, while Oguchi [40] uses a expansion in spherical

functions together with the eigenvalue eigenvector method. More recently Shieh [32] solved the VRTE by combining the iterative technique with the finite element technique allowing him to include both vertical and horizontal inhomogeneity in the plane parallel medium. These methods were implemented for spherical particles. We choose to use the solution developed by Ishimaru because it can handle spheroidal raindrops.

Fourier Expansion

Let us expand each term of the integrodifferential equation (4.24) into Fourier series with regard to the variable ϕ. First :

$$[I_s(z, \mu, \phi)] = [I_i]e^{-\gamma_{ii}\frac{z}{\mu_i}}\left\{\sum_{m=0}^{\infty}[F]_m^a(z, \mu)\cos m\phi + \sum_{m=1}^{\infty}[F]_m^b(z, \mu)\sin m\phi\right\} \tag{4.26}$$

with :

$$[F]_0^a(z, \mu) = \frac{1}{2\pi}\int_0^{2\pi}[F](z, \mu, \phi)d\phi$$

$$[F]_m^a(z, \mu) = \frac{1}{\pi}\int_0^{2\pi}[F](z, \mu, \phi)\cos m\phi d\phi$$

$$[F]_m^b(z, \mu) = \frac{1}{\pi}\int_0^{2\pi}[F](z, \mu, \phi)\sin m\phi d\phi$$

The Fourier matrices defined above are 4x1 matrices that satisfy :

$$[F]_m^a = \begin{bmatrix} F_{m1} \\ F_{m2} \\ 0 \\ 0 \end{bmatrix} \quad \text{and} \quad [F]_m^b = \begin{bmatrix} 0 \\ 0 \\ F_{m3} \\ F_{m4} \end{bmatrix}$$

because of the parity of the scattering coefficients. Similarly we have :

$$[S_s(\mu, \phi - \phi')] = \frac{1}{2\pi}[S]_0^a(\mu, \mu') + \frac{1}{\pi}\left\{\sum_{m=0}^{\infty}[S]_m^a(\mu, \mu')\cos m(\phi - \phi') + \sum_{m=1}^{\infty}[S](\mu, \mu')_m^b \sin m(\phi - \phi')\right\} \tag{4.27}$$

with :

$$[S]_m^a(\mu) = \begin{bmatrix} [S_1]_m^a(\mu) & 0 \\ 0 & [S_4]_m^a(\mu) \end{bmatrix}$$

$$[S]_m^b(\mu) = \begin{bmatrix} 0 & [S_2]_m^a(\mu) \\ [S_3]_m^a(\mu) & 0 \end{bmatrix}$$

where $[S_i]_m^{a \text{ or } b}$ are 2x2 matrices satisfying :

$$[S_i]_m^a(\mu) = \int_0^{2\pi}[S_i](\mu, \phi)\cos m(\phi - \phi')d(\phi - \phi') \qquad \text{for } i = 1 \text{ or } 4$$

$$[S_i]_m^b(\mu) = \int_0^{2\pi}[S_i](\mu, \phi)\sin m(\phi - \phi')d(\phi - \phi') \qquad \text{for } i = 2 \text{ or } 3$$

Finally:

$$[I_{inc}(z, \mu, \phi)] = \sum_{m=0}^{\infty} [I]_m^a(z, \mu) \cos m\phi + \sum_{m=1}^{\infty} [I](z, \mu)_m^b \sin m\phi \tag{4.28}$$

Ishimaru has shown that the first order scattering Stokes parameter matrix of the incoherent wave is proportional to [F], that the second order scattering Stokes parameter matrix is proportional to [S][F] and so on. Consequently , the first two elements of the Stokes parameter matrix $[I_{inc}]$ are even functions of ϕ while the last two are odd functions of ϕ. One can therefore write :

$$[I]_m^a(z, \mu) = \begin{bmatrix} I_{m1}(z, \mu) \\ I_{m2}(z, \mu) \\ 0 \\ 0 \end{bmatrix}$$

$$[I]_m^b(z, \mu) = \begin{bmatrix} 0 \\ 0 \\ I_{m3}(z, \mu) \\ I_{m4}(z, \mu) \end{bmatrix}$$

These are the unknown quantities. We now use (4.26)-(4.28) into (4.25) and thus obtain :

$$\mu \frac{d}{dz}\left(\sum_{m=0}^{\infty}[I]_m^a(z,\mu)\cos m\phi + \sum_{m=1}^{\infty}[I]_m^b(z,\mu)\sin m\phi\right) =$$

$$[\Lambda(\mu)]\left[\sum_{m=0}^{\infty}[I]_m^a(z,\mu)\cos m\phi + \sum_{m=1}^{\infty}[I]_m^b(z,\mu)\sin m\phi\right]$$

$$+\int_{-1}^{1}d\mu'\int_{0}^{2\pi}d(\phi-\phi')\left(\frac{1}{2\pi}[S]_m^a\right. \qquad (4.29)$$

$$\left.+\frac{1}{\pi}\sum_{m=1}^{\infty}[S]_m^a(\mu)\cos m(\phi-\phi') + [S]_m^b(\mu)\sin m(\phi-\phi')\right)[I_{inc}](\mu',\phi')$$

$$+[I_i]e^{-\gamma_{II}\frac{z}{\mu_i}}\left[\sum_{m=0}^{\infty}[F_m]_m^a\cos m\phi + \sum_{m=1}^{\infty}[F_m]_m^b\sin m\phi\right]$$

Let us compute the integral part of (4.29) J :

$$J=\int_{-1}^{1}d\mu'\int_{0}^{2\pi}d(\phi-\phi')\left\{\frac{1}{2\pi}[S]_0^a[I]_0^a\right.$$

$$+\frac{1}{\pi}\sum_{m=1}^{\infty}\sum_{n=0}^{\infty}\left([S]_m^a(\mu)[I]_n^a(z,\mu')\cos m(\phi-\phi')\cos n\phi'\right.$$

$$\left.+[S]_m^b(\mu)[I]_n^a(z,\mu')\sin m(\phi-\phi')\cos n\phi'\right) \qquad (4.30)$$

$$+\frac{1}{\pi}\sum_{m=1}^{\infty}\sum_{n=1}^{\infty}\left([S]_m^a(\mu)[I]_n^b(z,\mu')\cos m(\phi-\phi')\sin n\phi'\right.$$

$$\left.\left.+[S]_m^b(\mu)[I]_n^b(z,\mu')\sin m(\phi-\phi')\sin n\phi'\right)\right\}$$

Let us interchange summation and integration in the above equation and then perform the integration relative to ϕ' using :

$$\int_0^{2\pi} d(\phi - \phi') \frac{1}{2\pi} [S]_0^a [I]_0^a = [S]_0^a [I]_0^a$$

$$\int_0^{2\pi} \frac{1}{\pi} \cos m(\phi' - \phi) \cos n(\phi') d(\phi - \phi') = \delta_{mn} \cos(m\phi)$$

$$\int_0^{2\pi} \frac{1}{\pi} \cos m(\phi' - \phi) \sin n(\phi') d(\phi - \phi') = \delta_{mn} \sin(m\phi) \tag{4.31}$$

$$\int_0^{2\pi} \frac{1}{\pi} \sin m(\phi' - \phi) \cos n(\phi') d(\phi - \phi') = -\delta_{mn} \sin(m\phi)$$

$$\int_0^{2\pi} \frac{1}{\pi} \sin m(\phi' - \phi) \sin n(\phi') d(\phi - \phi') = \delta_{mn} \cos(m\phi)$$

where δ_{mn} is the Kronecker symbol. So:

$$\begin{aligned} J = \int_1^{-1} d\mu' \Big\{ & [S]_0^a(\mu, \mu')[I]_0^a(z, \mu) \\ & + \sum_{m=1}^{\infty} \Big([S]_m^a(\mu, \mu')[I]_m^a(z, \mu') + [S]_m^b(\mu, \mu')[I]_m^b(z, \mu') \Big) \cos m\phi \\ & + \Big(-[S]_m^b(\mu, \mu')[I]_m^a(z, \mu') + [S]_m^a(\mu, \mu')[I]_m^b(z, \mu') \Big) \sin m\phi \Big\} \end{aligned} \tag{4.32}$$

Substituting this into (4.29) and separating the cosine and sine series yields:

For m = 0:

$$\begin{aligned} \mu \frac{d}{dz} [I]_0(\mu, z) = & -[\Lambda(\mu)][I]_0(\mu, z) + \int_{-1}^{1} d\mu' [L]_0(\mu, \mu')[I]_0(z, \mu') \\ & + I_i e^{-\gamma_{II} \frac{z}{\mu_i}} [F]_0(\mu, \mu_i) \end{aligned} \tag{4.33}$$

with :

$$[I]_0 = \begin{bmatrix} I_{01} \\ I_{02} \end{bmatrix}$$

$$[L]_0 = [S_1]_0^a$$

$$[F]_0 = \begin{bmatrix} F_{01} \\ F_{02} \end{bmatrix}$$

For m ≠ 0

$$\begin{aligned} \mu \frac{d}{dz} [I]_m^a(\mu, z) = & - [\Lambda(\mu)][I]_m^a(\mu, z) \\ & + \int_{-1}^{1} d\mu' \left([S]_m^a(\mu, \mu')[I]_m^a(z, \mu') + [S]_m^b(\mu, \mu')[I]_m^b(z, \mu') \right) \\ & + I_i e^{-\gamma_{II} \frac{z}{\mu_i}} [F]_m^a(\mu, \mu_i) \end{aligned} \tag{4.34}$$

and:

$$\begin{aligned} \mu \frac{d}{dz} [I]_m^b(\mu, z) = & - [\Lambda(\mu)][I]_m^b(\mu, z) \\ & + \int_{-1}^{1} d\mu' \left([S]_m^b(\mu, \mu')[I]_m^a(z, \mu') + [S]_m^a(\mu, \mu')[I]_m^b(z, \mu') \right) \\ & + I_i e^{-\gamma_{II} \frac{z}{\mu_i}} [F]_m^a(\mu, \mu_i) \end{aligned}$$

This can also be written in a condensed form as :

$$\begin{aligned} \mu \frac{d}{dz} [I]_m(\mu, z) = & - [\Lambda(\mu)][I]_m(\mu, z) + \int_{-1}^{1} d\mu' [L]_m(\mu, \mu')[I]_m(z, \mu') \\ & + I_i e^{-\gamma_{II} \frac{z}{\mu_i}} [F]_m(\mu, \mu_i) \end{aligned} \tag{4.36}$$

with:

$$[I]_m = [I]^a_m + [I]^b_m$$

$$[F]_m = [F]^a_m + [F]^b_m$$

$$[L(\mu, \mu')]_m = \begin{bmatrix} [S_1]^a_m & [S_2]^b_m \\ -[S_3]^b_m & [S_4]^a_m \end{bmatrix}$$

The boundary conditions are :

$$\begin{aligned} &[I_{inc}(z = 0, \mu)]_m = 0 \qquad \text{for} \quad 0 \leq \mu \leq 1 \\ &[I_{inc}(z = d, \mu)]_m = 0 \qquad \text{for} \quad -1 \leq \mu \leq 0 \end{aligned} \tag{4.38}$$

Gauss Quadrature

The integral in (4.33) and (4.36) can approximated using the Gauss quadrature formula [51] :

$$\int_{-1}^{1} [L(\mu, \mu')]_m [I(z, \mu')]_m d\mu' = \sum_{k=1}^{N} a_k \{[L(\mu, \mu_k)]_m [I(z, \mu_k)]_m + [L(\mu, \mu_{-k})]_m [I(z, \mu_{-k})]\} \tag{4.37}$$

where :

$(\mu_k)(k \in [-N, +N])$ are the roots of the Legendre polynomial of degree 2N $P_{2N}(\mu)$. They satisfy : $-1 \leq \mu_{-N} < \mu_{-N+1} < \ldots \mu_{-1} < 0 < \mu_1 < \ldots \mu_{N-1} < \mu_N \leq 1$ and $\mu_k = -\mu_{-k}$ and a_k are the Gauss quadrature coefficients.

Substituting this into (4.36) yields for $I \in [-N, N]$:

$$\mu_l \frac{d}{dz}[I(z,\mu_l)]_m = -[\Lambda(\mu_l)][I(z,\mu_l)]_m + \sum_{k=1}^{N} a_k\{[L(\mu_l,\mu_k)]_m[I(z,\mu_k)]_m + [L(\mu_l,\mu_{-k})]_m[I(z,\mu_{-k})]_m\} + [F(\mu_l,\mu_i)]_m e^{-\gamma_{ii}\frac{z}{\mu_i}}[I_i] \tag{4.39}$$

Let us define the following 2N x 1 matrices :

$$[X(z)]_m = [[I(z,\mu_N)]_m \cdots [I(z,\mu_{-N})]_m]^T$$
$$[X_i(z)]_m = \left[\frac{1}{\mu_N}[F(\mu_N,\mu_i)]_m \ \cdots \ \frac{1}{\mu_{-N}}[F(\mu_{-N},\mu_i)]_m\right]^T \tag{4.40}$$

and the 2N x 2N matrix :

$$[\xi]_m = \begin{bmatrix} [K(\mu_N,\mu_N)]_m & \cdots & [K(\mu_N,\mu_{-N})]_m \\ [K(\mu_{-N},\mu_N)]_m & \cdots & [K(\mu_{-N},\mu_{-N})]_m \end{bmatrix} \tag{4.41}$$

with :

$$[K(\mu_k,\mu_l)]_m = -\frac{1}{\mu_k}\{a_l[L(\mu_k,\mu_l)]_m - \delta_{kl}[\Lambda(\mu_k)]\}$$

Using (4.40) and (4.41) into (4.39) the infinite set of first order differential equations :

$$\frac{d}{dz}[X(z)]_m + [\xi]_m[X(z)]_m = [I_i][X_i]_m e^{-\gamma_{ii}\frac{z}{\mu_i}} \tag{4.42}$$

For m = 0 the above expression represents a set of 4N first order differential equations while for $m \neq 0$ it represents a set of 8N first order differential equations. The unknown is the matrix $[X(z)]_m$ it is the mth Fourier coefficient of the Stokes parameter matrix of the incoherent field in a plane z = constant. Each coefficient of this matrix represents the Fourier coefficient in a direction μ_k. The boundary conditions become for $k \in [0\ ,\ N]$:

$$[I_{inc}(0, \mu_k)]_m = 0$$
$$[I_{inc}(d, \mu_{-k})]_m = 0 \tag{4.43}$$

Matrix Eigenvalue Method

Let us write (4.42) as :

$$\frac{d}{dz}[X(z)] + [\xi][X(z)] = [I_i][X_i]e^{-\gamma_{ii}\frac{z}{\mu_i}} \tag{4.44}$$

We note that $[\xi]$ is a real symmetric matrix, so it is diagonalizable and has 2N eigenvectors $[\beta_k]_{k\epsilon[-N...-1,1...N]}$ which form a complete set . Let us call the corresponding set of eigenvalues λ_k. The homogeneous equation :

$$\frac{d}{dz}X(z) + [\xi][X(z)] = 0 \tag{4.45}$$

has for solution :

$$[X_h(z)] = \sum_{k=-K}^{k=K} c_k[\beta_k]e^{-\lambda_k z} \tag{4.46}$$

where (c_k) is a set of constants which will be found from the boundary conditions at z=0 and z=d.

A particular solution to (4.44) is :

$$[X]_p(z) = \left[[\xi] - \frac{\gamma_{ii}}{\mu_i}[U]\right]^{-1}[I_i][X_i]e^{-\gamma_{ii}\frac{z}{\mu_i}} \tag{4.47}$$

where [U] is the K x K identity matrix. Combining (4.46) and (4.47) gives the general form of the solution of (4.44):

$$[X(z)] = \sum_{k=-K}^{k=K} c_k[\beta_k]e^{-\lambda_k z} + [X_p](z) \tag{4.48}$$

Applying the boundary conditions to that equation yields :

- For z = 0 we have for $l \in [1, K]$:

$$0 = \sum_{k=-K}^{K} c_k \beta_{lk} + X_{pl}(0) \tag{4.49}$$

- For z = d we have for $l \in [-K, -1]$:

$$0 = \sum_{k=-K}^{K} c_k \beta_{lk} e^{-\lambda_k z} + (X_p)_l(d) \tag{4.50}$$

β_{lk} is the l^{th} element of the k^{th} eigenvector $[\beta_k]$, and similarly $(X_p)_l(d)$ is the l^{th} of the matrix $(X_p)_l(d)$.

Equations (4-49) and (4.50) form a set of 2 K linear equations with 2 K unknowns that can be solved for c_k. Equation (4.44) can then be completely solved and the Fourier matrices $[I]_m$ are determined; one can consequently calculate $[I]_{inc}$ as :

$$[I_{inc}(z, \mu, \phi)] = \begin{bmatrix} \sum_{m=0}^{\infty} I_{m1}(z, \mu) \cos m\phi \\ \sum_{m=0}^{\infty} I_{m2}(z, \mu) \cos m\phi \\ \sum_{m=1}^{\infty} U_m(z, \mu) \sin m\phi \\ \sum_{m=1}^{\infty} V_m(z, \mu) \sin m\phi \end{bmatrix} \qquad (4.51.a)$$

From this the co and cross polarized incoherent intensity can be computed as :

$$\begin{aligned} I_x &= \mu^2 \cos^2\phi I_1 + I_2 \sin^2 \sin^2\phi - U\mu \sin\phi \cos\phi \\ I_y &= \mu^2 \sin^2\phi I_1 + I_2 \cos^2 \sin^2\phi + U\mu \sin\phi \cos\phi \end{aligned} \qquad (4.51.b)$$

Numerical Implementation

In order to apply the solution developed in the previous section we used the following numerical methods :

1. First to compute the average on the drop size distribution

$$\rho[x] = \int_o^{\bar{a}_{max}} n(\bar{a}) x(\bar{a}) d\bar{a}$$

we use an extended Simpson rule with 15 points (see [51] for reference) and the MP drop size distribution defined in (2.5). We obtain:

$$\rho[x] \simeq \frac{16000}{12}\left[4x(0.25)e^{-0.25\Lambda} + x(3.5)e^{-3.5\Lambda} + \sum_{j=1}^{6} 2x(0.5j)e^{-05j\Lambda} + 4x(0.5j + 0.25)e^{-(0.5j+0.25)\Lambda}\right] \tag{4.52}$$

$\bar{a}$ is in mm.

2. The Fourier transforms are computed using a 25 points extended Simpson rule. The Fourier transform F_m of $f(z, \theta, \phi)$, an even or odd function is :

$$F_m = \int_0^{2\pi} f(z, \theta, \phi) q(m\phi) d\phi = 2\int_0^{\pi} f(z, \theta, \phi) q(m\phi) d\phi \tag{4.53}$$

where :

$$q(m\phi) = \begin{cases} \cos m\phi \text{ if f is even} \\ \text{or} \\ \sin m\phi \text{ if f is odd} \end{cases}$$

(4.53) becomes :

$$F_m = 5\frac{\pi}{180}\left\{q(0)f(z, \theta, 0) + q(m\pi)f(z, \theta, \pi) + 4\sum_{j=0}^{11} f(z, \theta, (2j + 1)\frac{\pi}{24})q(m(2j + 1)\frac{\pi}{24}) + 2\sum_{j=1}^{11} f(z, \theta, (2j)\frac{\pi}{24})q(m(2j)\frac{\pi}{24})\right\} \tag{4.54}$$

3. To implement the Gauss quadrature we choose N = 6 . This choice was based on the results in the literature [32], [46] which showed that a good convergence was reached for a 12 point Gauss quadrature .

4. The number of computations was reduced considerably by the use of symmetry. Specifically we used the fact that the scattering coefficient $f_{1 \text{ or } 2}(\theta_k, \theta_l, \phi) = f_{\theta 1 \text{ or } 2}(\theta_k, \theta_l, \phi)\hat{\theta} + f_{\phi 1 \text{ or } 2}(\theta_k, \theta_l, \phi)\hat{\phi}$ with $\theta_k = arcos\mu_k$ and 1 and 2 corresponding to the 2 possible polarizations of the incident field satisfies :

$$\begin{aligned} f_{\theta 1}(\theta_k, \theta_l, \phi) &= f_{\theta 1}(\theta_{-k}, \theta_{-l}, \phi) \\ f_{\theta 2}(\theta_k, \theta_l, \phi) &= -f_{\theta 2}(\theta_{-k}, \theta_{-l}, \phi) \\ f_{\phi 1}(\theta_k, \theta_l, \phi) &= -f_{\phi 1}(\theta_{-k}, \theta_{-l}, \phi) \\ f_{\phi 2}(\theta_k, \theta_l, \phi) &= f_{\phi 2}(\theta_{-k}, \theta_{-l}, \phi) \end{aligned} \tag{4.55}$$

A computer code (see Appendix B)was written to solve the VRTE for a plane parallel medium. We used the numerical method described above and IMSL routines to calculate the eigenvalues and eigenvectors as well as to solve the system of complex and real equations that are described above. Calculations using this program are presented in the following section.

4.1.4 Results and Application to the Interference Problem

The results obtained for an incident angle $\theta_i = 0$ (see geometry in Figure 23) at a frequency of 30 GHz, and for a rain thickness of 1 km are plotted in Figures (23-26). These curves have the same shape as those presented by Ishimaru [48], but have a magnitude order significantly higher. This divergence can be partially explained by the fact that Ishimaru used spherical

raindrops thus Mie scattering coefficient and a diagonal therefore simpler extinction matrix while we used spheroidal raindrops. In addition, the solution to the VRTE is extremely sensitive to the value of the eigenvalues λ_k. Because of this fact the matrix involved in solving equations (4.49)-(4.50) becomes ill-conditioned for a rain thickness above 2.5 km.

Let us call I the first component of the resultant Stokes vector, and let us calculate the power received by an antenna located at a distance R from the rain medium.

$$P_i = \int \frac{I}{4\pi R^2} \lambda^2 G(\theta, \phi) d\Omega \tag{4.56}$$

Assuming a gaussian pattern $G(\theta) = G_0 e^{-4 \ln 2 (\frac{\theta}{\theta_{hp}})}$, θ_{hp} being the half power beamwidth and integrating yields:

$$P_i = \frac{G_0 \lambda^2 I \pi \theta_{HP}^2}{(4\pi R)^2 4 \ln 2} \tag{4.57}$$

The power received directly from a wanted satellite like OLYMPUS assuming that a unit intensity is incident on the rain medium is :

$$P_r = e^{-\alpha L} G_r \frac{\lambda^2}{4\pi R2} \tag{4.58}$$

where:

$$\begin{aligned} &G_r \text{ is the gain of the receiving antenna} \\ &e^{-\alpha L} \text{ is the attenuation} \end{aligned} \tag{4.59}$$

and the power ratio is :

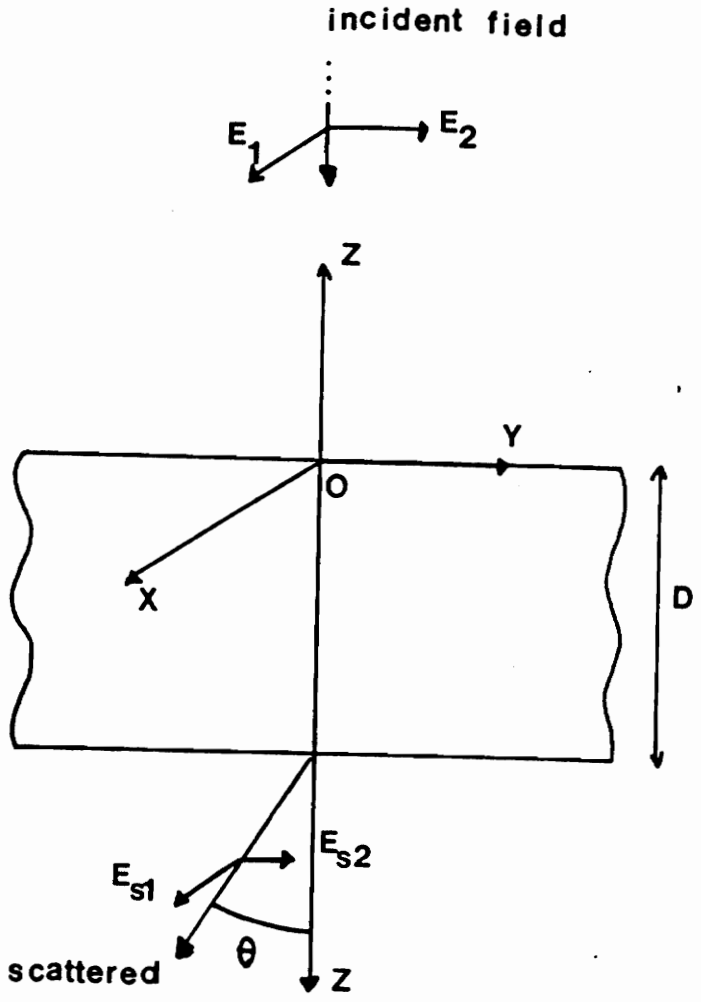

Figure 23. Geometry of the plane parallel medium used for calculations.

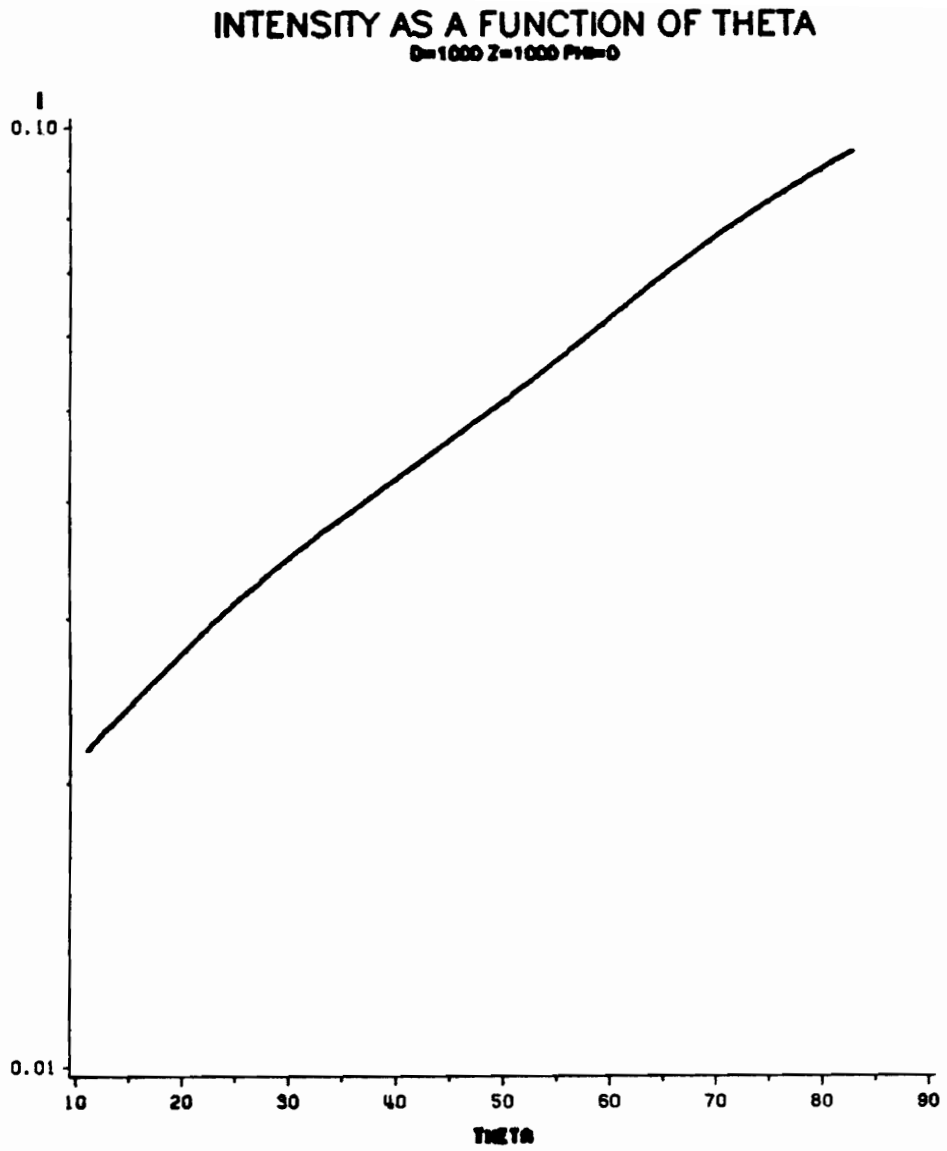

Figure 24. Incoherent intensity for a 1 km plane parallel medium; transmitted intensity at z=d; horizontal polarization.

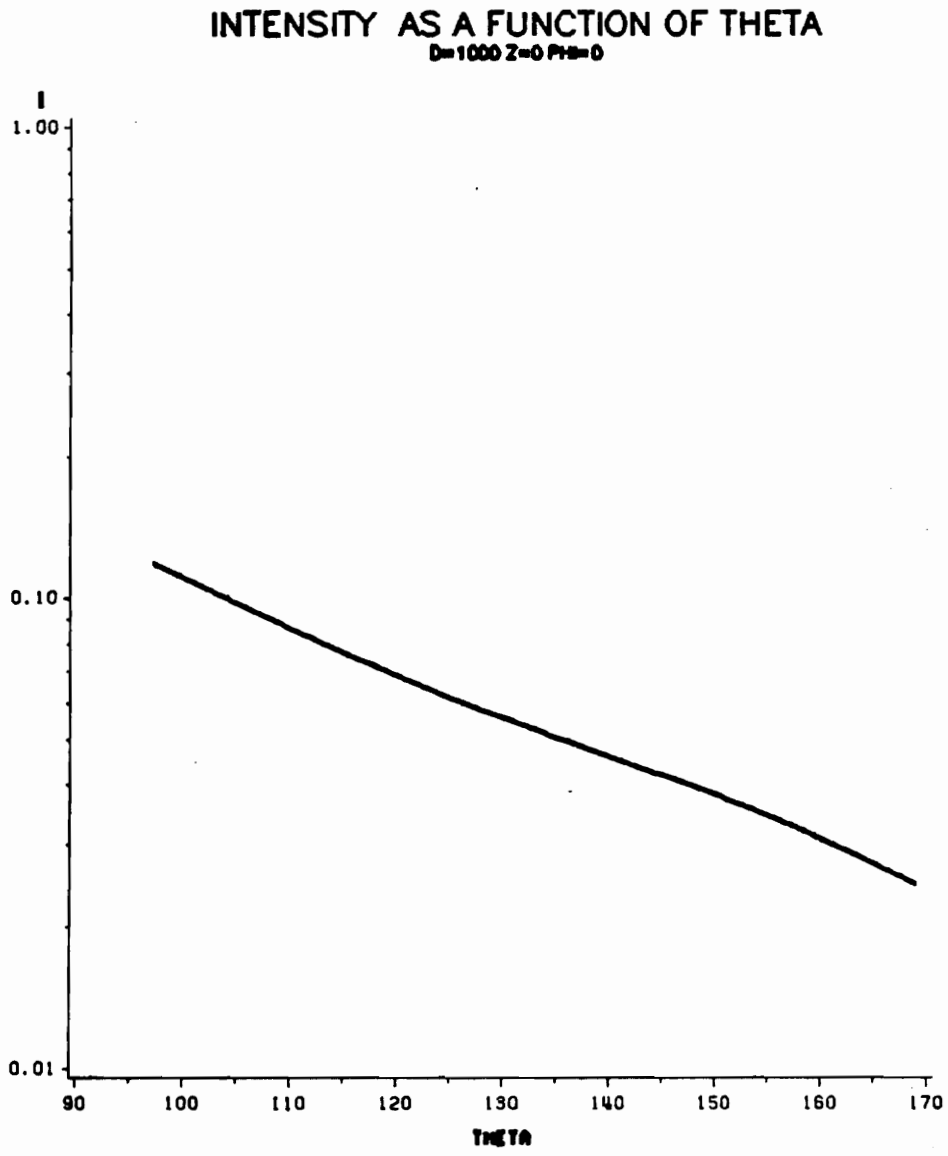

Figure 25. Incoherent intensity for a 1 km plane parallel medium; reflected intensity at z=0; horizontal polarization.

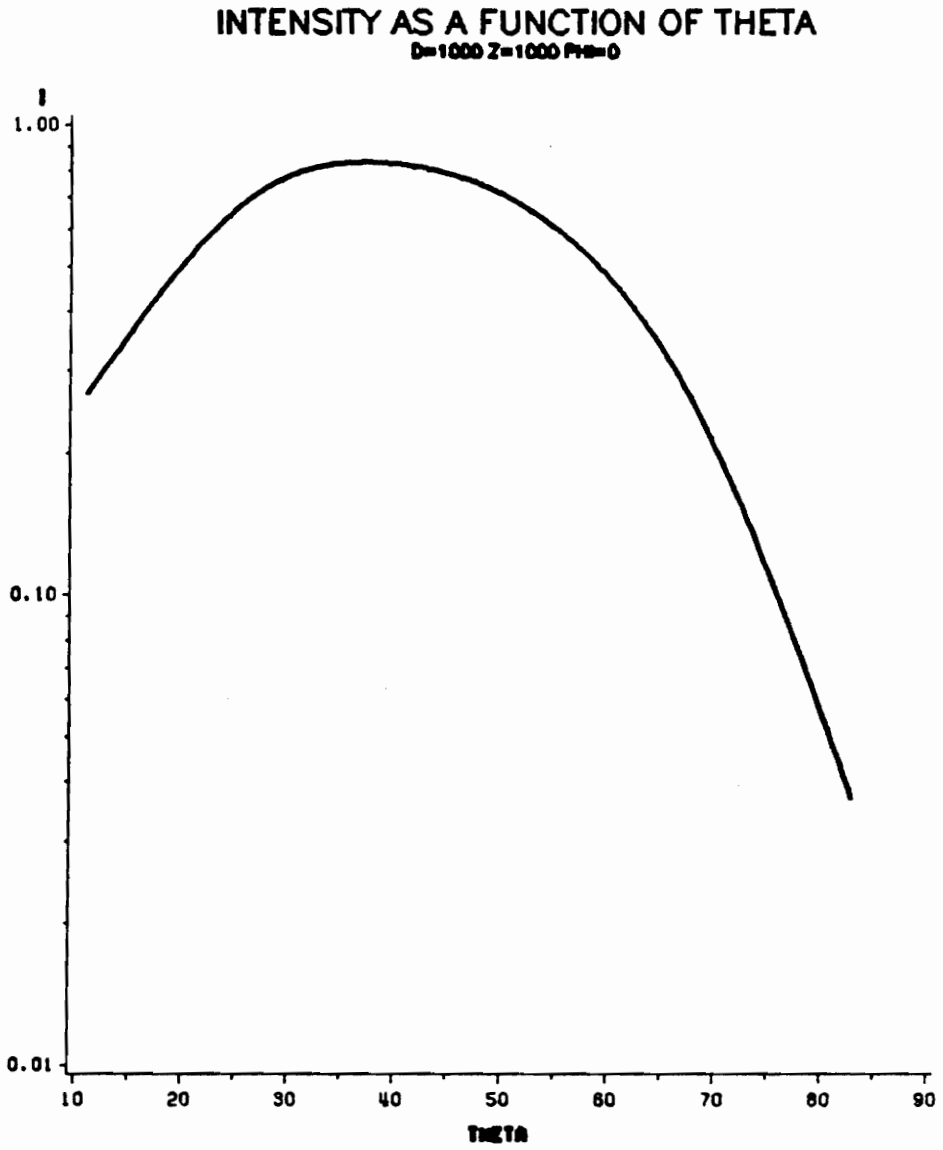

Figure 26. Incoherent intensity for a 1 km plane parallel medium; transmitted intensity at z=d; vertical polarization.

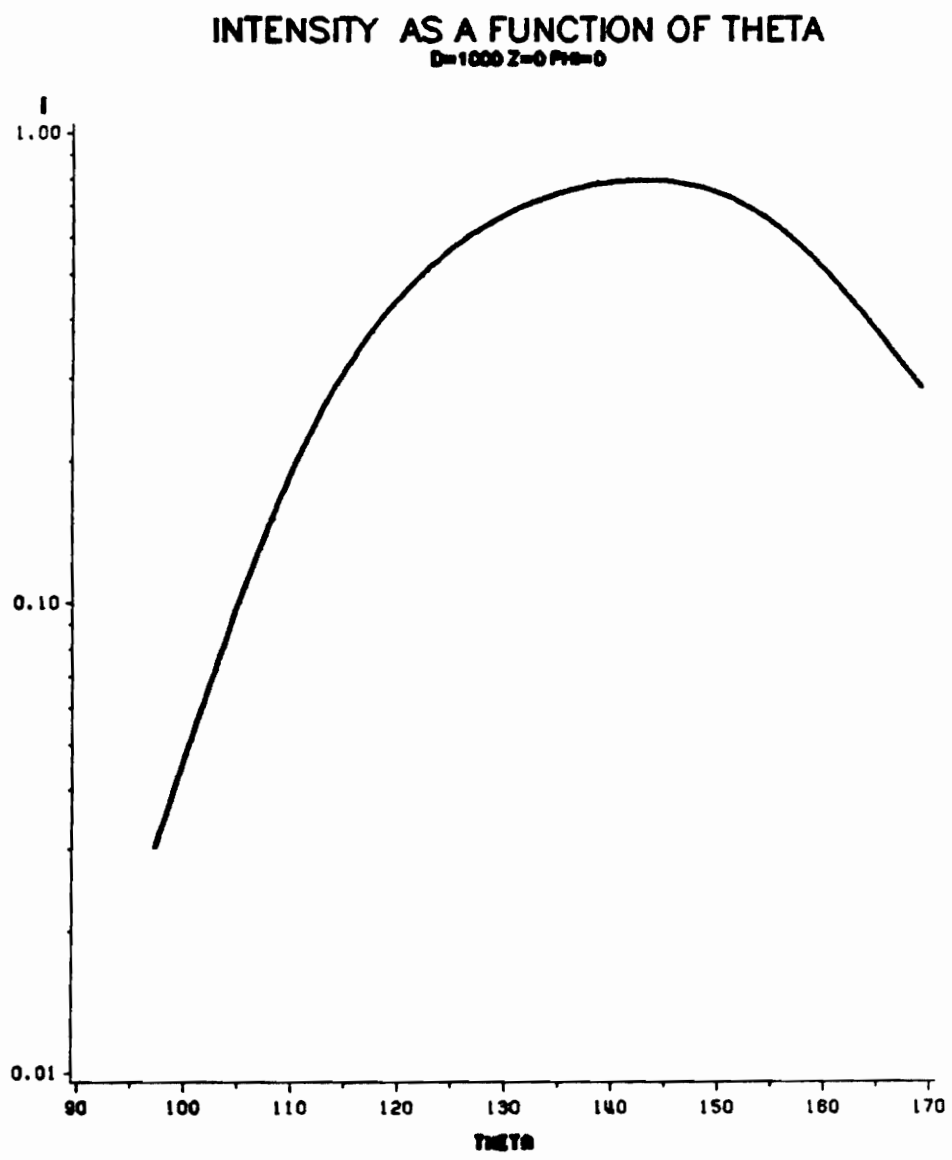

Figure 27. Incoherent intensity for a 1 km plane parallel medium; reflected intensity at $z=0$; vertical polarization.

$$\frac{P_i}{P_r} = \frac{G_0 \pi l \theta_{HP}^2 e^{\alpha L}}{G_r A \ln 2} \tag{4.60}$$

The result found by Ishimaru [46] for 30 GHz and rain rate of 12.5mm/hr are used to evaluate this formula with a half power beamwidth of 1 degree , a rain height of 3 km, and equal gains: Ishimaru finds I=-20 dB for normal incidence so the power ratio is $\frac{P_i}{P_r} = -45dB$. This result is comparable to that obtained with the two following techniques.

4.2 BRE and Chu 's Methods

For comparison purpose we study the problem using the bistatic radar equation and a technique derived by Chu. We assume for this that the attenuation in the common volume is $e^{-\alpha L}$ where L is the path length in the common volume and α is the extinction coefficient. The section of the path in the common volume is negligible compared to the range from the satellite to the common volume D_1.

4.2.1 Chu's Method

Let us replace Chu's assumption of isotropic scattering by supposing that the scattering is anisotropic. The scattering cross section used in (3.9) becomes, therefore, the bistatic scattering cross section $\sigma_{bi}(\bar{a}, \hat{i}, \hat{o})$, and (2.11) giving the interfering power becomes :

$$P_i = P_s e^{-\alpha L} \frac{\lambda^2}{4\pi} \left[\int \sigma(\bar{a}, \hat{i}, \hat{o}) n(\bar{a}) d\bar{a} \right] \int_0^L \int_0^{2\pi} \int_0^{\infty} \frac{2}{\pi\omega^2} e^{-\frac{2\rho^2}{\omega^2}} \rho d\rho d\phi dz \tag{4.61}$$

Let us evaluate the triple integral in the above expression :

$$I = \int_0^L \int_0^{2\pi} \int_0^{\infty} \frac{2}{\pi\omega^2} e^{-\frac{2\rho^2}{\omega^2}} \rho d\rho d\phi dz \tag{4.62}$$

Integrating with regard to ϕ and writing the integrand as a derivative with regard to ρ gives :

$$I = 2\pi \int_0^L \int_0^{\infty} \frac{-1}{2\pi} \frac{d}{d\rho} \left[e^{-\frac{2\rho^2}{\omega^2}} \right] \rho d\rho d\phi dz = \int_0^L \left[e^{\frac{-2\rho^2}{\omega^2}} \right]_0^{\infty} dz \tag{4.63}$$

and finally :

$$I = \int_0^L dz = L \tag{4.64}$$

The interfering power is then :

$$P_i = P_s e^{-\alpha L} \frac{\lambda^2}{4\pi} \left[\int \sigma(\bar{a}, \hat{i}, \hat{o}) n(\bar{a}) d\bar{a} \right] L \tag{4.65}$$

The power of the direct signal, which in the case of our proposed experiment would be coming from OLYMPUS, is attenuated by the rain and can be written as in (3.8) :

$$P_r = P_s A_g e^{-\alpha L} \tag{4.66}$$

and the ratio between interfering and direct received power is simply:

$$\frac{P_i}{P_s} = \frac{L}{G} \bar{\sigma}_{bi}(\bar{a}, \hat{i}, \hat{o}). \tag{4.67}$$

where

$G =$ gain of the ES antenna receiving the direct signal from OLYMPUS

$L =$ length of the rain path

$\bar{\sigma}_{bi}(\bar{a}, \hat{i}, \hat{o}) =$ the bistatic cross section per unit volume as in (2.11)

This result is equivalent to that of (3.10) but is expressed as a function of the bistatic scattering cross section per unit volume.It is plotted versus attenuation and rain rate for 30 GHz and elevation angles of 14 and 45 ° (Figures 28 to 31).

4.2.2 Use of the BRE

We start from the general form of the BRE as in (3.2) giving the expression of the power scattered P_i by the rain as a function of the transmitted power P_t . We assume that all the attenuation occurs within the common volume therefore $\gamma(D_1) = 1$ and $\gamma(D_2) = e^{-\alpha L}$. The pattern of the receiving antenna is supposed to a gaussian with a maximum in the scattering direction $\hat{o}$; thus the gain can be written as :

$$G_r(\hat{o}) = G_0 e^{-4 \ln 2 (\frac{\theta}{\theta_{HP}})^2} \tag{4.68}$$

Where θ_{HP} is the half power beamwidth of the antenna . θ can be expressed as $\theta = \tan^{-1}(\frac{\rho}{z})$. The interfering power is then:

$$P_i = P_t \frac{G_t(\hat{i}) G_0 \bar{\sigma}_{bi} \lambda^2 e^{-\alpha L}}{(4\pi)^3 D_1^2} \int_0^{2\pi} d\delta \int_{D_2}^{D_2+L} \frac{dz}{z^2} \int_0^{\infty} e^{-\frac{4 \ln 2}{\theta_{HP}^2} (\frac{\rho}{z})^2} \rho d\rho \tag{4.69}$$

Integrating this expression, using the fact that θ is small, and that the exponential in the integrand decreases rapidly, yields:

$$P_i = P_t \frac{G_t(\hat{i}) G_0 \bar{\sigma}_{bi} \lambda^2 e^{-\alpha L} L \theta_{HP}^2}{(4\pi)^2 D_1^2 16 \ln 2} \tag{4.70}$$

Besides the power directly received from the wanted satellite (e.g. OLYMPUS) is :

$$P_r = \frac{P_t G_t(\hat{i}) \lambda^2 G_r(\hat{i}) e^{-\alpha L}}{4\pi^2 D_1^2} \tag{4.71}$$

The ratio between the interfering power and the direct power from the satellite is finally :

$$\frac{P_i}{P_r} = \frac{G_0 L \bar{\sigma}_{bi} \theta_{HP}^2}{G_r(\hat{i}) 16 \ln 2} \tag{4.72}$$

This result is plotted and compared with the result obtained using Chu's technique in Figures 28 to 31. The two methods agree within 1 dB. In fact, if we replace G_0 by $\frac{30000}{\theta_{HP}^2}$ we find that the two formulas are equivalent.

4.3 Effect on Commercial Systems

In the preceding sections we computed the power of the interference due to rain scattering, here we are interested in analyzing the effects of potential interference on commercial satellite communication systems. More specifically, we study the performances of FM/FDM systems and digital TDM systems in presence of interference.

4.3.1 FDM/FM Systems

We follow the analysis developed by Gaines [52] to evaluate the performance of FM systems subject to rain induced attenuation and depolarization. Gaines has expressed the overall signal to noise ratio (SNR) of the system as a function of the attenuation and the isolation (XPD) by combining the signal to noise ratio due only to the thermal noise to that related to the cross-polarized interfering signal. We adapt this to our problem by replacing the

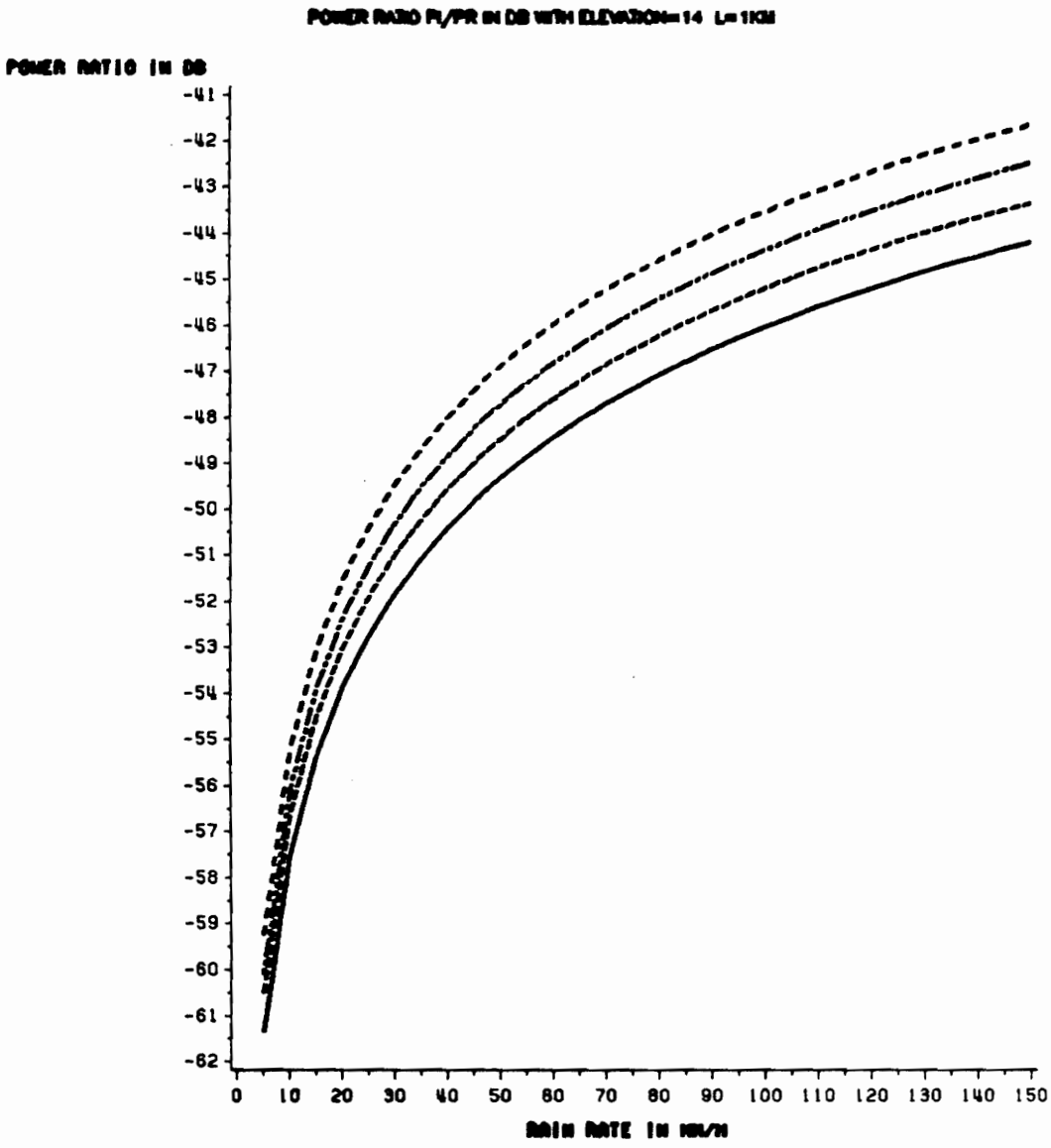

Figure 28. Comparison between the power ratio interfering power to direct power calculated using the BRE or Chu's technique.

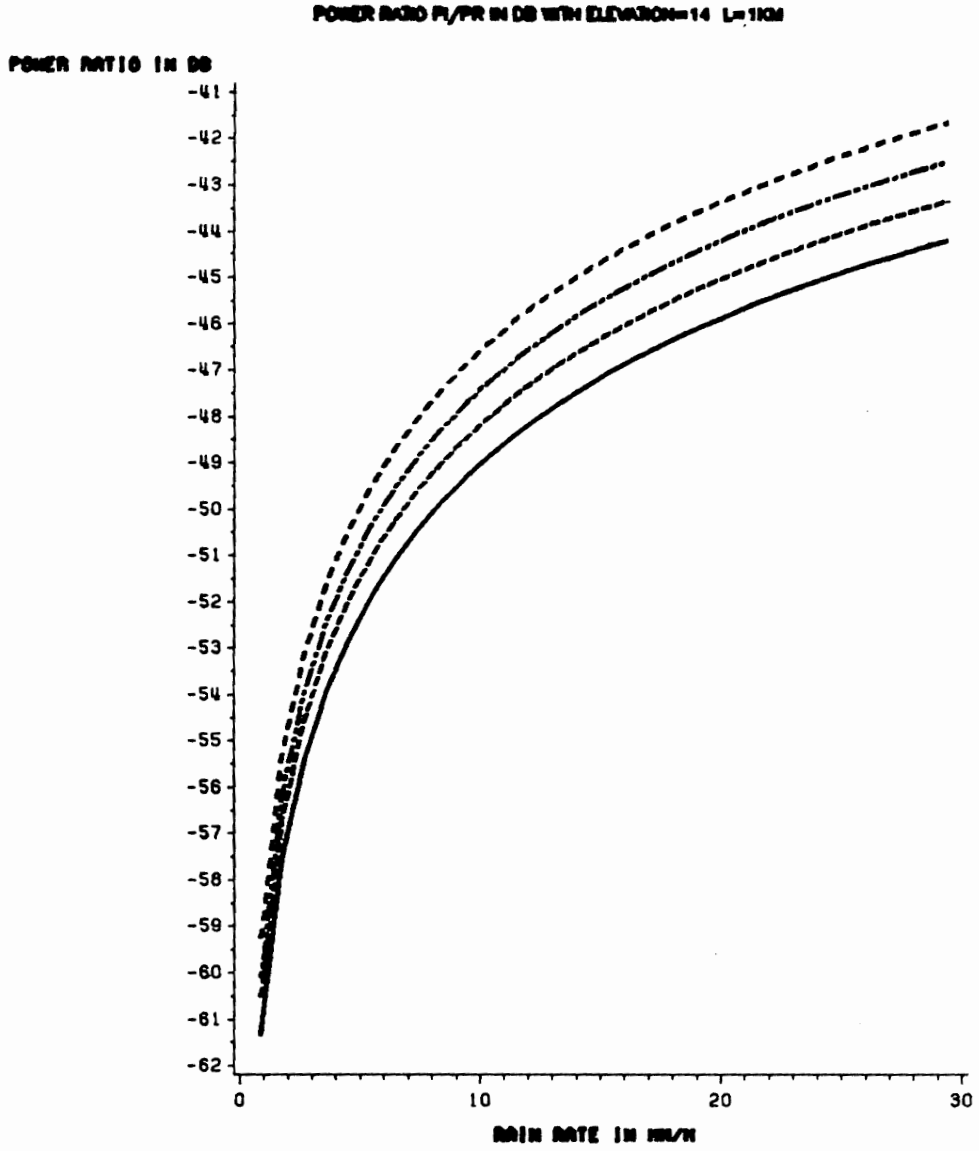

Figure 29. Comparison between the power ratio interfering power to direct power calculated using the BRE or Chu's technique.

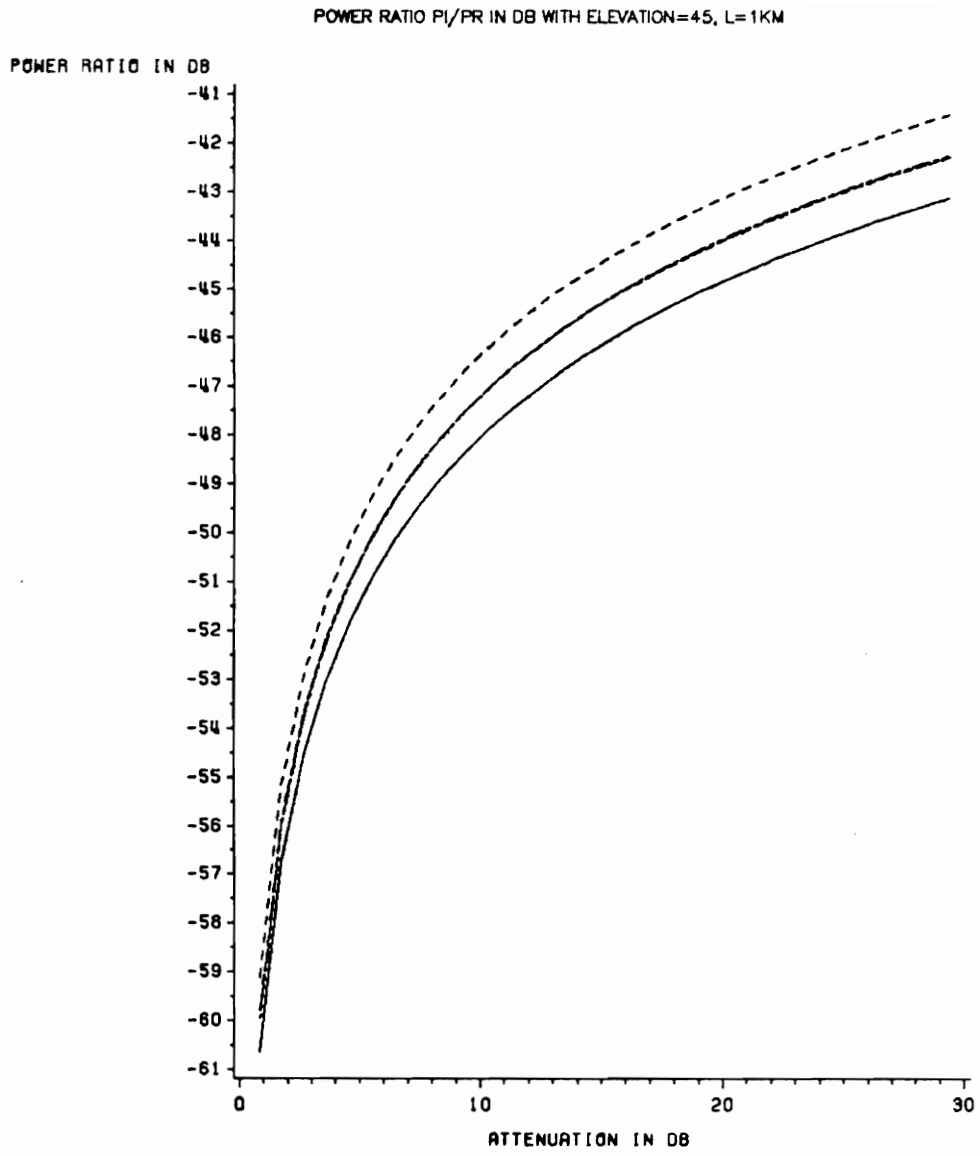

Figure 30. **Comparison between the power ratio interfering power to direct power calculated using the BRE or Chu's technique.**

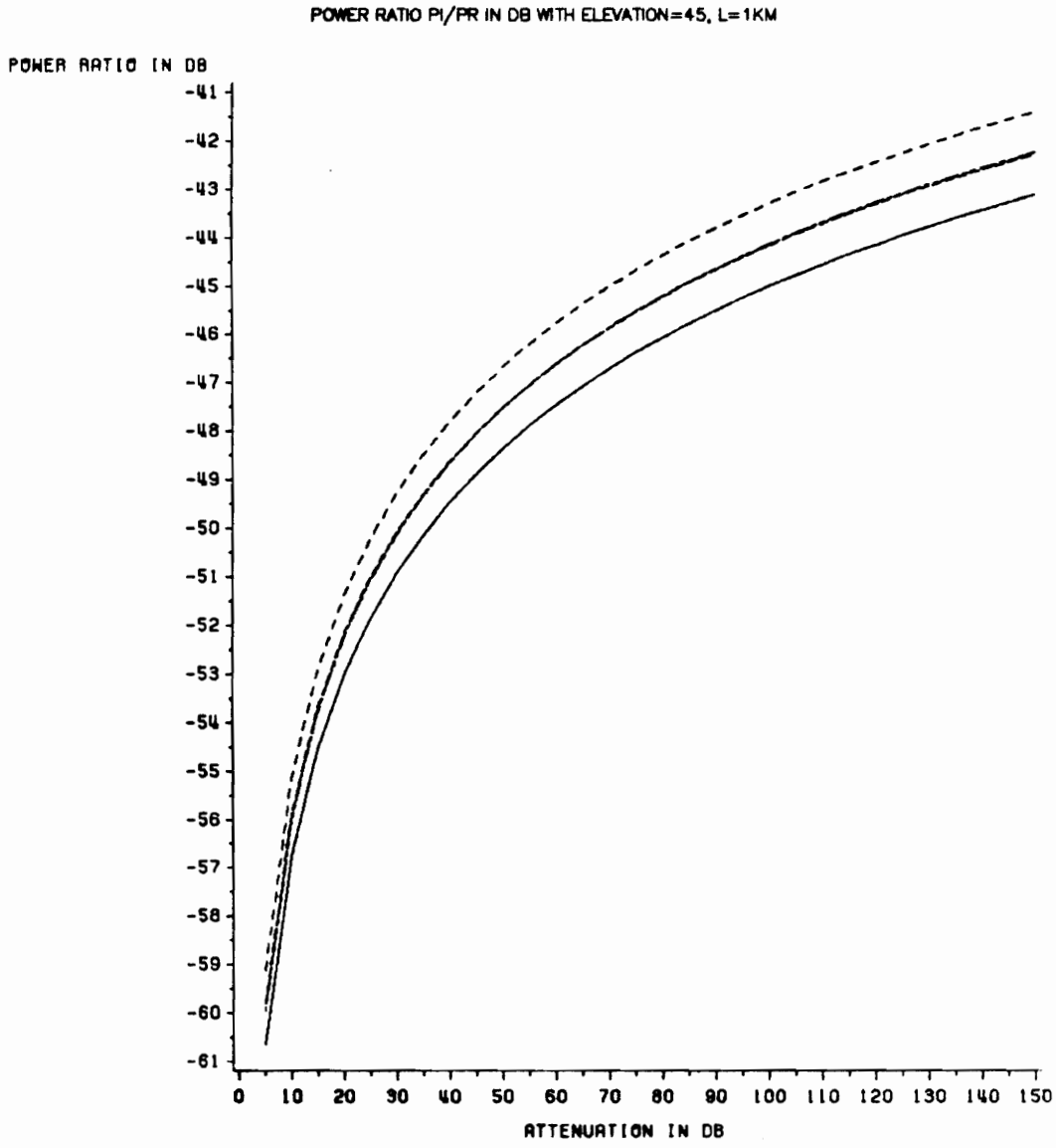

Figure 31. Comparison between the power ratio interfering power to direct power calculated using the BRE or Chu's technique.

cross-polarized interfering signal by the the rain scattered interfering signal assuming the worst case where the totality of the interfering signal is co-polarized with the wanted signal. This supposes that the interferer occupies the same frequency band as the wanted signal.

For a N channel telephone system the signal to noise ratio related to the interference is [52]:

$$\begin{aligned} SNR_I &= NPR + 2 + 6\log_{10}N \quad for\ N \leq 240 \\ SNR_I &= NPR + 16 \qquad\quad for\ N \geq 240 \end{aligned} \tag{4.73}$$

with :

$$SNR_I = \frac{\text{0 dBm test tone level}}{\frac{I}{C}}$$

and:

$NPR =$ noise power ratio

$$NPR = \frac{L/C}{I/C}$$

$C =$ carrier power level

$I =$ interfering power level

$L =$ load per channel

The thermal noise related signal to noise ratio on the other hand is :

$$SNR_t = CNR_1 + 10\log_{10}\left[\frac{B}{b}\right] + 20\log_{10}\left[\frac{\Delta f_{rms}}{f_n}\right] + p + W \tag{4.74}$$

where :

CNR_1 is the signal to noise ratio of the wanted signal
with no interference, but including possible attenuation
$CNR_1 = CNR_o - A$
CNR_0 being the clear weather carrier to noise ratio
and A the attenuation
B is the IF bandwidth
b is the baseband channel bandwidth
Δf_{rms} is the rms test tone deviation
f_n is the frequency of the the test channel in the multichannel FDM baseband
p is the preemphasis factor
W is the psophometric weighting factor

Combining the two signal to noise ratios yields the overall SNR:

$$SNR = \frac{1}{\frac{1}{SNR_I} + \frac{1}{SNR_T}} \tag{4.75}$$

To illustrate this formula we use an example [52] representing a typical FM telephone system with :

$N = 900 \quad b = 3.1KHz \quad B = 36MHz$ and $f_n = 4028KHz$
$p = 4dB \quad W = 2.5dB$

Using the (4.73) and (4.74) yields :

$$\begin{aligned} SNR_I &= \left[\frac{C}{I} \right] + 30.46 \\ SNR_T &= CNR_1 + 33.2 \end{aligned} \tag{4.76}$$

The overall signal to noise ratio is plotted in Figure 32 on page 103 page= no. as a function of the interfering signal for different CNR_1. The curve show that for systems with a high threshold the wanted signal may not be properly detected. Problems could occur when the

carrier to interference ratio is small (≤ 10) and when the interfering satellite sends a signal much stronger than the wanted signal.

4.3.2 Digital Systems

Prabhu [53], Castle [54] and Juroshek [55] studied the effect of noise plus interference on digital M-ary PSK systems. For this type of system the parameter which characterize the performance of the system is P_e the symbol error probability. P_e has for M-ary system a complex expression [53] to which Juroshek found a upper bound:

$$P_{ub} = erfc\left\{\rho \sin\left(\frac{\pi}{M}\left[1 - \frac{R_1}{\sin\left(\frac{\pi}{M}\right)}\right]\right)\right\} \tag{4.77}$$

where :

erfc is the complementary error function

$\rho = \sqrt{10^{0.1CNR_0}}$ with $CNR_0 =$ clear air carrier to noise ratio

$R_1 = \sqrt{10^{-0.1(C/I)}}$ with $\frac{C}{I} =$ carrier to interference ratio

The symbol error probability for a QPSK (M=4) is plotted with its upper bound in Figure 33, taken from the paper of Gaines et al [52].

The above formulation supposes that the interferer occupies the same frequency bandwidth as the the wanted signal. It is more realistic to assume that interfering and wanted signal occupy different but overlapping frequency bands as it is the case when a wide band FM/FDM signal is interfering in a narrow band PSK digital system. P.Constantinou [56] studied

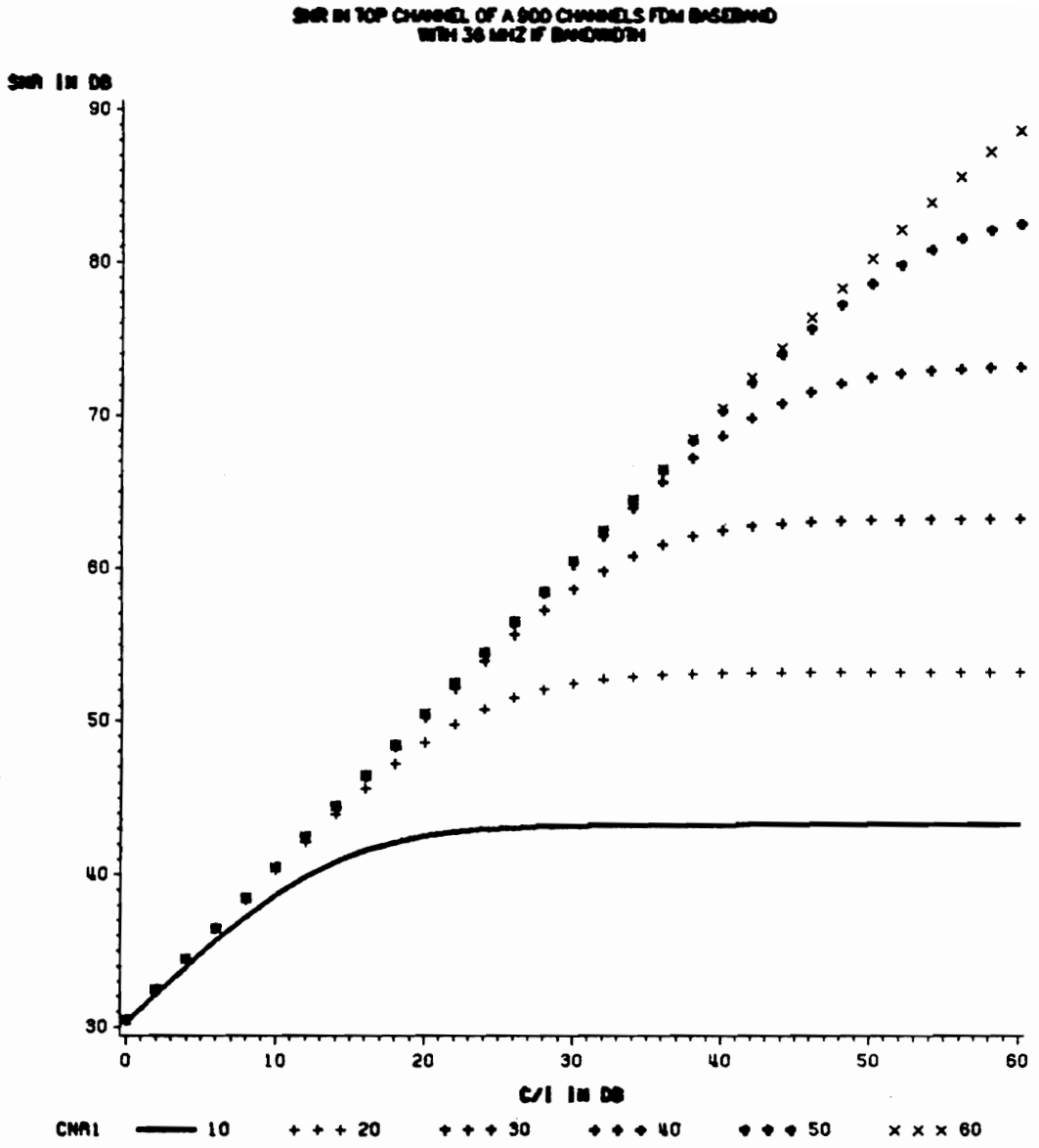

Figure 32. SNR in top channel of a 900 channels FDM/FM telephone system. The IF bandwidth is 36 MHz.

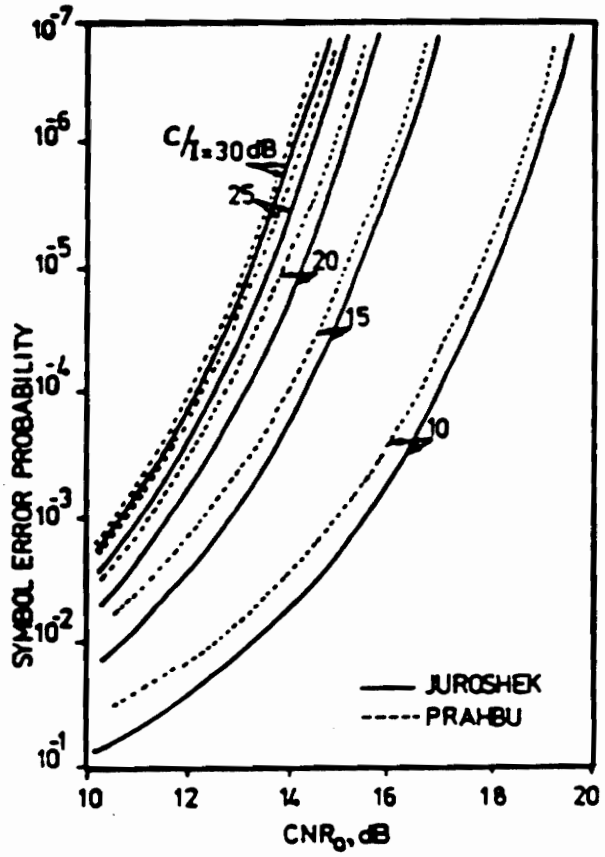

Figure 33. Symbol error probability calculated from Juroshek's model and Prabhu's model from reference [52]

this problem and found that the carrier to interference ratio at the input of the phase detector is:

$$\left(\frac{C}{I}\right)_0 = \left(\frac{C}{I}\right)_i - IRF \quad dB \tag{4.78}$$

where :

$\left(\frac{C}{I}\right)$ = carrier to interference ratio at the input of the band pass filter

IRF = interference reduction factor

$= 10 \log[S_0(f)]$

and

$$S_0(f) = \int_{f_1}^{f_2} S_i(f + \Delta f)\,|H(f)|^2 df$$

where : $f_2 - f_1 =$ common frequency band

S_i = normalized power spectral density of the interfering signal at the input of the band pass filter

This carrier to interference ratio is the one that should be used in equation (4.77).

5.0 Proposed Experiment

In this chapter we make recommendation for an experiment to measure rain scatter interference using OLYMPUS and ACTS. ACTS is the Advanced Communications Technology Satellite. It will enable 20/30 GHz propagation and communication experiments to be made after its launch, planned for 1992. We are proposing to use the 30 GHz beacon, which has characteristics:

Frequency = 27.505 GHz

EIRP = 16.7 dBW

Vertical polarization

On the other hand OLYMPUS, a European (ESA) large experimental three axis stabilized geostationary satellite will be launched in 1989. Its look angles from Blacksburg will be 14 degrees elevation and 108.2 degrees azimuth. Coherent 12, 20, and 30 GHz beacons are

included in the propagation package of OLYMPUS. The 30 GHz beacon that we would to use for a side scattering experiment has the following characteristics:

Frequency = 29.65589 GHz

EIRP (Blacksburg) = 16 dBW

Y polarization (90 $\pm$ 2° with respect to the equatorial plane of the earth).

We propose to have to have two antenna beams (A and B); the first (A), will be pointed at OLYMPUS and the second will look at an geostationary orbital spot 2 ° away from OLYMPUS. The angle between the two beams will therefore be 2.1 ° (see Figure 34). In clear air antenna A will receive the signal directly from OLYMPUS and antenna B will receive the same signal via its side lobes. During a rain event the main beam from antenna will receive the attenuated signal from OLYMPUS, and the off-path beam will receive the scattered signal. It is possible to implement this experiments two different ways :

- The first possibility consists of two separate antennas A and B. This offers more flexibility in pointing the off path beam around the direction of OLYMPUS.

- The second method is to use one antenna on which we will install two feeds, thus creating one beam looking at OLYMPUS and the other one pointed two degrees away. The offset beam is obtained by placing the second feed at a point displaced from the focal point of the reflector and at an optimum location for gain (see Ruze [58]). Since the two feeds will be in a central position and will have reasonable dimensions, the decrease in gain due to aperture blockage will be minor. The main problem will be the appearance of a coma lobe in the offset pattern on the side of the main beam. This may be a critical factor because discriminating against the direct signal from OLYMPUS with the side scatter

beam is important because the signal scattered by the rain is small compared to the direct signal. To solve this we propose to point the offset beam toward OLYMPUS and the central beam toward the interfering signal. Another important consideration is that the amount of scattered power increases with the beamwidth of the receiving antenna. We must therefore consider a trade-off between beamwidth and sidelobes discrimination.

The choice of two 1.22 meter 30 GHz prime focus parabolic reflectors would accommodate the above requirements. The receiver will have a low noise figure and a narrow bandwidth (integration) to minimize the thermal noise. To properly detect the predicted incoherent signal the receiver should have I and Q channels. The scattered signal will be measured simultaneously with downlink attenuation and our 2.8 GHz radar will be used to confirm the presence of rain.

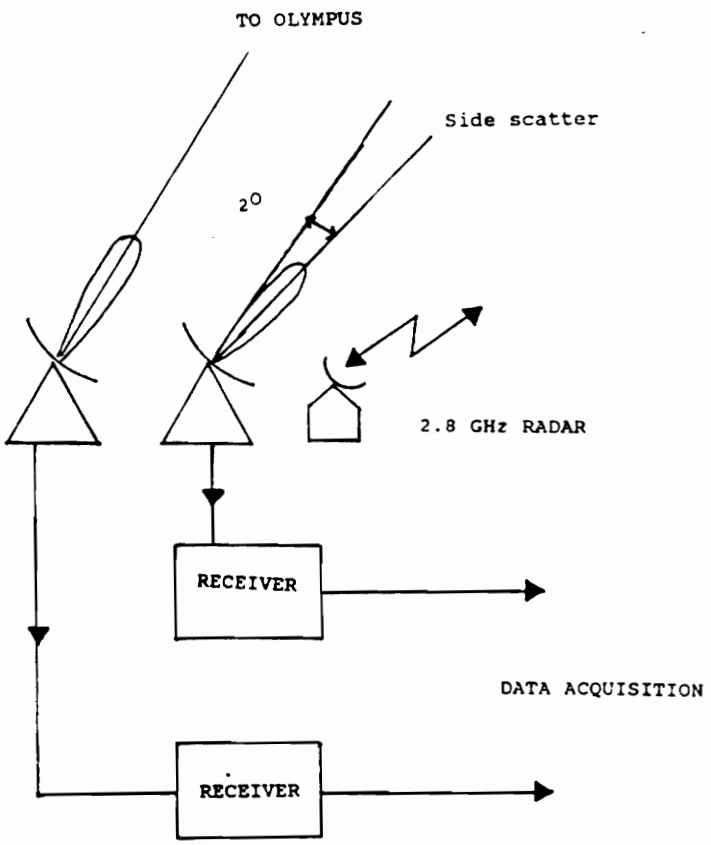

Figure 34. Configuration of the side-scatter experiment.

6.0 Conclusions

The results of this thesis studying the rain scattering interference on satellites link can be summarized as follow:

1. A mathematical formulation of the problem that includes both the rain and systems dependent parameters was presented in Chapter 2.

2. The program written by H. Barksdale to compute the forward scattering coefficient of raindrops using the EBCM was modified to generate scattering coefficient in all directions. The results as it is shown in Figures 11-18 are consistent with those obtained using the finite element technique.

3. Three prediction methods for the side scattered power were presented. The first method based on the vector radiative transfer equation includes the multiple scattering and compute the incoherent scattered power while the two other techniques assume single scattering. The results are consistent and show that the rain scattered power on a space-earth paths can be 40 dB to 60 dB lower than the direct signal from the interfering

satellite. This can create problems for both FM/FDM and digital/TDM VSAT links when the carrier to interference ratio is small and the margin of the system is low.

4. We propose an experiment that would measure the rain side scattering interference using the geostationary satellites OLYMPUS and ACTS. The results obtained in this work may be used to predict and understand the relative importance of rain side-scatter interference and may help in taking corrective actions such as the use of adaptive techniques to decrease potential degradation.

Future work could address the following issues:

1. As far as the multiple scattering is concerned, solve the radiative transfer equation for an arbitrary rain medium including the canting angle of the raindrops and allowing one to mix spherical and spheroidal drops. Also taking into account the dynamic behavior and the spatial structure of the rain could be considered. It would also be interesting to solve the same problem using the analytical multiple scattering theory because radiative transfer is a heuristic theory.

2. For the interference problem for satellite links it is recommended to derive statistical models. Also by conducting experiments in the 10-30 GHz range the verification of the predictions or the derivations of new models will be possible.

List of References

1. T. Oguchi, "Electromagnetic wave propagation in rain and other hydrometeors", *Proc. IEEE,* vol. 71, no.9,pp.1029-1078, Sept. 1983

2. W.L.Stutzman, "A review of theoretical modeling of millimeter wave propagation through precipitation", VPI & SU Technical Report no. T80-1, , 1980

3. B. Ray, "Broadband complex refractive indices of ice and water", *Appl. Opt.*, vol. 11, pp. 1836-1844, Aug. 1972

4. H. Barksdale, " Millimeter wave scattering in the near field of an antenna", Va Tech Ph.D. Dissertation , Dec.1987

5. H.R. Pruppacher and R.L. Pitter, "A semi-empirical determination of the shape of cloud and rain drops", *J. Atmos. Sci.*, vol. 28, pp. 86-94, Jan. 1971

6. J.O. Laws and D.A. Parsons, "The relation of raindrop size to intensity", *Ann. Geophy. Union Trans.*, vol. 24, pp. 452-460, 1943

7. J.S. Marshall and W. Palmer, "The distribution of raindrops with size", *J. Meteor.*, vol. 5, pp. 166-167, Aug. 1948

8. J. Joss, "Raindrop size distribution and sampling size errors", *J. Atmos. Sci.*, vol. 26, pp. 566-569, May. 1969

9. T. Oguchi, "Scattering properties of Pruppacher and Pitter form raindrops and cross polarization due to rain: Calculation at 11, 13, 19.3, and 34.8 GHz", *Radio Sci.*, vol. 12, pp. 247-256, 1970

10. D. E. Setzer, " Anisotropic scattering due to rain at radio relay frequencies.", *BSTJ,* vol. 50, pp. 86-868, March 1971.

11. T. Oguchi, "Scattering from Hydrometeors : A survey", *Radio Sci.*, vol. 16, pp. 691-730, Sept-Oct. 1981

12. M.A. Morgan, "Finite element computation of microwave scattering by raindrops", *Radio Sci.*, vol. 15, pp. 1109-1119, 1980

13. P. Barber and C. Yeh, "Scattering of electromagnetic waves by arbitrarily shaped dielectric bodies", *Appl. Opt.*, vol. 14, pp. 2864-2872, 1975

14. Van de Hulst, *Light Scattering by Small Particles*, Dover Publication Inc., N.Y., 1957

15. A. Ishimaru, *Wave Propagation and Scattering in Random Media*, Academic Press, New York, 1978

16. P.C. Waterman, "Scattering dielectric obstacles", *Alt. Freq.*, vol. 38, pp. 348-352, 1969

17. R.F. Harrington, *Time Harmonic Electromagnetic Fields*, Mc Graw Hill, New York, 1961

18. J.A. Stratton, *Electromagnetic Theory*, Mc Graw Hill, New York, 1941

19. C.W. Bostian *Notes on dyadic Green functions*, unpublished manuscript

20. Chandrasekhar, *Radiative Transfer*, Dover Publication Inc., N.Y., 1960

21. Kraus, *Radio astronomy*, Cygnus-Quasar Books, 1966

22. L.H.Doherty and A Stone, " Forward scatter from rain ", *IRE Trans. Ant. and Prop.*, July 1960, pp. 414-418

23. D. C. Hogg, R.A. Semplak and D.A. Gray, " Measurement of microwave interference at 4 Gc due to scatter by rain .", *Proc. IRE*, pp. 500, March 1963

24. L.T. Gusler and D.C. Hogg, "Some calculation on coupling between satellite communications and terrestrial radio relay systems due to scattering by rain ", *BSTJ*, vol. 49, pp. 1491-1512, Sept. 1970

25. R.K. Crane, " Bistatic scatter from rain ", *IEEE Trans. Ant. and Prop.*, vol. AP-22, no.2, pp. 310-320, March 1974

26. R. W. Hubbard, "Measurement and Prediction of Bistatic Radio Scattering due to Precipitation", *J. Res. Atmos.*, vol. 8, pp. 365-373, Jan. 1974

27. S. Sagakami, "Some Experimental Results on Bistatic Scatter from Rain", *IEEE Trans. Ant. and Prop.*, vol AP-28, no.2, pp. 161-165, March 1980

28. J. Awaka, " A prediction method for the received power from rain scattering ", *Radio Sci.*, vol. 19, no.2, pp. 643-651, March-Apr 1987

29. C. Paraboni, et al "Interference due to rain scatter: preliminary results obtained in the framework of the SIRIO SHF experiment by radar simulation and bistatic link experiment", *Alt. Freq.*, vol. 56, pp. 161-166, Jan.-Apr. 1987

30. W.L. Flock *Propagation Effects on Satellite Systems at Frequencies below 10 GHz* , NASA Reference Publication 1108 , Sept. 1983

31. CCIR, *Recommendations and Reports of the CCIR Group 5*, 1982

32. H. C. Shieh, " The modelling of bistatic rain scatter interference including a consideration of multiple scattering effects " Dissertation, Darmouth College, June, 1987

33. T. S. Chu, " Rain scatter interference on a earth space path ", *IEEE Trans. Ant. and Prop.*, vol. AP-25, pp.287-288, March 1977

34. D. Cox, H. Arnold and H. Hoffman, "Measured bounds on rain scatter coupling between space-earth radio paths ", *IEEE Trans. on Ant. and Prop.*, vol. AP-30, no. 3, pp.493-497, May 1982

35. T. Li, W. C. Jakes, and J A Morisson ," Forward scattering due to rain at 11 GHz", *IEEE Trans. Ant. and Prop.*, vol. AP-25, pp. 646-649, Sept 1977

36. R. L. Olsen " A review of theories of coherent radio wave propagation through precipitation media of randomly oriented scatterers , and the role of multiple scattering. ", *Radio Sci.*, vol. 17, no. 5, pp. 913-828, Sept-Oct 1982.

37. P. Delogne and M. Lobelle, " Numerical calculations on microwave propagation through rain", *Ann. des Telecomm.*, vol. 32, no. 11-12 , 1987.

38. P. Delogne and P. Sobiesky, " Fine structure of microwave cross polarization due to precipitation ", *Ann. des Telecomm.*, vol. 32, no. 11-12 , 1987.

39. T. Oguchi, "Effect of incoherent scattering on attenuation and depolarization of millimeter and optical waves due to hydrometeors ", *Radio Sci.*, vol. 21, no.4, pp. 717-730, July-Aug. 1986.

40. T. Oguchi, "Effect of incoherent scattering on attenuation and cross polarization of millimeter waves due to rain: Preliminary calculations at 34.8 and 82 GHz for spherical raindrops", *Ann. des Telecomm.*, vol. 35, no. 11-12, pp. 380-389, 1980

41. T. Oguchi, "Attenuation and phase rotation of radio waves due to rain: Calculations at 19.3 and 34.8 GHz ", *Radio Sci.*, vol. 8, no.1, pp. 31-38 Jan. 1973

42. A. Tsolakis and W. L. Stutzman, " Multiple scattering effect of electromagnetic waves by rain ", *Radio Sci.*, vol. 17, no. 6 , pp. 1495-1502, Nov.-Dec. 1982

43. C. Capsoni et Al, "Incoherent effects in electromagnetic propagation through rain ", *Ann. des Telecomm.*, vol. 32, no. 11-12, pp. 409-414, 1977

44. W.G. Tam and A. Zardecki, "Off-axis propagation of a laser beam in low visibility weather condition", *Appl. Opt.*, vol. 19, no. 6, Aug. 1980

45. A. Ishimaru, " Theory and application of wave propagation and scattering in random media ", *Proc. of IEEE*, vol. 65, no. 7, pp. 1030-1061, Jul. 1977

46. A. Ishimaru, " Multiple scattering calculations for non spherical particles based on the vector radiative transfer theory ", *Radio Sci.*, vol. 19, no. 5, pp. 1356-1366, Sept-Oct 1984

47. A. Ishimaru and C W Yeh, " Matrix representation of the vector radiative transfer theory for randomly distributed non spherical particles ", *J. Opt. Soc. Am.*, vol. 1, no. 4, pp. 359-364, Apr. 1984

48. A. Ishimaru, R Woo, J W Armstrong and D C Blackman, " Multiple scattering calculation on rain effect ", *Radio Sci.*, vol. 17, no.6, pp. 1425-1433, Nov-Dec, 1982

49. A. Ishimaru, and R.L.T. Cheung, " Multiple scattering effects on wave propagation due to rain ", *Ann. des Telecomm.*, vol. 35, no. 11-12, pp. 373-379, Nov-Dec 1980

50. R.K. Crane, " Propagation phenomena affecting satellite communication systems operating in the centimeter and millimeter bands", *Proc. IEEE*, vol. 58, pp. 173-188, 1971

51. M. Abramovitz and I. Stegun, *Handbook of Mathematical Functions with Formulas Graphs and Mathematical Tables*, New York, Dover Publications, 1970

52. T. Pratt et al, " System performance of dual polarization satellite communication links affected by attenuation and depolarization", *Proc. IEEE. Milcom 83 Conference*, pp. 135-139, Nov. 1983.

53. V.K. Prabhu, " Error rate consideration for coherent PSK systems with co-channel interferences", *BSTJ*, pp. 743-761, Mar. 1969

54. R.E. Castle and C.W. Bostian, " Combining the effect of rain induced attenuation and depolarization in digital satellite systems", *IEEE Trans. on Aero. and Elec. Sys.*, vol. AES-15 , no. 12, pp. 299-301, Mar. 1979

55. J.R. Juroshek, " An approximate method for calculating the performance of CPSK and NCFSK modems in gaussian noise and interference ", U.S. Dept. of Commerce , Office of Telecommunication, Boulder Colorado, OF-Rep 77-109

56. P. Constantinou, " FM-TV interference into digital communication systems", unpublished manuscript

57. ACTS/OLYMPUS Experiments, *Report EE SATCOM 88-4*, Sept. 1988

58. J. Ruze, "Lateral feed displacement in a paraboloid " , *IEEE Trans. Ant. and Prop.*, vol. AP 13, pp. 660-665, Sept.1965

Appendix A. EBCM

This Appendix contains the program SCAMP computing the scattering of single raindrops using the EBCM.

```
C****** SCATTERING PARAMETERS - OBLATE SPHEROIDAL RAINDROPS *********
C                                                                      *
C   THIS PROGRAM USES THE EBCM TO COMPUTE SCATTERING PARAMETERS        *
C  FOR OBLATE SPHEROIDAL RAINDROPS.  THE PARAMETERS COMPUTED ARE       *
C  THE SCATTERING AMPLITUDE.                                           *
C                                                                      *
C   USER INPUTS TO THE PROGRAM ARE:                                    *
C                                                                      *
C        FREQ= FREQUENCY OF OPERATION IN GHZ.                          *
C                                                                      *
C        RIRE(RIIM)= REAL(IMAG) PART OF THE REFRACTIVE                 *
C                INDEX OF WATER AT THE FREQUENCY                       *
C                AND TEMPERATURE OF INTEREST.                          *
C                                                                      *
C        TETA,PHI   OBSERVATION ANGLES                                 *
C                                                                      *
C        EVR        DROP RADIUS                                        *
C**********************************************************************

      COMPLEX*16 K,FSAMP1,FSAMP2,AB(60),Y(60),CD(60),SNTRNL(0:30,60,60)
      COMPLEX*16 NTRNL(60,60),SCTR(60,60),FSAMP01,FSAMP02,KR(248)
      COMPLEX*16 BESSEL(6,30,248),CHI(0:30,30,30,4,2)
      COMPLEX IMAG,RI
      REAL*8 SCRS,WGTS(8),NDS(8),PI,K0,CSALPHA,R(248),CSTETA,SNTETA
      REAL*8 LGNDR(3,30,248),VR(248),VTH(248),SNPHI,CSPHI,CPHI,SPHI
      REAL*8 R2TAU(248),ETA(248),K0R(248),SNALPHA,FMAG1,FMAG2,SCRS0
      REAL*8 FSAMPR1,FSAMPR2,FSAMPI1,FSAMPI2
      REAL*8 FACT(0:50)
      REAL*8 TESTR1,TESTI1,TESTR2,TESTI2,TESTSC,MU(6)
      REAL MAX,PHI,MPHI,TETAK(12)
      INTEGER IPIVOT(0:30,59),KAPO,LAPO
      COMMON /BLOC1/ K,K0,EVR,IPOL
      COMMON /BLOC2/ CSALPHA,IMAG,CSTETA
      COMMON /BLOC3/ WGTS,NDS,PI
      COMMON /BLOC4/ M,LMIN,LMAX,ISAVE
      COMMON /BLOC5/ RI
      COMMON /BLOC6/ AB,CD,SCTR
      COMMON /BLOC7/ SCRS,FSAMP1,FSAMP2
      COMMON /BLOC8/ NTRNL,SNTRNL,IPIVOT,N,IER
      COMMON /BLOC9/ NQI,NQP
      COMMON /BLOC10/ VR,VTH,R2TAU
      COMMON /BLOC11/ BESSEL
      COMMON /BLOC12/ LGNDR
      COMMON /BLOC13/ ETA
      COMMON /BLOC14/ K0R,KR
      COMMON /BLOC15/ CHI
      COMMON /BLOC16/ Y
      COMMON /BLOC17/ CSPHI,SNPHI
      COMMON /BLOC18/ FACT

C-----------------------------------------------------------------
      FACT(0)=1
      FACT(1)=1
      DO 2345 IJKL=2,50
2345  FACT(IJKL)=IJKL*FACT(IJKL-1)
C-----------------------------------------------------------------
      READ(5,*) KAPO,LAPO
      MU(1)=0.981560634246719
      MU(4)=0.587317954286617
      MU(2)=0.904117256370475
      MU(5)=0.367831498998180
      MU(3)=0.769902674194305
      MU(6)=0.125233408511469
      IMAG=(0.,1.)
      PI=3.141592653589793
      DO 9000 IKK=1,6
```

```
      TETAK(IKK)=ARCOS(MU(IKK))/PI*180.
 9000  TETAK(13-IKK)=ARCOS(-MU(IKK))/PI*180.

   66 CONTINUE
      READ(5,*,END=500)FREQ,RIRE,RIIM,EVR
CC  CALCUL POUR ALPHA =0
      RI=CMPLX(RIRE,RIIM)
      K0=2.*PI*FREQ/30.
      K=K0*RI
  777 CONTINUE
C     WRITE(8,100)FREQ,RIRE,RIIM,EVR
      NU1=EVR*(2.-EVR)
      NU2=EVR*DBLE((1.-EVR)**(2./3.))

C  CHOOSE INITIAL LMAX.

      RAD=EVR/(1.-EVR)**(1./3.)
      DO 1000 NANG=0,24
      TETA=0.
      PHI=0.
      CSTETA=1.
      SNTETA=0.
      CSPHI=1.
      SNPHI=0.
      LMAX=2.*K0*RAD+1.
   55 Z0=FLOAT(LMAX)+.5
      Z1=(EXP(1.)*K0*RAD/(2.*Z0))**Z0
      IF(Z1.GT.5.0E-05) THEN
        LMAX=LMAX+1
        GO TO 55
      ENDIF
      LLL=LMAX
      LL=LMAX+8
      NQI=LL+1
      NQP=8*NQI

C  DETERMINE THE QUADRATURE NODES AND COMPUTE THE SPHERICAL
C  BESSEL FUNCTIONS.

      CALL QPTS
      CALL BESFIL

C  ALPHA=0 DEGREES.

      ISAVE=0
      IPOL=1
      ALPHA=0.
      IF(ALPHA.EQ.90.) THEN
        CSALPHA=0.
        SNALPHA=1.
      ELSE
        IF(ALPHA.EQ.180.) THEN
          CSALPHA=-1.
          SNALPHA=0.
        ELSE
          CSALPHA=DCOS(PI*ALPHA/180.)
          SNALPHA=DSIN(PI*ALPHA/180.)
        ENDIF
      ENDIF
      M=1
      LMIN=1
      TESTR1=0.
      TESTR2=0.
      TESTI1=0.
      TESTI2=0.
      FSAMP01=(0.,0.)
```

```
      FSAMP02=(0.,0.)
   70 FSAMP1=(0.,0.)
      FSAMP2=(0.,0.)
      SCRS=0.
      N=2*LMAX

CC  COMPUTE SURFACE INTEGRALS FOR AZIMUTHAL MODE M=1.

      CALL LGNFIL
      CALL CHIFIL

CC  COMPUTE T-MATRIX FOR AZIMUTHAL MODE M=1.

      CALL MATFIL(NTRNL,2,1)
      CALL FACTOR
      IF(IER.EQ.2) THEN
C       WRITE(8,103)IPOL,M
C       WRITE(8,104)
      ENDIF
      CALL MATFIL(SCTR,1,1)
      CALL VECFIL
      CALL SOLVE

CC  COMPUTE EXPANSION COEFFICIENTS FOR THE SCATTERED FIELD.

      CALL COEFF(M,N)

CC   CALCULATE SCATTERING PARAMETERS AND CHECK FOR CONVERGENCE.

      CSPHI=DCOS(PI*M*PHI/180.)
      SNPHI=DSIN(PI*M*PHI/180.)
      CALL PARAM
      IF (DREAL(FSAMP1).NE.0.) THEN
         TESTR1=DABS(DREAL(FSAMP1-FSAMP01)/DREAL(FSAMP1))
      ENDIF
      IF (DIMAG(FSAMP1).NE.0.) THEN
         TESTI1=DABS(DIMAG(FSAMP1-FSAMP01)/DIMAG(FSAMP1))
      ENDIF
      IF (DREAL(FSAMP2).NE.0.) THEN
         TESTR2=DABS(DREAL(FSAMP2-FSAMP02)/DREAL(FSAMP2))
      ENDIF
      IF (DIMAG(FSAMP2).NE.0.) THEN
         TESTI2=DABS(DIMAG(FSAMP2-FSAMP02)/DIMAG(FSAMP2))
      ENDIF
      IF((TESTR1.GT.1.E-3).OR.(TESTI1.GT.1.E-3).OR.(TESTR2.GT.1.E-3).OR.
     &(TESTI2.GT.1.E-3)) THEN
         LLL=LLL+1
         IF(LLL.GT.LL) GO TO 201
         LMAX=LMAX+1
         FSAMP01=FSAMP1
         FSAMP02=FSAMP2
         ISAVE=1
         GO TO 70
      ENDIF
  201 TEST=MAX(TESTR1,TESTI1,TESTR2,TESTI2)
      FSAMPR1=DREAL(FSAMP1)/K0
      FSAMPI1=DIMAG(FSAMP1)/K0
      FSAMPR2=DREAL(FSAMP2)/K0
      FSAMPI2=DIMAG(FSAMP2)/K0
      CRSS=SCRS*PI/K0**2
C     WRITE(9,102)ALPHA,PHI,TETA,FSAMPR1,FSAMPI1,FSAMPR2,FSAMPI2,EVR
CC-----------------------------------------------------------------------
C BOUCLE POUR TETA OU PHI VARIABLE
      TETA=TETAK(KAPO)
      PHI=FLOAT(NANG)*180./24.
      IF(TETA.EQ.90.) THEN
```

```
        CSTETA=0.
        SNTETA=1.
      ELSE
        IF(TETA.EQ.180.) THEN
          CSTETA=-1.
          SNTETA=0.
        ELSE
          CSTETA=DCOS(PI*TETA/180.)
          SNTETA=DSIN(PI*TETA/180.)
        ENDIF
      ENDIF
C     WRITE(8,250) TETA,PHI

C  COMPUTE SURFACE INTEGRALS FOR AZIMUTHAL MODE M=0.
      ALPHA=TETAK(LAPO)
      IF(ALPHA.EQ.90.) THEN
        CSALPHA=0.
        SNALPHA=1.
      ELSE
        IF(ALPHA.EQ.180.) THEN
          CSALPHA=-1.
          SNALPHA=0.
        ELSE
          CSALPHA=DCOS(PI*ALPHA/180.)
          SNALPHA=DSIN(PI*ALPHA/180.)
        ENDIF
      ENDIF
      ISAVE=0
      M=0
      LMIN=1
      N=LMAX
      CALL LGNFIL
      CALL CHIFIL
      CALL MATFIL(NTRNL,2,1)
      CALL FACTOR

C  POLARIZATIONS 1 AND 2, ALPHA 90 DEGREES AND TETA AND PHI VARIABLE

      MMAX=1
  333 CONTINUE
C     WRITE(8,105)IPOL
      FSAMP01=(0.,0.)
      FSAMP02=(0.,0.)
      SCRS=0.
C     SCRS0=0.
C     TESTSC=0.
      TESTR1=0
      TESTR2=0.
      TESTI1=0.
      TESTI2=0.
303   FSAMP1=(0.,0.)
      FSAMP2=(0.,0.)
      M=0
C     IF (DABS(CSTETA).EQ.1.) M=1
  304 LMIN=M
      IF(M.EQ.0) LMIN=1
      N=2*(LMAX-LMIN+1)
      IF(M.EQ.0) N=LMAX
      IF(M.LE.MMAX) GO TO 733

CC  COMPUTE SURFACE INTEGRALS.

      CALL LGNFIL
      CALL CHIFIL
  733 CONTINUE
```

```
CC  COMPUTE T-MATRICIES.

      IF(M.LE.MMAX.AND.IPOL.EQ.1) GO TO 744
      CALL MATFIL(NTRNL,2,IPOL)
      CALL FACTOR
      IF(IER.EQ.2) THEN
C       WRITE(8,103)IPOL,M
C       WRITE(8,104)
      ENDIF
  744 CONTINUE
      CALL MATFIL(SCTR,1,IPOL)
      CALL VECFIL
      CALL SOLVE

CC  COMPUTE EXPANSION COEFFICIENTS FOR THE SCATTERED FIELD.

      CALL COEFF(M,N)

CC  COMPUTE SCATTERING PARAMETERS AND CHECK FOR CONVERGENCE.
      MPHI=M*PHI
      IF (INT(MPHI/90.)-MPHI/90..NE.0.) THEN
        CSPHI=DCOS(PI*MPHI/180.)
        SNPHI=DSIN(PI*MPHI/180.)
      ELSE
        RESTE=INT(MPHI/360.)-MPHI/360.
        IF(RESTE.EQ.0.) THEN
          CSPHI=1.
          SNPHI=0.
        ENDIF
        IF (ABS(RESTE).EQ..25) THEN
          CSPHI=0.
          SNPHI=1.
        ENDIF
        IF (ABS(RESTE).EQ..5) THEN
          CSPHI=-1.
          SNPHI=0.
        ENDIF
          IF (ABS(RESTE).EQ..75) THEN
          CSPHI=0.
          SNPHI=-1.
          ENDIF
      ENDIF
      CALL PARAM
      IF (DREAL(FSAMP1).NE.0.) THEN
         TESTR1=DABS(DREAL(FSAMP1-FSAMP01)/DREAL(FSAMP1))
      ENDIF
      IF (DIMAG(FSAMP1).NE.0.) THEN
         TESTI1=DABS(DIMAG(FSAMP1-FSAMP01)/DIMAG(FSAMP1))
      ENDIF
      IF (DREAL(FSAMP2).NE.0.) THEN
         TESTR2=DABS(DREAL(FSAMP2-FSAMP02)/DREAL(FSAMP2))
      ENDIF
      IF (DIMAG(FSAMP2).NE.0.) THEN
         TESTI2=DABS(DIMAG(FSAMP2-FSAMP02)/DIMAG(FSAMP2))
      ENDIF
      IF((TESTR1.GT.1.E-3).OR.(TESTI1.GT.1.E-3).OR.(TESTR2.GT.1.E-3).OR.
     &(TESTI2.GT.1.E-3).OR.((M.EQ.0).AND.((SNTETA.EQ.0.).OR.(SNALPHA.EQ.
     1)))) THEN
         M=M+1
         FSAMP01=FSAMP1
         FSAMP02=FSAMP2
         IF(M.LE.LMAX) GO TO 304
      ENDIF
      TEST=MAX(TESTR1,TESTI1,TESTR2,TESTI2)
      FSAMPR1=DREAL(FSAMP1)/K0
      FSAMPI1=DIMAG(FSAMP1)/K0
```

```
      FSAMPR2=DREAL(FSAMP2)/K0
      FSAMPI2=DIMAG(FSAMP2)/K0
      CRSS=SCRS*PI/K0**2
      WRITE(8,102)ALPHA,PHI,TETA,FSAMPR1,FSAMPI1,FSAMPR2,FSAMPI2,EVR
      IF(M.GT.MMAX) MMAX=M
      IPOL=IPOL+1
      IF(IPOL.EQ.2) GO TO 333
C     WRITE(6,104)
1000  CONTINUE
      GO TO 66
  100 FORMAT(26X,'FREQUENCY=',F4.1,' GHZ',/,22X,'REF INDEX=(',
     &F6.4,',',F7.4,')',/,20X,'EQUIVOLUMETRIC RADIUS=',F5.3,
     &' CM',/,20X,30('-'))
  101 FORMAT(//,1X,'DEBUT          ',//,22X,'F(0,0)',30X,'SCRS',/,
     &23X,'(CM)',17X,'(CMSQ)',8X,'TEST',5X,'LMAX',/,3X,E11.5,
     &',',E12.5,2X,E11.5,',',E12.5,3X,E11.5,3X,E10.4,3X,I2)
  105 FORMAT(//,1X,'POLARIZATION ',I1,':',//,3X,'ALPHA',12X,
     &'F(0,TETA)',36X,'SCRS',/,1X,'(DEGREES)',13X,'(CM)',38X,
     &'(CMSQ)',8X,'TEST',5X,'MMAX')
C 102 FORMAT(1X,F6.2,1X,F6.2,1X,F6.2,1X,F6.2,1X,E14.8,1X,E14.7,2X,E14.8,1X,E14.8
C     &,2X,E11.5,1X,E10.4,1X,I2,1X,I1)
  102 FORMAT(1X,F6.2,1X,F6.2,1X,F6.2,1X,F6.2,1X,E21.15,1X,E21.14,2X,E21.15,1X,
     &E21.15,2X,F9.5)
  103 FORMAT(1X,'IER=2 FOR POLARIZATION ',I1,' M = ',I2)
  104 FORMAT(1X,92('*'),/)
  250 FORMAT (/,3X ,'TETA=',F5.1,2X,'PHI=',F5.1)
 1200 FORMAT(2X,F6.2,2X,F6.2,4X,E10.5,2X,F8.3,4X,E10.5,2X,F8.3,2X,I1)
  500 STOP
      END



      SUBROUTINE MATFIL(C,IBES,IPOL)
      COMPLEX RI
      COMPLEX*16 C(60,60),CHI(0:30,30,30,4,2),D1,D2,D3,D4
      INTEGER P
      COMMON /BLOC4/ M,LMIN,LMAX,ISAVE
      COMMON /BLOC5/ RI
      COMMON /BLOC15/ CHI

      IMAX=LMAX-LMIN+1
      I=1
      DO 1 L=LMIN,LMAX
      II=I+IMAX
      J=1
      DO 2 P=LMIN,LMAX
      JJ=J+IMAX
      D1=CHI(M,L,P,1,IBES)
      D2=CHI(M,L,P,2,IBES)
      IF(M.EQ.0) THEN
        IF(IPOL.EQ.1) C(I,J)=D2+RI*D1
        IF(IPOL.EQ.2) C(I,J)=D1+RI*D2
      ELSE
        D3=CHI(M,L,P,3,IBES)
        D4=CHI(M,L,P,4,IBES)
        C(I,J)=D1+RI*D2
        C(I,JJ)=D3+RI*D4
        C(II,J)=-(D4+RI*D3)
        C(II,JJ)=D2+RI*D1
        IF(IPOL.EQ.2) THEN
          C(I,JJ)=-C(I,JJ)
          C(II,J)=-C(II,J)
        ENDIF
      ENDIF
    2 J=J+1
```

```
 1 I=I+1
   RETURN
   END



   SUBROUTINE CHIFIL
   COMPLEX*16 CHI(0:30,30,30,4,2),NTGRL
   INTEGER P
   COMMON /BLOC4/ M,LMIN,LMAX,ISAVE
   COMMON /BLOC15/ CHI

   IF(ISAVE.EQ.1) GO TO 100
   DO 1 L=LMIN,LMAX
   DO 1 P=LMIN,LMAX
   DO 1 IBES=1,2
   DO 1 I=1,4
   IF((I.EQ.3.OR.I.EQ.4).AND.M.EQ.0) GO TO 1
   CHI(M,L,P,I,IBES)=NTGRL(M,L,P,I,IBES)
 1 CONTINUE

100 LMAXM1=LMAX-1
   DO 2 I=1,4
   DO 2 IBES=1,2
   DO 3 L=LMIN,LMAXM1
   CHI(M,L,LMAX,I,IBES)=NTGRL(M,L,LMAX,I,IBES)
 3 CHI(M,LMAX,L,I,IBES)=NTGRL(M,LMAX,L,I,IBES)
 2 CHI(M,LMAX,LMAX,I,IBES)=NTGRL(M,LMAX,LMAX,I,IBES)
   RETURN
   END



   SUBROUTINE VECFIL
   COMPLEX*16 K,Y(60)
   COMPLEX IMAG,FJML
   REAL*8 K0,CSALPHA,LGNDR2,LGNDR3,FA,FB
   COMMON /BLOC1/ K,K0,EVR,IPOL
   COMMON /BLOC2/ CSALPHA,IMAG,CSTETA
   COMMON /BLOC4/ M,LMIN,LMAX,ISAVE
   COMMON /BLOC16/ Y
   I=1
   DO 2 L=LMIN,LMAX
   FA=LGNDR2(L,M,CSALPHA)
   FB=LGNDR3(L,M,CSALPHA)
   FJML=4.*IMAG**(-L)
   II=I+LMAX-LMIN+1
   IF(IPOL.EQ.1) THEN
     IF(M.EQ.0) THEN
       Y(I)=IMAG*FJML*FB
     ELSE
       Y(I)=FJML*FA
       Y(II)=IMAG*FJML*FB
     ENDIF
   ELSE
     Y(I)=-FJML*FB
     IF(M.NE.0) Y(II)=IMAG*FJML*FA
   ENDIF
 2 I=I+1
   RETURN
   END
```

```
      SUBROUTINE FACTOR
      COMPLEX*16 C(60,60),SC(0:30,60,60),Q,Z,TEMP
      INTEGER IPIVOT(0:30,59)
      COMMON /BLOC4/ M,LMIN,LMAX,ISAVE
      COMMON /BLOC8/ C,SC,IPIVOT,N,IER
      IER=1
      NM1=N-1
      DO 1 I=1,N
      DO 1 J=1,N
    1 SC(M,I,J)=C(I,J)
      DO 8 I=1,NM1
      PIVOT=0.
      DO 3 J=I,N
      RTEMP=CDABS(SC(M,J,I))
      IF(PIVOT.GE.RTEMP) GO TO 3
      PIVOT=RTEMP
      IPIVOT(M,I)=J
    3 CONTINUE
      IF(PIVOT.EQ.0.) GO TO 13
      IF (IPIVOT(M,I).EQ.I) GO TO 5
      DO 4 K=I,N
      TEMP=SC(M,I,K)
      SC(M,I,K)=SC(M,IPIVOT(M,I),K)
    4 SC(M,IPIVOT(M,I),K)=TEMP
    5 IP1=I+1
      DO 7 K=IP1,N
      Q=-SC(M,K,I)/SC(M,I,I)
      SC(M,K,I)=Q
      DO 6 J=IP1,N
    6 SC(M,K,J)=Q*SC(M,I,J)+SC(M,K,J)
    7 CONTINUE
    8 CONTINUE
      Z=(0.,0.)
      IF(SC(M,N,N).EQ.Z) GO TO 13
      RETURN
   13 IER=2
      RETURN
      END



      SUBROUTINE SOLVE
      COMPLEX*16 SC(0:30,60,60),Y(60),CD(60),Q,TEMP
      COMPLEX*16 AB(60),SCTR(60,60),C(60,60)
      INTEGER IPIVOT(0:30,59)
      COMMON /BLOC4/ M,LMIN,LMAX,ISAVE
      COMMON /BLOC6/ AB,CD,SCTR
      COMMON /BLOC8/ C,SC,IPIVOT,N,IER
      COMMON /BLOC16/ Y
      NP1=N+1
      NM1=N-1
      DO 1 I=1,NM1
      TEMP=Y(I)
      Y(I)=Y(IPIVOT(M,I))
      Y(IPIVOT(M,I))=TEMP
      IP1=I+1
      DO 4 J=IP1,N
    4 Y(J)=Y(J)+Y(I)*SC(M,J,I)
    1 CONTINUE
      CD(N)=Y(N)/SC(M,N,N)
      DO 10 K=1,NM1
      Q=(0.,0.)
      DO 9 J=1,K
    9 Q=Q+SC(M,N-K,NP1-J)*CD(NP1-J)
```

```
10 CD(N-K)=(Y(N-K)-Q)/SC(M,N-K,N-K)
   RETURN
   END



   SUBROUTINE COEFF(M,N)
   COMPLEX*16 AB(60),CD(60),SCTR(60,60)
   COMMON /BLOC6/ AB,CD,SCTR
   DO 20 I=1,N
   AB(I)=(0.,0.)
   DO 20 J=1,N
20 AB(I)=AB(I)-SCTR(I,J)*CD(J)
   RETURN
   END



   SUBROUTINE PARAM
   COMPLEX*16 FSAMP1,FSAMP2,AB(60),CD(60),SCTR(60,60),K
   COMPLEX IMAG,JL
   REAL*8 FA,FB,LGNDR2,LGNDR3,D,D1,D2
   REAL*8 SCRS,K0,CSALPHA,PI,CSTETA,SNPHI,CSPHI
   REAL*8 FACT(0:50)
   COMMON /BLOC1/ K,K0,EVR,IPOL
   COMMON /BLOC2/ CSALPHA,IMAG,CSTETA
   COMMON /BLOC4/ M,LMIN,LMAX,ISAVE
   COMMON /BLOC6/ AB,CD,SCTR
   COMMON /BLOC7/ SCRS,FSAMP1,FSAMP2
   COMMON /BLOC17/ CSPHI,SNPHI
   COMMON /BLOC18/ FACT
   PI=3.141592653589793
   I=1
   DO 21 L=LMIN,LMAX
   II=I+LMAX-LMIN+1
   FA=LGNDR2(L,M,CSTETA)
   FB=LGNDR3(L,M,CSTETA)
   JL=IMAG**L
   D1=(2*L+1)*FACT(L-M)
   D2=4*L*(L+1)*FACT(L+M)
   D=D1/D2
   IF(M.NE.0) D=2.*D
   IF(M.EQ.0) THEN
      IF(IPOL.EQ.1) FSAMP1=FSAMP1+JL*D*CSPHI*AB(I)*FB
      IF(IPOL.EQ.2) FSAMP1=FSAMP1+JL*D*SNPHI*AB(I)*FB
      IF(IPOL.EQ.1) FSAMP2=FSAMP2-IMAG*JL*D*SNPHI*AB(I)*FB
      IF(IPOL.EQ.2) FSAMP2=FSAMP2-IMAG*JL*D*CSPHI*AB(I)*FB
      SCRS=SCRS+D*CDABS(AB(I))**2
   ELSE
      IF(IPOL.EQ.1) FSAMP1=FSAMP1+JL*D*CSPHI*(AB(II)*FB+IMAG*AB(I)*FA
  &)
      IF(IPOL.EQ.2) FSAMP1=FSAMP1+JL*D*SNPHI*(AB(II)*FB-IMAG*AB(I)*FA
  &)
      IF(IPOL.EQ.1) FSAMP2=FSAMP2-JL*D*SNPHI*(AB(II)*FA+IMAG*AB(I)*FB
  &)
      IF(IPOL.EQ.2) FSAMP2=FSAMP2+JL*D*CSPHI*(AB(II)*FA-IMAG*AB(I)*FB
  &)
      SCRS=SCRS+D*(CDABS(AB(I))**2+CDABS(AB(II))**2)
   ENDIF
21 I=I+1
   RETURN
   END
```

```
      SUBROUTINE BESFIL
      COMPLEX*16 BESSEL(6,30,248),CBESJ,Y,KR(248),BES3(0:31)
      COMPLEX MIMAG
      REAL*8 K0R(248),BES1(0:31),BES2(0:31),SBESJ,SBESY,X
      COMMON /BLOC9/ NQI,NQP
      COMMON /BLOC11/ BESSEL
      COMMON /BLOC14/ K0R,KR
      MIMAG=(0.,-1.)
      NQIM1=NQI-1
      NQIM2=NQI-2
      DO 1 NP=1,NQP
      X=K0R(NP)
      Y=KR(NP)
      BES2(0)=-1.*DCOS(X)/X
      BES2(1)=BES2(0)/X-DSIN(X)/X
      DO 51 L=2,NQI
   51 BES2(L)=(2*L-1)*BES2(L-1)/X-BES2(L-2)
      BES1(NQI)=SBESJ(X,NQI)
      BES1(NQIM1)=SBESJ(X,NQIM1)
      BES3(NQI)=CBESJ(Y,NQI)
      BES3(NQIM1)=CBESJ(Y,NQIM1)
      L=NQIM2
      DO 52 I=0,NQIM2
      TLP3=2*L+3
      BES1(L)=TLP3*BES1(L+1)/X-BES1(L+2)
      BES3(L)=TLP3*BES3(L+1)/Y-BES3(L+2)
   52 L=L-1
      DO 53 L=0,NQI
      BES1(L)=DSIN(X)*BES1(L)/(X*BES1(0))
   53 BES3(L)=CDSIN(Y)*BES3(L)/(Y*BES3(0))
      DO 4 L=1,NQIM1
      TLP1=2*L+1
      BESSEL(1,L,NP)=BES1(L)
      BESSEL(2,L,NP)=BES1(L)+MIMAG*BES2(L)
      BESSEL(3,L,NP)=((L+1)*BES1(L-1)-L*BES1(L+1))/TLP1
      BESSEL(4,L,NP)=BESSEL(3,L,NP)+MIMAG*((L+1)*BES2(L-1)-L*
     &BES2(L+1))/TLP1
      BESSEL(5,L,NP)=BES3(L)
    4 BESSEL(6,L,NP)=((L+1)*BES3(L-1)-L*BES3(L+1))/TLP1
    1 CONTINUE
      RETURN
      END



      SUBROUTINE LGNFIL
      REAL*8 LGNDR(3,30,248),LGNDR1,LGNDR2,LGNDR3,ETA(248)
      COMMON /BLOC4/ M,LMIN,LMAX,ISAVE
      COMMON /BLOC9/ NQI,NQP
      COMMON /BLOC12/ LGNDR
      COMMON /BLOC13/ ETA
      LL=LMIN
      IF(ISAVE.EQ.1) LL=LMAX
      DO 1 NP=1,NQP
      DO 1 L=LL,LMAX
      LGNDR(1,L,NP)=LGNDR1(L,M,ETA(NP))
      LGNDR(2,L,NP)=LGNDR2(L,M,ETA(NP))
    1 LGNDR(3,L,NP)=LGNDR3(L,M,ETA(NP))
      RETURN
      END
```

```
      SUBROUTINE QPTS
      COMPLEX*16 K,KR(248)
      REAL*8 D1,ARG,PI,WGTS(8),NDS(8),ETA(248),TAU,FTHTA,R
      REAL*8 R2TAU(248),K0R(248),VR(248),VTH(248),K0,NET
      REAL NU
      COMMON /BLOC1/ K,K0,EVR,IPOL
      COMMON /BLOC3/ WGTS,NDS,PI
      COMMON /BLOC9/ NQI,NQP
      COMMON /BLOC10/ VR,VTH,R2TAU
      COMMON /BLOC13/ ETA
      COMMON /BLOC14/ K0R,KR
      D1=1.
      NP=1
      DO 2 I=1,NQI
      DO 3 J=1,8
      ARG=PI*(NDS(J)+DBLE(2.*I-1.))/(2.*NQI)
      ETA(NP)=DCOS(ARG)
      TAU=DSQRT(D1-ETA(NP)**2)
      NU=EVR*(2.-EVR)
      NET=NU*ETA(NP)*TAU
      FTHTA=D1-NU*TAU**2
      R=EVR*(D1-DBLE(EVR))**(2./3.)/DSQRT(FTHTA)
      R2TAU(NP)=TAU*R**2
      K0R(NP)=K0*R
      KR(NP)=K*R
      VR(NP)=D1/DSQRT(D1+(NET/FTHTA)**2)
      VTH(NP)=VR(NP)*NET/FTHTA
    3 NP=NP+1
    2 CONTINUE
      RETURN
      END
```

```
      REAL FUNCTION MAX(A,B)
      IF(A.GE.B) MAX=A
      IF(B.GT.A) MAX=B
      RETURN
      END
```

```
      COMPLEX FUNCTION NTGRL*16(M,L,P,N,IBES)
      COMPLEX*16 NTGRND
      COMPLEX*16 BESSEL(6,30,248),Y,FBES,KR(248)
      REAL*8 X,VR(248),VTH(248),R2TAU(248),R2,V1,V2
      REAL*8 LGNDR(3,30,248),FLGNDR,K0R(248)
      REAL*8 NDS(8),WGTS(8),PI
      INTEGER P
      COMMON /BLOC10/ VR,VTH,R2TAU
      COMMON /BLOC11/ BESSEL
      COMMON /BLOC12/ LGNDR
      COMMON /BLOC14/ K0R,KR
      COMMON /BLOC3/ WGTS,NDS,PI
      COMMON /BLOC9/ NQI,NQP
      NP=1
      NTGRL=(0.,0.)
      DO 1 I=1,NQI
```

```
      DO 2 J=1,8
C      NTGRL=NTGRL+WGTS(J)*NTGRND(M,L,P,N,IBES,NP)
C-----------------------------------------------------------------------
      R2=R2TAU(NP)
      X=K0R(NP)
      Y=KR(NP)
      V1=VR(NP)
      V2=VTH(NP)
      IF(N.EQ.1.OR.N.EQ.2) THEN
        IF(M.EQ.0) THEN
          FLGNDR=LGNDR(3,L,NP)*LGNDR(3,P,NP)
        ELSE
          FLGNDR=LGNDR(2,L,NP)*LGNDR(2,P,NP)+
     &         LGNDR(3,L,NP)*LGNDR(3,P,NP)
        ENDIF
        FBES=BESSEL(5,P,NP)*BESSEL(IBES,L,NP)
        IF(N.EQ.1) THEN
          NTGRND=(V1*BESSEL(IBES+2,L,NP)*BESSEL(5,P,NP)*
     &           FLGNDR+V2*L*(L+1)*FBES*LGNDR(1,L,NP)*
     &           LGNDR(3,P,NP)/X)*R2
        ELSE
          NTGRND=-(V1*BESSEL(IBES,L,NP)*BESSEL(6,P,NP)*FLGNDR+
     &           V2*P*(P+1)*FBES*LGNDR(3,L,NP)*LGNDR(1,P,NP)/Y)*R2
        ENDIF
      ELSE
        FLGNDR=LGNDR(2,L,NP)*LGNDR(3,P,NP)+
     &       LGNDR(3,L,NP)*LGNDR(2,P,NP)
        IF(N.EQ.3) THEN
          NTGRND=(V1*BESSEL(IBES+2,L,NP)*BESSEL(6,P,NP)*
     &           FLGNDR+V2*(P*(P+1)*BESSEL(IBES+2,L,NP)*
     &           BESSEL(5,P,NP)*LGNDR(2,L,NP)*
     &           LGNDR(1,P,NP)/Y+L*(L+1)*BESSEL(IBES,L,NP)*
     &           BESSEL(6,P,NP)*LGNDR(1,L,NP)*
     &           LGNDR(2,P,NP)/X))*R2
        ELSE
          NTGRND=V1*BESSEL(IBES,L,NP)*BESSEL(5,P,NP)*
     &           FLGNDR*R2
        ENDIF
      ENDIF
C-----------------------------------------------------------------------
      NTGRL=NTGRL+WGTS(J)*NTGRND
    2 NP=NP+1
    1 CONTINUE
      NTGRL=-NTGRL*PI*PI/(2.*NQI)
      RETURN
      END




      REAL FUNCTION LGNDR1*8(N,M,ETA)
      REAL*8 ETA,DP1,DM1,D0
      REAL*8 FACT(0:50)
      COMMON /BLOC18/ FACT
      DP1=DBLE(1.)
      DM1=DBLE(-1.)
      D0=DBLE(0.)
      IF(M.GT.N) THEN
        LGNDR1=0.
        RETURN
      ENDIF
      IF(ETA.EQ.DP1.OR.ETA.EQ.DM1) GO TO 200
```

```
      KMAX=(N-M)/2
      IF(ETA.EQ.D0) THEN
        IF((FLOAT(N-M)/2.).NE.FLOAT(KMAX)) THEN
          LGNDR1=0.
        ELSE
          LGNDR1=(-1.)**KMAX*FACT(2*N-2*KMAX)/
     &           (FACT(KMAX)*FACT(N-KMAX)*2.**N)
        ENDIF
        RETURN
      ELSE
        LGNDR1=0.
        DO 1 K=0,KMAX
    1   LGNDR1=LGNDR1+(-1.)**K*FACT(2*N-2*K)*ETA**(N-M-2*K)/
     &         (FACT(K)*FACT(N-K)*FACT(N-M-2*K))
        IF(M.EQ.0) THEN
          LGNDR1=LGNDR1/2.**N
        ELSE
          LGNDR1=(DP1-ETA**2)**(FLOAT(M)/2.)*LGNDR1/2.**N
        ENDIF
        RETURN
      ENDIF
  200 CONTINUE
      IF(M.NE.0) THEN
        LGNDR1=0.
      ELSE
        IF(ETA.EQ.DP1) LGNDR1=1.
        IF(ETA.EQ.DM1) LGNDR1=(-1.)**N
      ENDIF
      RETURN
      END



      REAL FUNCTION LGNDR2*8(N,M,ETA)
      REAL*8 LGNDR1,ETA,DP1,DM1,D0
      REAL*8 FACT(0:50)
      COMMON /BLOC18/ FACT
      DP1=DBLE(1.)
      DM1=DBLE(-1.)
      D0=DBLE(0.)
      IF(M.EQ.0) THEN
        LGNDR2=0.
        RETURN
      ENDIF
      IF(ETA.EQ.DP1.OR.ETA.EQ.DM1) GO TO 200
      IF(ETA.EQ.D0) GO TO 300
      KMAX=(N-M)/2
      LGNDR2=0.
      DO 1 K=0,KMAX
    1 LGNDR2=LGNDR2+(-1.)**K*FACT(2*N-2*K)*ETA**(N-M-2*K)/
     &(FACT(K)*FACT(N-K)*FACT(N-M-2*K))
      IF(M.EQ.1) THEN
        LGNDR2=LGNDR2/2.**N
      ELSE
        LGNDR2=M*(DP1-ETA**2)**(FLOAT(M-1)/2.)*LGNDR2/2.**N
      ENDIF
      RETURN
  200 CONTINUE
      IF(M.NE.1) THEN
        LGNDR2=0.
        RETURN
      ENDIF
      IF(ETA.EQ.DP1) PN0=1.
      IF(ETA.EQ.DM1) PN0=(-1.)**N
      LGNDR2=ETA*(N*(N+1)*PN0)/2.
```

```
      RETURN
  300 LGNDR2=M*LGNDR1(N,M,D0)
      RETURN
      END



      REAL FUNCTION LGNDR3*8(N,M,ETA)
      REAL*8 LGNDR1,ETA,DP1,DM1
      DP1=DBLE(1.)
      DM1=DBLE(-1.)
      IF(M.NE.0) THEN
        LGNDR3=((N-M+1)*(N+M)*LGNDR1(N,M-1,ETA)-LGNDR1(N,M+1,ETA))/2.
      ELSE
        IF(ETA.EQ.DP1.OR.ETA.EQ.DM1) THEN
          LGNDR3=0.
        ELSE
          LGNDR3=-((N+1)*ETA*LGNDR1(N,M,ETA)-(N-M+1)*
     &           LGNDR1(N+1,M,ETA))/DSQRT(DP1-ETA**2)
        ENDIF
      ENDIF
      RETURN
      END



      REAL FUNCTION SBESJ*8(X,N)
      REAL*8 X,Z,SBESST,Q0,Q1,Q2,QN
      Z=DSIN(X)/X
      IF(N.EQ.0) THEN
        SBESJ=Z
        RETURN
      ENDIF
      IF(.5*X*X/(2.*N+3.).LT.1.0) THEN
        SBESJ=SBESST(X,N)
        RETURN
      ENDIF
      M=X+10.
      IF(M.LE.N) M=N+5
      Q2=SBESST(X,M+1)
      Q1=SBESST(X,M)
      MM=M
      DO 1 I=1,M
      IF(MM.EQ.N) QN=Q0
      Q0=(2*MM+1)*Q1/X-Q2
      Q2=Q1
      Q1=Q0
    1 MM=MM-1
      SBESJ=Z*QN/Q0
      RETURN
      END



      REAL FUNCTION SBESST*8(X,N)
      REAL*8 X,F,Q1,Q2,Z
      F=1.
      DO 1 I=1,N
    1 F=F*X/(2.*I+1.)
      K1=1
      K2=2*N+3
      Z=-.5*X*X
      Q1=1.
```

```
      Q2=Z/FLOAT(K2)
    2 Q1=Q1+Q2
      IF(DABS(Q2).GT.1.0D-16) THEN
        K1=K1+1
        K2=K2+2
        Q2=Q2*Z/FLOAT(K1*K2)
        GO TO 2
      ENDIF
      SBESST=F*Q1
      RETURN
      END



      COMPLEX FUNCTION CBESJ*16(Y,N)
      COMPLEX*16 Y,Z,Q0,Q1,Q2,QN,CBESST
      Z=CDSIN(Y)/Y
      IF(N.EQ.0) THEN
        CBESJ=Z
        RETURN
      ENDIF
      IF(CDABS(.5*Y*Y/(2.*N+3.)).LT.1.0) THEN
        CBESJ=CBESST(Y,N)
        RETURN
      ENDIF
      M=CDABS(Y)+10.
      IF(M.LE.N) M=N+5
      Q2=CBESST(Y,M+1)
      Q1=CBESST(Y,M)
      MM=M
      DO 1 I=1,M
      IF(MM.EQ.N) QN=Q0
      Q0=(2*MM+1)*Q1/Y-Q2
      Q2=Q1
      Q1=Q0
    1 MM=MM-1
      CBESJ=Z*QN/Q0
      RETURN
      END



      COMPLEX FUNCTION CBESST*16(Y,N)
      COMPLEX*16 Y,Z,F,Q1,Q2
      F=(1.,0.)
      DO 1 I=1,N
    1 F=F*Y/(2.*I+1.)
      K1=1
      K2=2*N+3
      Z=-.5*Y*Y
      Q1=(1.,0.)
      Q2=Z/FLOAT(K2)
    2 Q1=Q1+Q2
      IF(CDABS(Q2).GT.1.0D-16) THEN
        K1=K1+1
        K2=K2+2
        Q2=Q2*Z/FLOAT(K1*K2)
        GO TO 2
      ENDIF
      CBESST=F*Q1
      RETURN
      END
```

```
      BLOCK DATA WTSNDS
      COMMON /BLOC3/ WGTS,NDS,PI
      REAL*8 WGTS(8),NDS(8),PI
      DATA WGTS/.101228536290376,.222381034453374,.313706645877887,
     &.362683783378362,.362683783378362,.313706645877887,
     &.222381034453374,.101228536290376/
      DATA NDS/-.960289856497536,-.796666477413627,-.525532409916329,
     &-.18343464249565,.18343464249565,.525532409916329,
     &.796666477413627,.960289856497536/
      END
```

Appendix B. Radiative Transfer Programs

This appendix contains the following programs:

1. GAM1: program computing γ_{ll} for the two incident polarizations.

2. LAMDK: program computing the $[\Lambda_k]$ for the two incident polarizations.

3. LMUKL: program computing $[I(\mu_k, \mu_l)]_m$.

4. XII: program computing $[X]_m$ for the two incident polarizations.

5. RADTRO: program solving the VRTE for the plane parallel geometry.

```
C*********************************************************************
C THIS PROGRAMME COMPUTE GAMMAII FOR THE TWO DIFFERENT POLRIZATIONS   *
C THE INPUT ARE THE ARRAY CONTAINING THE FORWARD SCATERING COEFFICIENTS*
C FOR THE INCIDENT ANGLES (45,0,14 DEGREES) FOR 14 DIFFERENTS RAIN DROP*
C SIZES.(0.025-3.5)                                                   *
C*********************************************************************
C INITIALIZATIONS AND DECLARATIONS
      COMPLEX*16 FTE1,FTE2,FFI1,FFI2,F(14),G
      COMPLEX*16 F11,F12,F21,F22,FFWD11(14),FFWD22(14)
      REAL*8 GAMA1,GAMA2
      REAL*8 PI,FTE1R,FTE1I,FTE2R,FTE2I,FFI1R,FFI1I,FFI2R,FFI2I
      COMPLEX IMAG
      COMMON /BLOCK1/ RR
C
      IMAG=(0.,1.)
      WL=.01
C ENTREE DES DONNEES
      DO 1000 I=1,14
      READ (5,*,END=1001 ) ALPHA,PHI,TETA,FTE1R,FTE1I,FFI1R,FFI1I,EVR
      READ (5,*,END=1001 ) ALPHA,PHI,TETA,FTE2R,FTE2I,FFI2R,FFI2I,EVR
1001  FTE1=FTE1R+IMAG*FTE1I
      FFI1=FFI1R+IMAG*FFI1I
      FTE2=FTE2R+IMAG*FTE2I
      FFI2=FFI2R+IMAG*FFI2I
      CALL TRANSF(ALPHA,PHI,TETA,FTE1,FTE2,FFI1,FFI2,F11,F12,F21,F22)
      FFWD11(I)=F11
      FFWD22(I)=F22
1000  CONTINUE
C MARCHALL AND PALMER AVERAGE
      RR=100.0
      DO 2000 I=1,14
2000  F(I)=-2*WL*DIMAG(FFWD11(I))
      CALL MPAVE (F,G)
      GAMA1=DREAL(G)
      I=1
      WRITE(8,*) I,GAMA1,RR
      DO 2100 I=1,14
2100  F(I)=-2*WL*DIMAG(FFWD22(I))
      CALL MPAVE (F,G)
      GAMA2=DREAL(G)
      I=2
      WRITE(8,*) I,GAMA2,RR
 99   END


C THIS PROGRAM READS AND TRANSFORMS THE SCATTERING COEFFICIENTS IN TO
C THE  VAN DE HULST FORM I.E. F11,F12,F22,F21
C THE INPUT DATA ARE:
C THE SCATTERING COEFFICIENTS
C                FTETA1
C                FTETA2
C                FFI1
C                FFI2
C AND THE ANGLES FOR WHIHICH THEY ARE COMPUTED
C                ALPHA INCIDENT ANGLE
C                PHI
C                TETA OBSERVATION ANGLE
C SUBROUTINE TRANSFORMING F(TETA,ALPHA,PHI) IN F11,F22,F12,F21
      SUBROUTINE TRANSF(ALPHA,FI,TETA,FTE1,FTE2,FFI1,FFI2,F11,F12,F21,
     &F22)
      COMPLEX*16 FTE1,FTE2,FFI1,FFI2
      COMPLEX*16 F11,F12,F21,F22
      REAL*8 CT,ST,SA,CA,CF,SF,U,U2,A,B,C,D,PI
      PI=3.141592653589793
C CASE OF FORWARD OR BACKWARD SCATTERING
      IF (((ALPHA.EQ.TETA).OR.(ALPHA.EQ.180.-TETA)).AND.((FI.EQ.0.).OR.
```

```
     &(ABS(FI).EQ.180.))) THEN
      F12=(0.,0.)
      F21=(0.,0.)
      F11=FTE1
      F22=FFI2
      GO TO 99
      ENDIF
C GENERAL CASE(JE SUPPOSE ICI QUE J'AI LA BONNE VALEUR DE TETA ET FI)
      IF (TETA.EQ.90.) THEN
        CT=0.
        ST=1.
      ELSE
        IF (TETA.EQ.180.) THEN
         CT=-1.
         ST=0.
        ELSE
         CT=DCOS(TETA*PI/180.)
         ST=DSIN(TETA*PI/180.)
        ENDIF
      ENDIF
      IF (FI.EQ.90.) THEN
        CF=0.
        SF=1.
      ELSE
        IF (FI.EQ.180.) THEN
         CF=-1.
         SF=0.
        ELSE
         CF=DCOS(FI*PI/180.)
         SF=DSIN(FI*PI/180.)
        ENDIF
      ENDIF
      IF (ALPHA.EQ.90.) THEN
        CA=0.
        SA=1.
      ELSE
        IF (ALPHA.EQ.180.) THEN
         CA=-1.
         SA=0.
        ELSE
         CA=DCOS(ALPHA*PI/180.)
         SA=DSIN(ALPHA*PI/180.)
        ENDIF
      ENDIF
      U=CA*CT-SA*ST*CF
      U2=1-U*U
      A=-SA*SF
      B=SA*CF*CT-CA*ST
      C=-ST*SF
      D=CT*ST*CF-SA*CT
      F11=(A*(FTE1*C+FTE2*D)-B*(FFI1*C+FFI2*D))/U2
      F12=(A*(-FTE1*D+FTE2*C)-B*(-FFI1*D+FFI2*C))/U2
      F21=(B*(FTE1*C+FTE2*D)+A*(FFI1*C+FFI2*D))/U2
      F22=(B*(-FTE1*D+FTE2*C)+A*(-FFI1*D+FFI2*C))/U2
99     RETURN
      END


C THIS SUBROUTINE COMPUTE THE AVERAGE OF THE FUNCTION F BY USING THE
C MARSCHALL & PALMER DISTRIBUTION AND SNE DIT BACK IN G
C
C
      SUBROUTINE MPAVE(F,G)
      INTEGER J
      REAL N0,RR
      REAL*8 BETA
```

```
      COMPLEX*16 G,F(14),CINT
      COMMON /BLOCK1/ RR
C CONSTANTS
      CINT=(0.,0.)
      G=(0.,0.)
      N0=16000.0
      BETA=8.2*RR**(-.21)
C COMPUTE G FOR 0.25 AND 3.5 MM
      CINT=4*DEXP(-BETA*.25)*F(1)+DEXP(-BETA*3.5)*F(14)
C COMPUTATION FOR THE OTHER RADIUS (.5 TO 3.2)
      DO 10 J=1,6
      CINT=CINT+2*DEXP(-BETA*.5*J)*F(2*J)
      CINT=CINT+4*DEXP(-BETA*(.5*J+.25))*F(2*J+1)
10    CONTINUE
      G=CINT*N0/12.
      RETURN
      END
```

```
C*********************************************************************
C THIS PROGRAMME COMPUTE LAMDAK THE TWO DIFFERENT POLRIZATIONS        *
C THE INPUT ARE THE ARRAY CONTAINING THE SCATERING COEFFICIENTS       *
C FOR THE INCIDENT ANGLES (45,0,14 DEGREES) FOR 14 DIFFERENTS RAIN DROP*
C SIZES.(0.025-3.5) ,AND OBSERVATION ANGLES TETA(K)(12 VALUES)        *
C*********************************************************************
C INITIALIZATIONS AND DECLARATIONS
      INTEGER ICHOI,M,IPOL,I,J,K,IP
      COMPLEX*16 FTE1,FTE2,FFI1,FFI2,F(14),G
      COMPLEX*16 F11,F12,F21,F22,F1(14),F2(14),F3(14),F4(14)
      COMPLEX*16 FKK11(14),FKK22(14)
      REAL*8 LAMDA1,LAMDA2,LAMDA3,LAMDA4
      REAL*8 PI,FTE1R,FTE1I,FTE2R,FTE2I,FFI1R,FFI1I,FFI2R,FFI2I
      COMPLEX IMAG
      COMMON /BLOCK1/ RR
C
      IMAG=(0.,1.)
      PI=3.141592653589793
      WL=.01
C ENTREE DES DONNEES
      DO 5000 I=1,14
      DO 1000 IP=1,25
      READ (5,* ) ALPHA,PHI,TETA,FTE1R,FTE1I,FFI1R,FFI1I,EVR
      READ (5,* ) ALPHA,PHI,TETA,FTE2R,FTE2I,FFI2R,FFI2I,EVR
      IF (PHI.NE.0.) GO TO 1000
      FTE1=FTE1R+IMAG*FTE1I
      FFI1=FFI1R+IMAG*FFI1I
      FTE2=FTE2R+IMAG*FTE2I
      FFI2=FFI2R+IMAG*FFI2I
      CALL TRANSF(ALPHA,PHI,TETA,FTE1,FTE2,FFI1,FFI2,F11,F12,F21,F22)
      FKK11(I)=F11
      FKK22(I)=F22
1000  CONTINUE
5000  CONTINUE
C MARCHALL AND PALMER AVERAGE
      RR=100.0
      DO 2000 I=1,14
      F1(I)=-2*WL*DIMAG(FKK11(I))
      F2(I)=-2*WL*DIMAG(FKK22(I))
      F3(I)=-WL*DIMAG(FKK11(I)+FKK22(I))
      F4(I)=-WL*DREAL(FKK11(I)-FKK22(I))
2000  CONTINUE
      CALL MPAVE (F1,G)
      LAMDA1=DREAL(G)
      CALL MPAVE (F2,G)
      LAMDA2=DREAL(G)
      CALL MPAVE (F3,G)
      LAMDA3=DREAL(G)
      CALL MPAVE (F4,G)
      LAMDA4=DREAL(G)
      WRITE (8,*)LAMDA1,LAMDA2,LAMDA3,LAMDA4
 99   END


C THIS PROGRAM READS AND TRANSFORMS THE SCATTERING COEFFICIENTS IN TO
C THE  VAN DE HULST FORM I.E. F11,F12,F22,F21
C THE INPUT DATA ARE:
C THE SCATTERING COEFFICIENTS
C               FTETA1
C               FTETA2
C               FFI1
C               FFI2
C AND THE ANGLES FOR WHIHICH THEY ARE COMPUTED
C               ALPHA INCIDENT ANGLE
C               PHI
```

```
C                TETA OBSERVATION ANGLE
C SUBROUTINE TRANSFORMING F(TETA,ALPHA,PHI) IN F11,F22,F12,F21
      SUBROUTINE TRANSF(ALPHA,FI,TETA,FTE1,FTE2,FFI1,FFI2,F11,F12,F21,
     &F22)
      COMPLEX*16 FTE1,FTE2,FFI1,FFI2
      COMPLEX*16 F11,F12,F21,F22
      REAL*8 CT,ST,SA,CA,CF,SF,U,U2,A,B,C,D,PI
      PI=3.141592653589793
C CASE OF FORWARD OR BACKWARD SCATTERING
      IF (((ALPHA.EQ.TETA).OR.(ALPHA.EQ.180.-TETA)).AND.((FI.EQ.0.).OR.
     &(ABS(FI).EQ.180.))) THEN
      F12=(0.,0.)
      F21=(0.,0.)
      F11=FTE1
      F22=FFI2
      GO TO 99
      ENDIF
C GENERAL CASE(JE SUPPOSE ICI QUE J'AI LA BONNE VALEUR DE TETA ET FI)
      IF (TETA.EQ.90.) THEN
        CT=0.
        ST=1.
      ELSE
        IF (TETA.EQ.180.) THEN
         CT=-1.
         ST=0.
        ELSE
         CT=DCOS(TETA*PI/180.)
         ST=DSIN(TETA*PI/180.)
        ENDIF
      ENDIF
      IF (FI.EQ.90.) THEN
        CF=0.
        SF=1.
      ELSE
        IF (FI.EQ.180.) THEN
         CF=-1.
         SF=0.
        ELSE
         CF=DCOS(FI*PI/180.)
         SF=DSIN(FI*PI/180.)
        ENDIF
      ENDIF
      IF (ALPHA.EQ.90.) THEN
        CA=0.
        SA=1.
      ELSE
        IF (ALPHA.EQ.180.) THEN
         CA=-1.
         SA=0.
        ELSE
         CA=DCOS(ALPHA*PI/180.)
         SA=DSIN(ALPHA*PI/180.)
        ENDIF
      ENDIF
      U=CA*CT-SA*ST*CF
      U2=1-U*U
      A=-SA*SF
      B=SA*CF*CT-CA*ST
      C=-ST*SF
      D=CT*ST*CF-SA*CT
      F11=(A*(FTE1*C+FTE2*D)-B*(FFI1*C+FFI2*D))/U2
      F12=(A*(-FTE1*D+FTE2*C)-B*(-FFI1*D+FFI2*C))/U2
      F21=(B*(FTE1*C+FTE2*D)+A*(FFI1*C+FFI2*D))/U2
      F22=(B*(-FTE1*D+FTE2*C)+A*(-FFI1*D+FFI2*C))/U2
99    RETURN
      END
```

```
C THIS SUBROUTINE COMPUTE THE AVERAGE OF THE FUNCTION F BY USING THE
C MARSCHALL & PALMER DISTRIBUTION AND SNE DIT BACK IN G
C
C
      SUBROUTINE MPAVE(F,G)
      INTEGER J
      REAL N0,RR
      REAL*8 BETA
      COMPLEX*16 G,F(14),CINT
      COMMON /BLOCK1/ RR
C CONSTANTS
      CINT=(0.,0.)
      G=(0.,0.)
      N0=16000.0
      BETA=8.2*RR**(-.21)
C COMPUTE G FOR 0.25 AND 3.5 MM
      CINT=4*DEXP(-BETA*.25)*F(1)+DEXP(-BETA*3.5)*F(14)
C COMPUTATION FOR THE OTHER RADIUS (.5 TO 3.2)
      DO 10 J=1,6
      CINT=CINT+2*DEXP(-BETA*.5*J)*F(2*J)
      CINT=CINT+4*DEXP(-BETA*(.5*J+.25))*F(2*J+1)
10    CONTINUE
      G=CINT*N0/12.
      RETURN
      END
```

```
C*****************************************************************
C THIS PROGRAMME COMPUTE L(MUK,MUL)M                              *
C THE INPUT ARE THE ARRAY CONTAINING THE SCATERING COEFFICIENTS   *
C FOR THE INCIDENT ANGLES TETA(K) FOR 14 DIFFERENTS RAIN DROP     *
C SIZES.(0.025-3.5) ,AND OBSERVATION ANGLES TETA(K)(12 VALUES)    *
C*****************************************************************
C INITIALIZATIONS AND DECLARATIONS
      INTEGER ICHOI,M,IPOL,I,J,K
      COMPLEX*16 FTE1,FTE2,FFI1,FFI2,F(25),G,SFFI1,SFTE2
      COMPLEX*16 F11,F12,F21,F22
      COMPLEX*16 FKL11(14,25),FKL22(14,25),FKL12(14,25),FKL21(14,25)
      COMPLEX*16 SFKL11(14,25),SFKL22(14,25),SFKL12(14,25),SFKL21(14,25)
      COMPLEX*16 S11(14),S12(14),S13(14),S14(14)
      COMPLEX*16 S21(14),S23(14)
      COMPLEX*16 S31(14),S32(14)
      COMPLEX*16 S41(14),S42(14)
      REAL*8 SMP(4,4,25),SM(4,4),STE
      REAL*8 PI,FTE1R,FTE1I,FTE2R,FTE2I,FFI1R,FFI1I,FFI2R,FFI2I
      COMPLEX IMAG
      COMMON /BLOCK1/ RR
C
      IMAG=(0.,1.)
      PI=3.141592653589793
      WL=.01
      RR=100.0
C ENTREE DES DONNEES
      DO 1000 I=1,14
      DO 1100 J=1,25
      READ (5,* ) ALPHA,PHI,TETA,FTE1R,FTE1I,FFI1R,FFI1I,EVR
      READ (5,* ) ALPHA,PHI,TETA,FTE2R,FTE2I,FFI2R,FFI2I,EVR
      FTE1=FTE1R+IMAG*FTE1I
      FFI1=FFI1R+IMAG*FFI1I
      FTE2=FTE2R+IMAG*FTE2I
      FFI2=FFI2R+IMAG*FFI2I
      CALL TRANSF(ALPHA,PHI,TETA,FTE1,FTE2,FFI1,FFI2,F11,F12,F21,F22)
      FKL11(I,J)=F11
      FKL22(I,J)=F22
      FKL12(I,J)=F12
      FKL21(I,J)=F21
C CAS SYMETRIQUE  SIL Y A LIEU PARTOUT SAUF SUR LA DIAGONALE
      IF (TETA.EQ.ALPHA) GO TO 1100
      SALPHA=180.-ALPHA
      STETA=180.-TETA
      ISYM=1
      SFFI1=-FFI1R-IMAG*FFI1I
      SFTE2=-FTE2R-IMAG*FTE2I
      CALL TRANSF(SALPHA,PHI,STETA,FTE1,SFTE2,SFFI1,FFI2,F11,F12,F21,
     $F22)
      SFKL11(I,J)=F11
      SFKL22(I,J)=F22
      SFKL12(I,J)=F12
      SFKL21(I,J)=F21
1100  CONTINUE
1000  CONTINUE
C MARCHALL AND PALMER AVERAGE FOR THE 78 FIRST CASE (PAS DE SYMETRIE)
      DO 2200 J=1,25
      DO 2000 I=1,14
      S11(I)=FKL11(I,J)*DCONJG(FKL11(I,J))
      S12(I)=FKL12(I,J)*DCONJG(FKL12(I,J))
      S13(I)=FKL21(I,J)*DCONJG(FKL21(I,J))
      S14(I)=FKL22(I,J)*DCONJG(FKL22(I,J))
      S21(I)=FKL11(I,J)*DCONJG(FKL12(I,J))
      S23(I)=FKL21(I,J)*DCONJG(FKL22(I,J))
      S31(I)=FKL11(I,J)*DCONJG(FKL21(I,J))
      S32(I)=FKL12(I,J)*DCONJG(FKL22(I,J))
      S41(I)=FKL11(I,J)*DCONJG(FKL22(I,J))
```

```
      S41(I)=S41(I)+FKL12(I,J)*DCONJG(FKL21(I,J))
      S42(I)=FKL11(I,J)*DCONJG(FKL22(I,J))
      S42(I)=S41(I)-FKL12(I,J)*DCONJG(FKL21(I,J))
2000  CONTINUE
C S1*********************
      CALL MPAVE (S11,G)
      SMP(1,1,J)=DREAL(G)
      CALL MPAVE (S12,G)
      SMP(1,2,J)=DREAL(G)
      CALL MPAVE (S13,G)
      SMP(1,3,J)=DREAL(G)
      CALL MPAVE (S14,G)
      SMP(1,4,J)=DREAL(G)
C S2*********************
      CALL MPAVE (S21,G)
      SMP(2,1,J)=DREAL(G)
      SMP(2,2,J)=-DIMAG(G)
      CALL MPAVE (S23,G)
      SMP(2,3,J)=DREAL(G)
      SMP(2,4,J)=-DIMAG(G)
C S3*********************
      CALL MPAVE (S31,G)
      SMP(3,1,J)=2.*DREAL(G)
      SMP(3,3,J)=2.*DIMAG(G)
      CALL MPAVE (S32,G)
      SMP(3,2,J)=2.*DREAL(G)
      SMP(3,4,J)=2.*DIMAG(G)
C S4*********************
      CALL MPAVE (S41,G)
      SMP(4,1,J)=DREAL(G)
      SMP(4,3,J)=DIMAG(G)
      CALL MPAVE (S42,G)
      SMP(4,4,J)=DREAL(G)
      SMP(4,2,J)=-DIMAG(G)
2200  CONTINUE
C COMPUTATION OF THE FIRST 9 FOURIER TRANSFORMS
      DO 2300 M=0,5
      DO 2400 N=1,4
      DO 2500 P=1,4
      DO 2600 J=1,25
2600  F(J)=SMP(N,P,J)
      IF ((N.EQ.1).OR.(N.EQ.4)) ICHOI=0
      IF ((N.EQ.2).OR.(N.EQ.3)) ICHOI=1
      CALL FOURIER (F,M,ICHOI,STE)
2500  SM(N,P)=STE*2.
2400  WRITE (8,88) M,N,SM(N,1),SM(N,2),SM(N,3),SM(N,4)
2300  CONTINUE
      IF (ISYM.EQ.0) GO TO 99
C CAS SYMETRIQUE ***********************************************************
C MARCHALL AND PALMER AVERAGE FOR THE 66 SYMETRIC CASE
      DO 3200 J=1,25
      DO 3000 I=1,14
      S11(I)=SFKL11(I,J)*DCONJG(SFKL11(I,J))
      S12(I)=SFKL12(I,J)*DCONJG(SFKL12(I,J))
      S13(I)=SFKL21(I,J)*DCONJG(SFKL21(I,J))
      S14(I)=SFKL22(I,J)*DCONJG(SFKL22(I,J))
      S21(I)=SFKL11(I,J)*DCONJG(SFKL12(I,J))
      S23(I)=SFKL21(I,J)*DCONJG(SFKL22(I,J))
      S31(I)=SFKL11(I,J)*DCONJG(SFKL21(I,J))
      S32(I)=SFKL12(I,J)*DCONJG(SFKL22(I,J))
      S41(I)=SFKL11(I,J)*DCONJG(SFKL22(I,J))
      S41(I)=S41(I)+SFKL12(I,J)*DCONJG(SFKL21(I,J))
      S42(I)=SFKL11(I,J)*DCONJG(SFKL22(I,J))
      S42(I)=S41(I)-SFKL12(I,J)*DCONJG(SFKL21(I,J))
3000  CONTINUE
C S1*********************
```

```
      CALL MPAVE (S11,G)
      SMP(1,1,J)=DREAL(G)
      CALL MPAVE (S12,G)
      SMP(1,2,J)=DREAL(G)
      CALL MPAVE (S13,G)
      SMP(1,3,J)=DREAL(G)
      CALL MPAVE (S14,G)
      SMP(1,4,J)=DREAL(G)
C S2*********************
      CALL MPAVE (S21,G)
      SMP(2,1,J)=DREAL(G)
      SMP(2,2,J)=-DIMAG(G)
      CALL MPAVE (S23,G)
      SMP(2,3,J)=DREAL(G)
      SMP(2,4,J)=-DIMAG(G)
C S3*********************
      CALL MPAVE (S31,G)
      SMP(3,1,J)=2.*DREAL(G)
      SMP(3,3,J)=2.*DIMAG(G)
      CALL MPAVE (S32,G)
      SMP(3,2,J)=2.*DREAL(G)
      SMP(3,4,J)=2.*DIMAG(G)
C S4*********************
      CALL MPAVE (S41,G)
      SMP(4,1,J)=DREAL(G)
      SMP(4,3,J)=DIMAG(G)
      CALL MPAVE (S42,G)
      SMP(4,4,J)=DREAL(G)
      SMP(4,2,J)=-DIMAG(G)
3200  CONTINUE
C COMPUTATION OF THE FIRST 9 FOURIER TRANSFORMS
      DO 3300 M=0,5
      DO 3400 N=1,4
      DO 3500 P=1,4
      DO 3600 J=1,25
3600  F(J)=SMP(N,P,J)
      IF ((N.EQ.1).OR.(N.EQ.4)) ICHOI=0
      IF ((N.EQ.2).OR.(N.EQ.3)) ICHOI=1
      CALL FOURIER (F,M,ICHOI,STE)
3500  SM(N,P)=STE*2.
3400  WRITE (8,88) M,N,SM(N,1),SM(N,2),SM(N,3),SM(N,4)
3300  CONTINUE
88    FORMAT(I1,2X,I1,2X,E28.20,2X,E28.20,2X,E28.20,2X,E28.20)
 99   END


C THIS PROGRAM READS AND TRANSFORMS THE SCATTERING COEFFICIENTS IN TO
C THE  VAN DE HULST FORM I.E. F11,F12,F22,F21
C THE INPUT DATA ARE:
C THE SCATTERING COEFFICIENTS
C               FTETA1
C               FTETA2
C               FFI1
C               FFI2
C AND THE ANGLES FOR WHIHICH THEY ARE COMPUTED
C               ALPHA INCIDENT ANGLE
C               PHI
C               TETA OBSERVATION ANGLE
C SUBROUTINE TRANSFORMING F(TETA,ALPHA,PHI) IN F11,F22,F12,F21
      SUBROUTINE TRANSF(ALPHA,FI,TETA,FTE1,FTE2,FFI1,FFI2,F11,F12,F21,
     &F22)
      COMPLEX*16 FTE1,FTE2,FFI1,FFI2
      COMPLEX*16 F11,F12,F21,F22
      REAL*8 CT,ST,SA,CA,CF,SF,U,U2,A,B,C,D,PI
      PI=3.141592653589793
C CASE OF FORWARD OR BACKWARD SCATTERING
```

```
      IF (((ALPHA.EQ.TETA).OR.(ALPHA.EQ.180.-TETA)).AND.((FI.EQ.0.).OR.
     &(ABS(FI).EQ.180.))) THEN
      F12=(0.,0.)
      F21=(0.,0.)
      F11=FTE1
      F22=FFI2
      GO TO 99
      ENDIF
C GENERAL CASE(JE SUPPOSE ICI QUE J'AI LA BONNE VALEUR DE TETA ET FI)
      IF (TETA.EQ.90.) THEN
        CT=0.
        ST=1.
      ELSE
        IF (TETA.EQ.180.) THEN
          CT=-1.
          ST=0.
        ELSE
          CT=DCOS(TETA*PI/180.)
          ST=DSIN(TETA*PI/180.)
        ENDIF
      ENDIF
      IF (FI.EQ.90.) THEN
        CF=0.
        SF=1.
      ELSE
        IF (FI.EQ.180.) THEN
          CF=-1.
          SF=0.
        ELSE
          CF=DCOS(FI*PI/180.)
          SF=DSIN(FI*PI/180.)
        ENDIF
      ENDIF
      IF (ALPHA.EQ.90.) THEN
        CA=0.
        SA=1.
      ELSE
        IF (ALPHA.EQ.180.) THEN
          CA=-1.
          SA=0.
        ELSE
          CA=DCOS(ALPHA*PI/180.)
          SA=DSIN(ALPHA*PI/180.)
        ENDIF
      ENDIF
      U=CA*CT-SA*ST*CF
      U2=1-U*U
      A=-SA*SF
      B=SA*CF*CT-CA*ST
      C=-ST*SF
      D=CT*ST*CF-SA*CT
      F11=(A*(FTE1*C+FTE2*D)-B*(FFI1*C+FFI2*D))/U2
      F12=(A*(-FTE1*D+FTE2*C)-B*(-FFI1*D+FFI2*C))/U2
      F21=(B*(FTE1*C+FTE2*D)+A*(FFI1*C+FFI2*D))/U2
      F22=(B*(-FTE1*D+FTE2*C)+A*(-FFI1*D+FFI2*C))/U2
99    RETURN
      END


C THIS SUBROUTINE COMPUTE THE AVERAGE OF THE FUNCTION F BY USING THE
C MARSCHALL & PALMER DISTRIBUTION AND SNE DIT BACK IN G
C
C
      SUBROUTINE MPAVE(F,G)
      INTEGER J
      REAL N0,RR
```

```
      REAL*8 BETA
      COMPLEX*16 G,F(14),CINT
      COMMON /BLOCK1/ RR
C CONSTANTS
      CINT=(0.,0.)
      G=(0.,0.)
      N0=16000.0
      BETA=8.2*RR**(-.21)
C COMPUTE G FOR 0.25 AND 3.5 MM
      CINT=4*DEXP(-BETA*.25)*F(1)+DEXP(-BETA*3.5)*F(14)
C COMPUTATION FOR THE OTHER RADIUS (.5 TO 3.2)
      DO 10 J=1,6
      CINT=CINT+2*DEXP(-BETA*.5*J)*F(2*J)
      CINT=CINT+4*DEXP(-BETA*(.5*J+.25))*F(2*J+1)
10    CONTINUE
      G=CINT*N0/12.
      RETURN
      END

C THIS PROGRAM COMPUTE THE FOURIER TRANSFORM WITH REGARD TO THE
C AZIMUTHAL ANGLE PHI OF THE INPUT FUNCTION F USING A 25 POINT SIMPSON
C INTEGRATION.
C THE INPUT DATA ARE
C       *THE ARRAY CONTAINING THE FUNCTION  AT THE 25
C        VALUES OF PHI (0(7.5)180) F(25)

C       *THE ORDER M OF THE FOURIER COEFFICIENT WANTED

C       *THE VARIABLE ICHOI TO CHOOSE BETWEEN A COSINE OR A SINE
C        TRANSFORM : ICHOI=0 FOR A COSINE TRANSFORM
C              AND  ICHOI=1 FOR A SINE TRANSFORM
      SUBROUTINE  FOURIER(F,M,ICHOI,FOUT)
      INTEGER MPAR,ICHOI,M,J
      REAL HFI
      REAL*8 FCO,FSI,PI
      COMPLEX*16 F(25),FOUT
      COMPLEX IMAG
C CONSTANTS
      IMAG=(0.,1.)
      PI=3.141592653589793
C INITIALIZATIONS
      HFI=180./24
      FOUT=(0.,0.)
c parity of m
      MPAR=M-2*INT(M/2)
C SIMPSON  INTEGRATION
      IF (ICHOI.EQ.0) THEN
        FOUT=F(1)
        IF(MPAR.EQ.0) THEN
          FOUT=FOUT+F(25)
        ELSE
          FOUT=FOUT-F(25)
        ENDIF
      ENDIF
      DO 10 J=0,11
      IF (J.EQ.0) THEN
        IF (ICHOI.EQ.0) FOUT=FOUT+4*F(2)*FCO(M*HFI)
        IF (ICHOI.EQ.1) FOUT=FOUT+4*F(2)*FSI(M*HFI)
      ELSE
        IF (ICHOI.EQ.0) THEN
          FOUT=FOUT+4*F(2*J+2)*FCO(M*(2*J+1)*HFI)
          FOUT=FOUT+2*F(2*J+1)*FCO(M*2*J*HFI)
        ELSE
          FOUT=FOUT+4*F(2*J+2)*FSI(M*(2*J+1)*HFI)
          FOUT=FOUT+2*F(2*J+1)*FSI(M*2*J*HFI)
        ENDIF
```

```
      ENDIF
   10 CONTINUE
      FOUT=FOUT*HFI/3.*PI/180.
      RETURN
  999 END
C
      REAL FUNCTION FCO*8(X)
      REAL X
      REAL*8 PI,DTR
      PI=3.141592653589793
      DTR=PI/180.
      REST=X/360.
      REST=REST-INT(REST)
      IF (REST.EQ.0.) THEN
       FCO=1.
      ELSE
       IF (REST.EQ..75) THEN
         FCO=0.
       ELSE
         IF (REST.EQ..5) THEN
          FCO=-1.
         ELSE
          IF (REST.EQ..25) THEN
            FCO=0.
          ELSE
            FCO=DCOS(X*DTR)
          ENDIF
         ENDIF
       ENDIF
      ENDIF
      RETURN
      END

      REAL FUNCTION FSI*8(X)
      REAL X
      REAL*8 PI,DTR
      PI=3.141592653589793
      DTR=PI/180.
      REST=X/360.
      REST=REST-INT(REST)
      IF (REST.EQ.0.) THEN
       FSI=0.
      ELSE
       IF (REST.EQ..75) THEN
         FSI=-1.
       ELSE
         IF (REST.EQ..5) THEN
          FSI=0.
         ELSE
          IF (REST.EQ..25) THEN
            FSI=1.
          ELSE
            FSI=DSIN(X*DTR)
          ENDIF
         ENDIF
       ENDIF
      ENDIF
      RETURN
      END
```

```
C*********************************************************************
C THIS PROGRAMME COMPUTE XI FOR THE TWO DIFFERENT POLRIZATIONS        *
C THE INPUT ARE THE ARRAY CONTAINING THE SCATERING COEFFICIENTS       *
C FOR THE INCIDENT ANGLES (45,0,14 DEGREES) FOR 14 DIFFERENTS RAIN DROP*
C SIZES.(0.025-3.5) ,AND OBSERVATION ANGLES TETA(K)(12 VALUES)        *
C*********************************************************************
C INITIALIZATIONS AND DECLARATIONS
      INTEGER ICHOI,M,IPOL,I,J,K
      COMPLEX*16 FTE1,FTE2,FFI1,FFI2,F(14),G
      COMPLEX*16 F11,F12,F21,F22,F1(14),F2(14),F3(14),F4(14)
      COMPLEX*16 FIK11(14,25),FIK22(14,25),FIK12(14,25),FIK21(14,25)
      REAL*8 FM1,FM2,FM3,FM4,FMP1(25),FMP2(25),FMP3(25),FMP4(25)
      REAL*8 PI,FTE1R,FTE1I,FTE2R,FTE2I,FFI1R,FFI1I,FFI2R,FFI2I
      COMPLEX IMAG
      COMMON /BLOCK1/ RR
C
      IMAG=(0.,1.)
      PI=3.141592653589793
      WL=.01
C ENTREE DES DONNEES
      DO 1000 I=1,14
      DO 1100 J=1,25
      READ (5,*,END=1100) ALPHA,PHI,TETA,FTE1R,FTE1I,FFI1R,FFI1I,EVR
      READ (5,*,END=1100 ) ALPHA,PHI,TETA,FTE2R,FTE2I,FFI2R,FFI2I,EVR
      FTE1=FTE1R+IMAG*FTE1I
      FFI1=FFI1R+IMAG*FFI1I
      FTE2=FTE2R+IMAG*FTE2I
      FFI2=FFI2R+IMAG*FFI2I
      CALL TRANSF(ALPHA,PHI,TETA,FTE1,FTE2,FFI1,FFI2,F11,F12,F21,F22)
      FIK11(I,J)=F11
      FIK22(I,J)=F22
      FIK12(I,J)=F12
1100  FIK21(I,J)=F21
1000  CONTINUE
C MARCHALL AND PALMER AVERAGE
      RR=100.0
C POLARIZATION 1
      IPOL=1
      DO 2200 J=1,25
      DO 2000 I=1,14
      F1(I)=FIK11(I,J)*DCONJG(FIK11(I,J))
      F2(I)=FIK21(I,J)*DCONJG(FIK21(I,J))
      F3(I)=FIK11(I,J)*DCONJG(FIK21(I,J))
      F4(I)=2*DIMAG(F3(I))
      F3(I)=2*DREAL(F3(I))
2000  CONTINUE
      CALL MPAVE (F1,G)
      FMP1(J)=DREAL(G)
      CALL MPAVE (F2,G)
      FMP2(J)=DREAL(G)
      CALL MPAVE (F3,G)
      FMP3(J)=DREAL(G)
      CALL MPAVE (F4,G)
2200  FMP4(J)=DREAL(G)
C COMPUTATION OF THE FIRST 8 FOURIER TRANSFORMS FOR POLARIZATION 1
      WRITE (8,*) IPOL
      DO 2300 M=0,5
      CALL FOURIER (FMP1,M,0,FM1)
      CALL FOURIER (FMP2,M,0,FM2)
      CALL FOURIER (FMP3,M,1,FM3)
      CALL FOURIER (FMP4,M,1,FM4)
      FM1=FM1/PI
      FM2=FM2/PI
      FM2=FM3/PI
      FM4=FM4/PI
      IF (M.NE.0) THEN
```

```
      FM1=FM1*2.
      FM2=FM2*2.
      FM2=FM3*2.
      FM4=FM4*2.
    ENDIF
    WRITE (8,*)M,FM1,FM2
2300  WRITE (8,*)M,FM3,FM4
C POLARIZATION 2
    IPOL=2
    DO 3200 J=1,25
    DO 3000 I=1,14
    F1(I)=FIK12(I,J)*DCONJG(FIK12(I,J))
    F2(I)=FIK22(I,J)*DCONJG(FIK22(I,J))
    F3(I)=FIK12(I,J)*DCONJG(FIK22(I,J))
    F4(I)=2*DIMAG(F3(I))
    F3(I)=2*DREAL(F3(I))
3000  CONTINUE
    CALL MPAVE (F1,G)
    FMP1(J)=DREAL(G)
    CALL MPAVE (F2,G)
    FMP2(J)=DREAL(G)
    CALL MPAVE (F3,G)
    FMP3(J)=DREAL(G)
    CALL MPAVE (F4,G)
3200  FMP4(J)=DREAL(G)
C COMPUTATION OF THE FIRST 8 FOURIER TRANSFORMS FOR POLARIZATION 2
    WRITE (8,*) IPOL
    DO 3300 M=0,5
    CALL FOURIER (FMP1,M,0,FM1)
    CALL FOURIER (FMP2,M,0,FM2)
    CALL FOURIER (FMP3,M,1,FM3)
    CALL FOURIER (FMP4,M,1,FM4)
    FM1=FM1/PI
    FM2=FM2/PI
    FM2=FM3/PI
    FM4=FM4/PI
    IF (M.NE.0) THEN
      FM1=FM1*2.
      FM2=FM2*2.
      FM2=FM3*2.
      FM4=FM4*2.
    ENDIF
    WRITE (9,*) M,FM1,FM2
3300  WRITE (9,*) M,FM3,FM4
 99   END


C THIS PROGRAM READS AND TRANSFORMS THE SCATTERING COEFFICIENTS IN TO
C THE  VAN DE HULST FORM I.E. F11,F12,F22,F21
C THE INPUT DATA ARE:
C THE SCATTERING COEFFICIENTS
C               FTETA1
C               FTETA2
C               FFI1
C               FFI2
C AND THE ANGLES FOR WHIHICH THEY ARE COMPUTED
C               ALPHA INCIDENT ANGLE
C               PHI
C               TETA OBSERVATION ANGLE
C SUBROUTINE TRANSFORMING F(TETA,ALPHA,PHI) IN F11,F22,F12,F21
    SUBROUTINE TRANSF(ALPHA,FI,TETA,FTE1,FTE2,FFI1,FFI2,F11,F12,F21,
   &F22)
    COMPLEX*16 FTE1,FTE2,FFI1,FFI2
    COMPLEX*16 F11,F12,F21,F22
    REAL*8 CT,ST,SA,CA,CF,SF,U,U2,A,B,C,D,PI
```

```
      PI=3.141592653589793
C CASE OF FORWARD OR BACKWARD SCATTERING
      IF (((ALPHA.EQ.TETA).OR.(ALPHA.EQ.180.-TETA)).AND.((FI.EQ.0.).OR.
     &(ABS(FI).EQ.180.))) THEN
      F12=(0.,0.)
      F21=(0.,0.)
      F11=FTE1
      F22=FFI2
      GO TO 99
      ENDIF
C GENERAL CASE(JE SUPPOSE ICI QUE J'AI LA BONNE VALEUR DE TETA ET FI)
      IF (TETA.EQ.90.) THEN
        CT=0.
        ST=1.
      ELSE
        IF (TETA.EQ.180.) THEN
          CT=-1.
          ST=0.
        ELSE
          CT=DCOS(TETA*PI/180.)
          ST=DSIN(TETA*PI/180.)
        ENDIF
      ENDIF
      IF (FI.EQ.90.) THEN
        CF=0.
        SF=1.
      ELSE
        IF (FI.EQ.180.) THEN
          CF=-1.
          SF=0.
        ELSE
          CF=DCOS(FI*PI/180.)
          SF=DSIN(FI*PI/180.)
        ENDIF
      ENDIF
      IF (ALPHA.EQ.90.) THEN
        CA=0.
        SA=1.
      ELSE
        IF (ALPHA.EQ.180.) THEN
          CA=-1.
          SA=0.
        ELSE
          CA=DCOS(ALPHA*PI/180.)
          SA=DSIN(ALPHA*PI/180.)
        ENDIF
      ENDIF
      U=CA*CT-SA*ST*CF
      U2=1-U*U
      A=-SA*SF
      B=SA*CF*CT-CA*ST
      C=-ST*SF
      D=CT*ST*CF-SA*CT
      F11=(A*(FTE1*C+FTE2*D)-B*(FFI1*C+FFI2*D))/U2
      F12=(A*(-FTE1*D+FTE2*C)-B*(-FFI1*D+FFI2*C))/U2
      F21=(B*(FTE1*C+FTE2*D)+A*(FFI1*C+FFI2*D))/U2
      F22=(B*(-FTE1*D+FTE2*C)+A*(-FFI1*D+FFI2*C))/U2
99    RETURN
      END


C THIS SUBROUTINE COMPUTE THE AVERAGE OF THE FUNCTION F BY USING THE
C MARSCHALL & PALMER DISTRIBUTION AND SNE DIT BACK IN G
C
C
      SUBROUTINE MPAVE(F,G)
```

```
      INTEGER J
      REAL N0,RR
      REAL*8 BETA
      COMPLEX*16 G,F(14),CINT
      COMMON /BLOCK1/ RR
C CONSTANTS
      CINT=(0.,0.)
      G=(0.,0.)
      N0=16000.0
      BETA=8.2*RR**(-.21)
C COMPUTE G FOR 0.25 AND 3.5 MM
      CINT=4*DEXP(-BETA*.25)*F(1)+DEXP(-BETA*3.5)*F(14)
C COMPUTATION FOR THE OTHER RADIUS (.5 TO 3.2)
      DO 10 J=1,6
      CINT=CINT+2*DEXP(-BETA*.5*J)*F(2*J)
      CINT=CINT+4*DEXP(-BETA*(.5*J+.25))*F(2*J+1)
10    CONTINUE
      G=CINT*N0/12.
      RETURN
      END

C THIS PROGRAM COMPUTE THE FOURIER TRANSFORM WITH REGARD TO THE
C AZIMUTHAL ANGLE PHI OF THE INPUT FUNCTION F USING A 25 POINT SIMPSON
C INTEGRATION.
C THE INPUT DATA ARE
C       *THE ARRAY CONTAINING THE FUNCTION  AT THE 25
C        VALUES OF PHI (0(7.5)180) F(25)
C       *THE ORDER M OF THE FOURIER COEFFICIENT WANTED
C       *THE VARIABLE ICHOI TO CHOOSE BETWEEN A COSINE OR A SINE
C        TRANSFORM : ICHOI=0 FOR A COSINE TRANSFORM
C              AND  ICHOI=1 FOR A SINE TRANSFORM
      SUBROUTINE  FOURIER(F,M,ICHOI,FOUT)
      INTEGER MPAR,ICHOI,M,J
      REAL HFI
      REAL*8 FCO,FSI,PI
      REAL*8 F(25),FOUT
      COMPLEX IMAG
C CONSTANTS
      IMAG=(0.,1.)
      PI=3.141592653589793
C INITIALIZATIONS
      HFI=180./24
      FOUT=0.
c parity of m
      MPAR=M-2*INT(M/2)
C SIMPSON  INTEGRATION
      IF (ICHOI.EQ.0) THEN
        FOUT=F(1)
        IF(MPAR.EQ.0) THEN
          FOUT=FOUT+F(25)
        ELSE
          FOUT=FOUT-F(25)
        ENDIF
      ENDIF
      DO 10 J=0,11
      IF (J.EQ.0) THEN
        IF (ICHOI.EQ.0) FOUT=FOUT+4*F(2)*FCO(M*HFI)
        IF (ICHOI.EQ.1) FOUT=FOUT+4*F(2)*FSI(M*HFI)
      ELSE
        IF (ICHOI.EQ.0) THEN
          FOUT=FOUT+4*F(2*J+2)*FCO(M*(2*J+1)*HFI)
          FOUT=FOUT+2*F(2*J+1)*FCO(M*2*J*HFI)
        ELSE
          FOUT=FOUT+4*F(2*J+2)*FSI(M*(2*J+1)*HFI)
          FOUT=FOUT+2*F(2*J+1)*FSI(M*2*J*HFI)
        ENDIF
```

```
      ENDIF
   10 CONTINUE
      FOUT=FOUT*HFI/3.*PI/180.
      RETURN
  999  END
C
      REAL FUNCTION FCO*8(X)
      REAL X
      REAL*8 PI,DTR
      PI=3.141592653589793
      DTR=PI/180.
      REST=X/360.
      REST=REST-INT(REST)
      IF (REST.EQ.0.) THEN
        FCO=1.
      ELSE
       IF (REST.EQ..75) THEN
         FCO=0.
       ELSE
         IF (REST.EQ..5) THEN
          FCO=-1.
         ELSE
          IF (REST.EQ..25) THEN
            FCO=0.
          ELSE
            FCO=DCOS(X*DTR)
          ENDIF
         ENDIF
       ENDIF
      ENDIF
      RETURN
      END

      REAL FUNCTION FSI*8(X)
      REAL X
      REAL*8 PI,DTR
      PI=3.141592653589793
      DTR=PI/180.
      REST=X/360.
      REST=REST-INT(REST)
      IF (REST.EQ.0.) THEN
        FSI=0.
      ELSE
       IF (REST.EQ..75) THEN
         FSI=-1.
       ELSE
         IF (REST.EQ..5) THEN
          FSI=0.
         ELSE
          IF (REST.EQ..25) THEN
            FSI=1.
          ELSE
            FSI=DSIN(X*DTR)
          ENDIF
         ENDIF
       ENDIF
      ENDIF
      RETURN
      END
```

```
C*****************************************************************
C THIS PROGAMME SOLVE THE RADIATIVE TRANSFER EQUATION FOR A PLANE *
C PARALLEL MEDIUM.THE INPUTS ARE :                                *
C D THE THICKNESS OF THE MEDIUM                                   *
C Z THE DISTANCE AT WHICH THE INCOHERENT FIELD IS COMPUTED        *
C GAMMAII                                                         *
C LAMBDAK                                                         *
C L(MUK,MUL)                                                      *
C XIM                                                             *
C                                                                 *
C*****************************************************************
C DECLARATIONS
      INTEGER IPOL,POL,M,MM,I,J,P,Q,L,K,IKK
      COMPLEX IMAG
      REAL DELT,D,DELT1,TETAK(12)
      REAL*8 PI,DTR,DD,H(0:4,12,12,4,4)
      REAL*8 MUI,A(12),MU(12),GAMAI,LAMD(12,4,4),XI(0:4,12,4)
      REAL*8 XIM(48),KSIM(48,48),AXP0M(48,48),XP0M(48)
      COMPLEX*16 EVALM(48),EVECM(48,48),ACM(48,48),BCM(48),CM(48),NORM
      REAL*8 XI0(24),KSI0(24,24),AXP00(24,24),XP00(24)
      REAL RWKSP(9622)
      COMPLEX*16 EVAL0(24),EVEC0(24,24),AC0(24,24),BC0(24),C0(24)
      COMPLEX*16 ELDP,SM(4,48),S0(24),I1(12),I2(12)
      COMMON /WORKSP/ RWKSP
      CALL IWKIN(9622)
C BLOCK DE DONNEES DATA POUR Ak ET MUk
      DATA A/0.047175336386512,0.106939325995318,0.160078328543346,
     &      0.203167426723066,0.233492536538355,0.249147045813403,
     &      0.249147045813403,
     &      0.233492536538355,
     &      0.203167426723066,
     &      0.160078328543346,
     &      0.106939325995318,
     &      0.047175336386512/
C INITIALIZATION DE MUk
      MU(1)=0.981560634246719
      MU(4)=0.587317954286617
      MU(2)=0.904117256370475
      MU(5)=0.367831498998180
      MU(3)=0.769902674194305
      MU(6)=0.125233408511469
      IMAG=(0.,1.)
      PI=3.141592653589793
      DTR=PI/180.
      PHI=0.0
      DO 9000 IKK=1,6
      TETAK(IKK)=ARCOS(MU(IKK))/PI*180.
      MU(13-IKK)=-MU(IKK)
9000  TETAK(13-IKK)=ARCOS(-MU(IKK))/PI*180.
C INITIALIZATIONS
      IPOL=1
      RR=12.5
      DO 9 K=1,12
      DO 10 I=4,4
      DO 11 J=4,4
11    LAMD(K,I,J)=0.
10    CONTINUE
09    CONTINUE
      MUI=1.
      TETAI=0.
      READ(4,*,END=1)D,Z
      UNITE=100.
      UNITE2=UNITE*UNITE
C**********************INPUT OF THE DATA**********************
C INPUT OF GAMMAII
      READ(5,*,END=1)POL,GAMAI,RR
```

```
      GAMAI=GAMAI/UNITE
      DD=DEXP(-D*GAMAI/MUI)
C INPUT OF XI
      DO 100 I=1,12
      DO 110 M=0,4
      READ(5,*,END=1)MM,XI(M,I,1),XI(M,I,2)
      READ(5,*,END=1)MM,XI(M,I,3),XI(M,I,4)
      IF ( DABS(XI(M,I,1)).LE.0.000001) THEN
      XI(M,I,1)=0.
      ELSE
      XI(M,I,1)=XI(M,I,1)/UNITE2
      ENDIF
      IF ( DABS(XI(M,I,2)).LE.0.000001) THEN
      XI(M,I,2)=0.
      ELSE
      XI(M,I,2)=XI(M,I,2)/UNITE2
      ENDIF
      IF ( DABS(XI(M,I,3)).LE.0.000001) THEN
      XI(M,I,3)=0.
      ELSE
      XI(M,I,3)=XI(M,I,3)/UNITE2
      ENDIF
      IF ( DABS(XI(M,I,4)).LE.0.000001) THEN
      XI(M,I,4)=0.
      ELSE
      XI(M,I,4)=XI(M,I,4)/UNITE2
      ENDIF
110   CONTINUE
100   CONTINUE
C INPUT OF LAMDA
      DO 150 K=1,12
      READ(5,*,END=1) LAMD(K,1,1),LAMD(K,2,2),LAMD(K,3,3),LAMD(K,3,4)
      IF (DABS(LAMD(K,1,1)).LE.0.000001) THEN
      LAMD(K,1,1)=0.0
      ELSE
      LAMD(K,1,1)=LAMD(K,1,1)/UNITE
      ENDIF
      IF (DABS(LAMD(K,2,2)).LE.0.000001) THEN
      LAMD(K,2,2)=0.0
      ELSE
      LAMD(K,2,2)=LAMD(K,2,2)/UNITE
      ENDIF
      IF (DABS(LAMD(K,3,3)).LE.0.000001) THEN
      LAMD(K,3,3)=0.0
      ELSE
      LAMD(K,3,3)=LAMD(K,3,3)/UNITE
      ENDIF
      IF (DABS(LAMD(K,3,4)).LE.0.000001) THEN
      LAMD(K,3,4)=0.0
      ELSE
      LAMD(K,3,4)=LAMD(K,3,4)/UNITE
      ENDIF
      LAMD(K,4,3)=-LAMD(K,3,4)
150   LAMD(K,4,4)=LAMD(K,3,3)
C INPUT OF H(MUK,MUL)
      DO 200 K=1,12
      DO 210 L=K,12
      DO 220 M=0,4
      READ(5,*,END=1)H(M,K,L,1,1),H(M,K,L,1,2),H(M,K,L,2,1),H(M,K,L,2,2)
      READ(5,*,END=1)H(M,K,L,1,3),H(M,K,L,1,4),H(M,K,L,2,3),H(M,K,L,2,4)
      READ(5,*,END=1)H(M,K,L,3,1),H(M,K,L,3,2),H(M,K,L,4,1),H(M,K,L,4,2)
      H(M,K,L,3,1)=-H(M,K,L,3,1)
      H(M,K,L,3,2)=-H(M,K,L,3,2)
      H(M,K,L,4,1)=-H(M,K,L,4,1)
      H(M,K,L,4,2)=-H(M,K,L,4,2)
      READ(5,*,END=1)H(M,K,L,3,3),H(M,K,L,3,4),H(M,K,L,4,3),H(M,K,L,4,4)
```

```
      DO 221 I=1,4
      DO 222 J=1,4
      IF (DABS(H(M,K,L,I,J)).LE.0.000001) THEN
      H(M,K,L,I,J)=0.0
      ELSE
      H(M,K,L,I,J)=H(M,K,L,I,J)/UNITE2
      ENDIF
222   CONTINUE
221   CONTINUE
220   CONTINUE
      IF (K.EQ.L) GO TO 210
C SYMETRIC  CASE
      DO 300 M=0,4
      P=13-K
      Q=13-L
      READ(5,*,END=1)H(M,P,Q,1,1),H(M,P,Q,1,2),H(M,P,Q,2,1),H(M,P,Q,2,2)
      READ(5,*,END=1)H(M,P,Q,1,3),H(M,P,Q,1,4),H(M,P,Q,2,3),H(M,P,Q,2,4)
      READ(5,*,END=1)H(M,P,Q,3,1),H(M,P,Q,3,2),H(M,P,Q,4,1),H(M,P,Q,4,2)
      H(M,P,Q,3,1)=-H(M,P,Q,3,1)
      H(M,P,Q,3,2)=-H(M,P,Q,3,2)
      H(M,P,Q,4,1)=-H(M,P,Q,4,1)
      H(M,P,Q,4,2)=-H(M,P,Q,4,2)
      READ(5,*,END=1)H(M,P,Q,3,3),H(M,P,Q,3,4),H(M,P,Q,4,3),H(M,P,Q,4,4)
      DO 301 I=1,4
      DO 302 J=1,4
302   H(M,P,Q,I,J)=H(M,P,Q,I,J)/UNITE2
301   CONTINUE
300   CONTINUE
210   CONTINUE
200   CONTINUE
C*******************LOOP FOR COMPUTATION FOR M[1:8]*****************
      DO 8000 M=1,4
      WRITE (6,*) M
C******************CALCUL DE KSIm**********************************
      DO 1000 K=1,12
      DO 1010 L=1,12
      IF (K.EQ.L) THEN
        DELT=1.
      ELSE
        DELT=0.
      ENDIF
      DO 1020 I=1,4
      DO 1030 J=1,4
      P=4*(K-1)+I
      Q=4*(L-1)+J
      IF (P.EQ.Q) THEN
        DELT1=1.
      ELSE
        DELT1=0.
      ENDIF
      KSIM(P,Q)=-(A(K)*H(M,K,L,I,J)-DELT*LAMD(K,I,J))/MU(K)
      AXP0M(P,Q)=KSIM(P,Q)-DELT1*GAMAI/MUI
1030  CONTINUE
1020  CONTINUE
1010  CONTINUE
1000  CONTINUE
C******************CALCUL DE XIM***********************************
      DO 1100 K=1,12
      DO 1110 I=1,4
      P=4*(K-1)+I
1110  XIM(P)=XI(M,K,I)/MU(K)
1100  CONTINUE
C******************EIGENVALUES AND EIGENVECTORS OF KSIM************
      CALL DEVCRG (48,KSIM,48,EVALM,EVECM,48)
C NORMALIZATION
C     DO 1105 P=1,48
```

```
C     NORM=EVECM(1,P)
C      DO 1106 Q=1,48
C1106  EVECM(Q,P)=EVECM(Q,P)/NORM
C1105  CONTINUE
C ****************SOLVE FOR XP(0)m*****************************
      CALL DLSARG(48,AXP0M,48,XIM,1,XP0M)
C*****************COMPUTE  CM*********************************
      DO 2000 I=1,24
2000  BCM(I)=-DCMPLX(XP0M(I))
      DO 2010 I=25,48
2010  BCM(I)=-DCMPLX(XP0M(I)*DD)
      DO 2020 P=1,48
      ELDP=CDEXP(-EVALM(P)*D)
      DO 2030 L=1,24
2030  ACM(L,P)=EVECM(L,P)
      DO 2040 L=25,48
2040  ACM(L,P)=EVECM(L,P)*ELDP
2020  CONTINUE
C     WRITE (6,*) ACM
      CALL DLSACG(48,ACM,48,BCM,1,CM)
C****COMPUTATION OF XM THE SOLUTION Mth FOURIER COMPONENT**********
      DO 2500 I=1,48
      SM(M,I)=(0.,0.)
      DO 2510 P=1,48
2510  SM(M,I)=SM(M,I)+CM(P)*EVECM(I,P)*CDEXP(-Z*EVALM(P))
2500  SM(M,I)=SM(M,I)+XP0M(I)*DEXP(-Z*GAMAI/MUI)
8000  CONTINUE
C******************LOOP FOR COMPUTATION FOR M=0******************
C******************CALCUL DE KSI0*********************************
      M=0
      WRITE (6,*) M
      DO 4000 K=1,12
      DO 4010 L=1,12
      IF (K.EQ.L) THEN
        DELT=1.
      ELSE
        DELT=0.
      ENDIF
      DO 4020 I=1,2
      DO 4030 J=1,2
      P=2*(K-1)+I
      Q=2*(L-1)+J
      IF (P.EQ.Q) THEN
        DELT1=1.
      ELSE
        DELT1=0.
      ENDIF
      KSI0(P,Q)=-(A(K)*H(M,K,L,I,J)-DELT*LAMD(K,I,J))/MU(K)
      AXP00(P,Q)=KSI0(P,Q)-DELT1*GAMAI/MUI
4030  CONTINUE
4020  CONTINUE
4010  CONTINUE
4000  CONTINUE
C******************CALCUL DE XI0**********************************
      DO 4100 K=1,12
      DO 4110 I=1,2
      P=2*(K-1)+I
4110  XI0(P)=XI(M,K,I)/MU(K)
4100  CONTINUE
C******************EIGENVALUES AND EIGENVECTORS OF KSI0************
      CALL DEVCRG(24,KSI0,24,EVAL0,EVEC0,24)
C     WRITE(6,*) EVAL0
C  NORMALIZATION
      DO 4105 P=1,24
      NORM=EVEC0(1,P)
```

```
      DO 4106 Q=1,24
4106  EVEC0(Q,P)=EVEC0(Q,P)/NORM
4105  CONTINUE
C ****************SOLVE FOR XP(0)m*******************************
      CALL DLSARG(24,AXP00,24,XI0,1,XP00)
C*****************COMPUTE  C0*************************************
      DO 5000 I=1,12
5000  BC0(I)=-DCMPLX(XP00(I))
      DO 5010 I=13,24
5010  BC0(I)=-DCMPLX(XP00(I)*DD)
      DO 5020 P=1,24
      ELDP=CDEXP(-EVAL0(P)*D)
      DO 5030 L=1,12
5030  AC0(L,P)=EVEC0(L,P)
      DO 5040 L=13,24
5040  AC0(L,P)=EVEC0(L,P)*ELDP
5020  CONTINUE
C     WRITE (6,*) AC0
      CALL DLSACG(24,AC0,24,BC0,1,C0)
C****COMPUTATION OF XM THE SOLUTION Mth FOURIER COMPONENT**********
      DO 5500 I=1,24
      S0(I)=(0.,0.)
      DO 5510 P=1,24
5510  S0(I)=S0(I)+C0(P)*EVEC0(I,P)*CDEXP(-Z*EVAL0(P))
5500  S0(I)=S0(I)+XP00(I)*DEXP(-Z*GAMAI/MUI)
C SUMMATION ON FOURIER COMPONENTS*********************************
      DO 6000 K=1,12
      I1(K)=S0(2*(K-1)+1)
      I2(K)=S0(2*(K-1)+2)
      DO 6010 M=1,4
      I1(K)=(I1(K)+SM(M,4*(K-1)+1))*COS(M*PHI*DTR)
6010  I2(K)=(I2(K)+SM(M,4*(K-1)+2))*COS(M*PHI*DTR)
      WRITE (9,*) TETAK(K),CDABS(I1(K)),CDABS(I2(K))
6000  WRITE (8,333) TETAK(K),I1(K),I2(K)
      WRITE (8,*) D,Z
333   FORMAT (F10.5,2X,E15.8,2X,E15.8,2X,E15.8,2X,E15.8)
1     END
```

Fatim Mah Soutoura Haidara was born in Bamako, Mali. She attended the 'classes preparatoires in mathematiques superieures et speciales ' at Lycee Saint Louis in Paris, France in 1979-1982 and was admitted to Ecole Speciale de Mecanique et d'Electricite (Paris) from where she received in 1985 the degree of Ingenieur de Mecanique et d'Electricite. After this she worked in Dakar, Senegal, as a pedagogic assistant for IBM and later joined the Ms program of Virginia Polytechnic Institute and State University in 1986. Upon completion of her M.s. Degree in 1988 she plans to pursue her study toward the Ph.D.degree in electrical engineering at VPI and SU where she is serving as a graduate research assistant.